

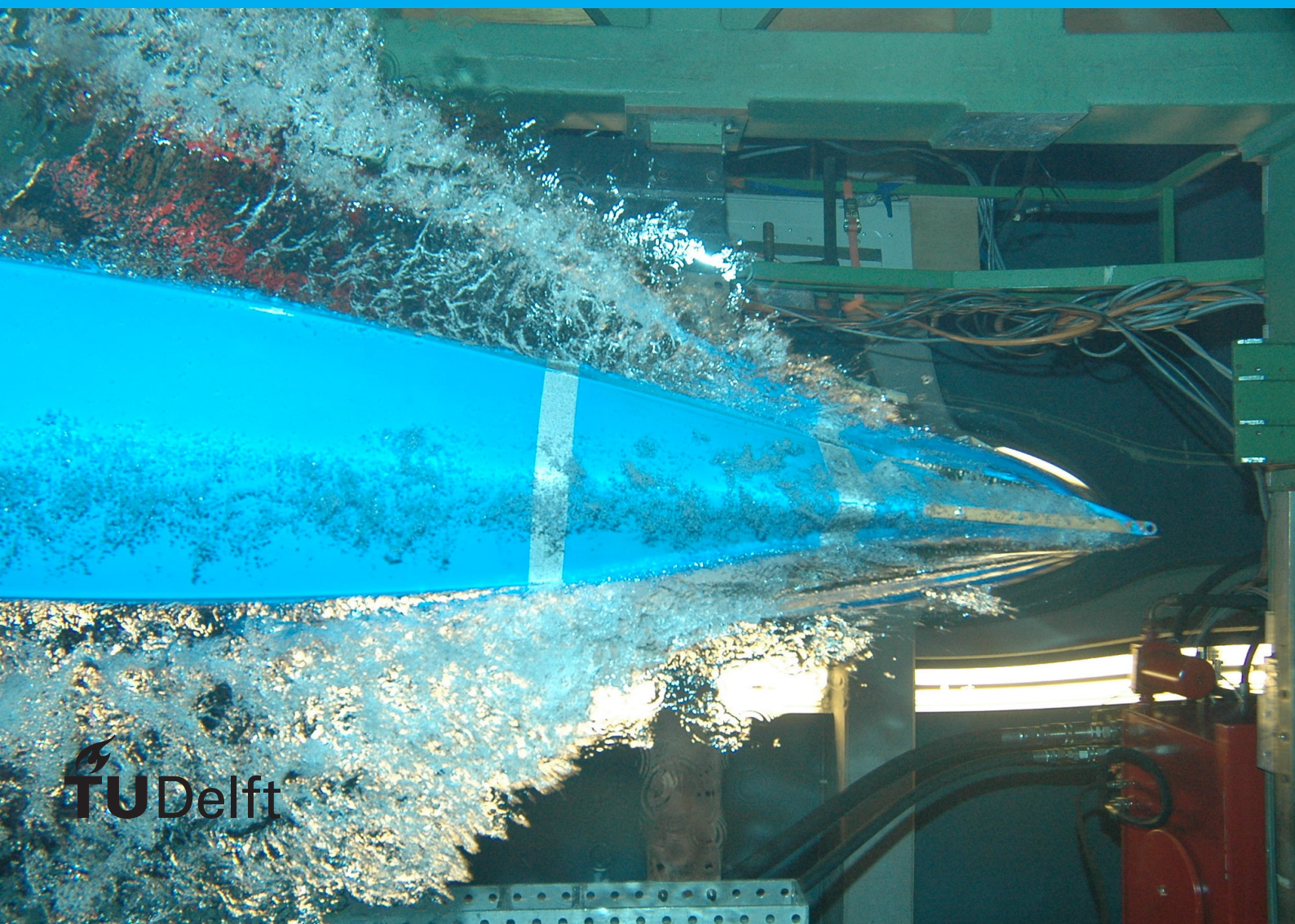
Waste heat recovery of future marine propulsion systems

A techno-economic process-oriented approach

A.P. Herweijer

2021/2022

StudentID: 4394267



Waste heat recovery of future marine propulsion systems

A techno-economic process-oriented approach

by

A.P. Herweijer

to obtain the degree of Master of Science
at the Delft University of Technology,
to be defended publicly on Friday September 23, 2022 at 13:00 PM.

Student number: 4394267
Project duration: October, 2021 – September, 2022
Thesis supervisors: Prof. dr. ir. R. Pecnik, TU Delft, supervisor
Dr. ir. L. van Biert, TU Delft, (co)supervisor
Ir. A. Munir, Vuyk Engineering Rotterdam, company supervisor
S. Bot Vuyk Engineering Rotterdam

An electronic version of this thesis is available at <http://repository.tudelft.nl/>.

Preface

I would like to thank my university supervisors René Pecnik and Lindert van Biert for their valuable input on the many topics that surfaced during the course of this project. Our frequent meetings were often inspiring and highly educational. Furthermore, their insight and advice regarding problems I encountered, as well as the results I obtained, kept me focused on the important parts and allowed for the creation of this thesis.

Additionally, I would like to thank my company supervisor Asif Munir from Vuyk Engineering Rotterdam for sharing his knowledge on the practical applications and considerations of waste heat recovery in marine vessels. Finally, I am also grateful to Sander Bot from Vuyk Engineering Rotterdam for checking in on me regularly, keeping me organised, and helping me approach my thesis with a clear structure.

A.P. Herweijer
Delft, September 2022

Abstract

In response to climate change, the marine sector is increasingly focused on the energy transition. New marine power plants operating more efficiently and on cleaner fuels are receiving significantly more attention. While the transition to different power plants and fuels results in reduced fossil fuel consumption and emissions, waste heat recovery systems can aid in obtaining both as well. Current as well as future marine power plants do not convert all of the energy contained in the fuel into useful power, with significant amounts of energy being wasted as heat. Waste heat recovery technologies can be applied to recover some of this energy and generate additional power, effectively boosting total system efficiency, with the resulting benefits of improved fuel economy and reduced specific emissions.

This study first provides an extensive summary of all the different marine power plants, fuels, and waste heat recovery technologies, of both the present and future. One type of power plant that could be an advantageous alternative for future marine propulsion is the solid oxide fuel cell (SOFC) due to its high efficiency and potential to run on clean fuels. SOFCs generate electricity from chemical energy using a high-temperature electrochemical process, resulting in high-temperature waste heat being expelled. Therefore, the potential for a waste heat recovery technology to boost system efficiency is high, and it is chosen to investigate several power cycles for the waste heat recovery of a case study vessel powered by a 2 MW SOFC system. The aim of this study is to develop and execute an approach to evaluate these waste heat recovery technologies regarding their efficiency, size, and associated cost.

While numerous power cycles for waste heat recovery are in existence, a selection of potentially suitable systems with a number of different setups is made to investigate further. Thermodynamic models are created for the selected power cycles to determine and compare their theoretical efficiencies. Subsequently, the size of the heat exchangers are calculated for the evaluation of system size, considering the size of other components such as turbomachinery as well. Two types of heat exchangers are considered in this study: the compact and innovative printed circuit heat exchanger (PCHE) and the classic but commonly large shell and tube heat exchanger (STHE). Finally, the investigated systems are subjected to an economic analysis based on the cost associated with the main components, with again considerations being made regarding excluded additional components.

The results indicate that various configurations of the (transcritical) Rankine cycle operating on steam and CO₂, as well as the (supercritical) Brayton cycle operating on CO₂ and air, present with significant theoretical efficiencies ranging from 41 to 52% and electrical power outputs ranging from approximately 530 kWe to over 670 kWe. From the evaluation of the system size it is concluded that the smallest systems are those operated on CO₂ equipped with PCHEs, while the largest are the air Brayton cycles equipped with STHEs. The economic analysis revealed that the systems with the lowest costs are the configurations of the (transcritical) Rankine cycle operating on steam, as well as certain air Brayton cycles equipped with PCHEs. The systems with the highest cost are found to be the air Brayton cycles equipped with STHEs, due to the significant sizes of the required heat exchangers. In general, it is concluded that no system outperforms the others simultaneously across all three investigated aspects of efficiency, size, and cost, and trade-offs will be required when selecting a waste heat recovery technology for the presented case study vessel. Nonetheless, a detailed process-oriented approach has been developed and executed to allow various waste heat recovery solutions to be compared, and it is proven that a significant amount of power can be produced from recovered waste heat. The results from this study can be directly consulted by ship owners and designers considering the application of waste heat recovery to an SOFC powered vessel. Furthermore, the developed approach can also be applied to waste heat recovery in other industries and power generation systems, as it provides a step-by-step guide on relevant calculations and considerations.

Contents

Preface	iii
Abstract	v
Nomenclature	x
1 Introduction	1
2 Background	3
2.1 Climate change	3
2.1.1 Shipping industry	3
2.2 Marine power plants	4
2.2.1 Turbines	4
2.2.2 Reciprocating engine	5
2.2.3 Full-electric	5
2.2.4 Assisted drive	7
2.3 Marine fuels	8
2.3.1 Marine fuel oils	8
2.3.2 Natural gas	8
2.3.3 Biofuels	9
2.3.4 Zero-carbon fuels	9
2.3.5 Other fuels	10
2.4 Waste heat recovery	12
2.4.1 Waste heat sources	12
2.4.2 Overview of waste heat sources	14
2.4.3 Waste heat recovery systems	15
2.4.4 Overview of waste heat recovery systems	20
3 The future of marine propulsion	21
3.1 Marine power plant evaluation	21
3.2 Marine fuel evaluation	22
3.3 Waste heat source evaluation	23
3.4 Waste heat recovery system evaluation	23
3.4.1 Waste heat recovery system variations & dependencies	24
3.5 Overview of evaluation	25
3.6 Scope of research	26
3.6.1 Summary	27
4 Research objective	29
4.1 Problem statement	29
4.2 Case study	29
4.2.1 In literature	30
4.3 Research questions	30
4.3.1 Main research question	31
4.3.2 Sub-research questions	31
4.4 Planned approach & methodology	31
5 System characteristics, selection, and design	33
5.1 Initial selection	33
5.2 System configurations	34
5.2.1 The basic configurations	34
5.2.2 Modified configurations	35

6	Efficiency of configurations	39
6.1	Assumptions	39
6.2	Thermodynamics	40
6.2.1	Combined reheating, intercooling & recompression BC	40
6.2.2	Regenerative RC	43
6.3	Validation of models	44
6.4	Comparison	46
6.4.1	Comparison of the SRC configurations	46
6.4.2	Comparison of the TCSRC configurations	47
6.4.3	Comparison of the CO ₂ TCRC configurations	47
6.4.4	Comparison of the air BC configurations	48
6.4.5	Comparison of the CO ₂ SBC configurations	48
6.5	Final comparison and conclusions.	50
7	Size of configurations	53
7.1	Heat exchanger size	53
7.1.1	Overall heat transfer coefficients.	53
7.1.2	Modelling	56
7.1.3	Results & conclusions	59
7.2	Additional size considerations	62
7.2.1	Turbines.	63
7.2.2	Compressors & pumps.	63
7.2.3	Turbomachinery in literature	63
7.2.4	Other components	64
7.3	Conclusions.	65
8	Component cost analysis	67
8.1	Purchased equipment cost.	67
8.1.1	Applied cost factors	69
8.1.2	Resulting purchased equipment costs.	70
8.2	Additional costs.	71
8.2.1	Cost of other components	71
8.2.2	Other cost factors.	72
8.3	Conclusions.	73
9	Conclusions and recommendations	75
9.1	Conclusions.	75
9.2	Recommendations	76
	Bibliography	79
A	Verification of intermediate pressures	89
A.1	Verification of reheating, intercooling, and regeneration pressures	89
B	Size of configurations	91
B.1	Electric power produced	91
B.2	Heat transfer area and heat exchanger volume.	91
C	Cost of configurations	93
C.1	Applied inputs to the PEC correlations	93
C.2	Detailed results of PEC	95
D	Alternative approaches	99
D.1	Same power output.	99
D.2	No additional cost correction.	101

Nomenclature

Subscripts

<i>amb</i>	ambient
<i>C</i>	Compressor (or Cold flow)
<i>e</i>	electric
<i>gen</i>	generator
<i>H</i>	Heater (or Hot flow)
<i>HEX</i>	Heat exchanger
<i>ise</i>	isentropic
<i>max</i>	maximum
<i>min</i>	minimum
<i>P</i>	Process fluid
<i>RH</i>	Reheater
<i>S</i>	Service fluid
<i>T</i>	Turbine
<i>th</i>	theoretical

Normal scripts

<i>A</i>	Area
<i>C*</i>	Cost scaling factor
<i>h</i>	Specific enthalpy
ΔH	Enthalpy change
\dot{m}	Mass flow rate
<i>P</i>	Pressure or power output
ΔP	Pressure drop
<i>PR</i>	Pressure ratio
<i>q</i>	Specific heat
\dot{Q}	Heat
<i>s</i>	Specific entropy
<i>split</i>	Flow split fraction
<i>T</i>	Temperature
ΔT	(Minimum) temperature difference

\bar{U}	Overall heat transfer coefficient
<i>W</i>	Work
<i>w</i>	Specific work
<i>x</i>	Vapour quality

Greek symbols

η	(isentropic) efficiency
--------	-------------------------

Acronyms

AFC	Alkaline fuel cell
BC	Brayton cycle
CAC	Charge-air cooling
CEPCI	Chemical engineering plant cost index
DIR	Direct internal reforming
DME	Dimethyl ether
FWH	Feedwater heater
GHG	Greenhouse gas
HFO	Heavy fuel oil
HP	High-pressure
HPC	High-pressure compressor
HPT	High-pressure turbine
HT-FC	High-temperature fuel cell
HTC	High-temperature compressor
HTP	High-temperature pump
HTR	High-temperature recuperator
ICE	Internal combustion engine
KC	Kalina cycle
LNG	Liquefied natural gas
LP	Low-pressure
LPC	Low-pressure compressor
LPG	Liquefied petroleum gas
LPT	Low-pressure turbine
LT-FC	Low-temperature fuel cell

LTC	Low-temperature compressor	SBC	Supercritical Brayton cycle
LTP	Low-temperature pump	SC	Stirling cycle
LTR	Low-temperature recuperator	sCO ₂	Supercritical CO ₂
MCFC	Molten carbonate fuel cell	SCRC	Supercritical Rankine cycle
ORC	Organic Rankine cycle	SOFC	Solid oxide fuel cell
PAFC	Phosphoric acid fuel cell	SRC	Steam Rankine cycle
PCHE	Printed circuit heat exchanger	STHE	Shell and tube heat exchanger
PEC	Purchased equipment cost	TCRC	Transcritical Rankine cycle
PEG	Piezoelectric generator	TCSRC	Transcritical steam Rankine cycle
PEMFC	Polymer electrolyte membrane fuel cell	TEC	Thermionic energy converter
PFD	Process flow diagram	TEG	Thermoelectric generator
PM	Particulate matter	TIT	Turbine inlet temperature
PT	Power turbine	TPV	Thermophotovoltaic
RC	Rankine cycle		

1

Introduction

Climate change has been a looming danger for many years now and is becoming increasingly catastrophic; with more extreme weather, a rising sea level, and other symptoms being the expected result. The cause of climate change has also been plainly evident for years now: harmful emissions such as carbon dioxide are resulting in global warming [69].

To even start mitigating climate change, a large decrease in emissions is required. One way to flatten the curve is through more stringent regulations on emissions, and several institutions such as the Intergovernmental Panel on Climate Change are advocating these. Besides international agreements to decrease emissions, there have been suggestions of more enforceable regulations such as carbon pricing.

The largest share of greenhouse gas emissions (GHG) are caused by the energy sector, which accounts for 73.2% of all GHG emissions [97]; this gives rise to the need for an energy transition. The world is slowly transitioning from highly polluting fossil fuels for energy to cleaner, or even fully renewable, energy; where the desired goal is to be fully transitioned by the second half of this century [15].

Approximately 80% of global trade goods is transported by marine vessels [5], and as a result the maritime transport sector is responsible for nearly 3% of all GHG emissions [31]. Therefore, the maritime transport sector is looking for an energy transition, incentivized by the International Maritime Organization (IMO) setting emission goals, companies are looking into alternative ways of propulsion and fuels. However, there are currently limited green alternatives available in this sector, and implementation of alternatives is at the moment a complex and costly endeavour.

Alternative prime movers and fuels could significantly reduce emissions, and although there is an increase in research and development into cleaner alternatives, many ships still use diesel engines that run on polluting heavy fuel oils (HFO). One of the drawbacks of alternative propulsion systems and fuels are the accompanying costs. Advanced propulsion technologies are expensive to design and implement, and the prices of alternative fuels are relatively high with respect to their energy content. Because of current emission regulations and higher (alternative) fuel prices, there is an ever growing desire for increased fuel efficiency to provide the necessary cost and emissions decrease.

Technological advancements have caused efficiencies to increase, with current marine diesel engines having relatively high efficiencies of approximately 50%; however, the remaining energy contained in the fuel is still lost and largely expelled as waste heat [38]. These losses are not unique to diesel engines, and other types of power plant display varying efficiencies and operational characteristics, expelling different amounts of waste heat at different temperatures. To improve the efficiency and fuel economy of any given power plant, the concept of waste heat recovery can be applied. Waste heat recovery technologies are designed to use the otherwise lost waste heat for purposes such as power generation for propulsion or heating. Application of waste heat recovery in current marine propulsion has been proven effective and increasingly applied, but the benefits to possible future marine propulsion may be even greater. Especially when considering relatively expensive alternative fuels, the use of waste heat recovery technologies to generate power for propulsion could lead to significant cost savings, and potentially make such alternative fuels more cost-competitive.

On the topic of waste heat recovery, a lot of research has focused on maximizing system efficiency through large waste heat recovery cascades; however, for marine applications, the size of a waste heat recovery technology is a largely limiting factor, which should not be ignored to achieve an incremental increase in efficiency. Additionally, while there has been significant research into waste heat recovery for current marine propulsion systems, extensive overviews of marine propulsion and waste heat recovery appear to be lacking, and there has been little research conducted into waste heat recovery for future marine propulsion. With the increased likelihood of a shift in marine propulsion, a structured approach to evaluate different waste heat recovery technologies for future marine applications may prove vital.

Therefore, this study has been conducted to provide such an extensive summary and overview of marine propulsion and waste heat recovery, and to apply a straightforward approach to investigate waste heat recovery options for future marine application. The first part of which has been achieved by structuring marine propulsion and waste heat recovery into separate sections, summarising relevant literature regarding each component, and finally evaluating these components to find promising technologies for further investigation, and therewith the research topic of the second part.

In chapter 2, first the scientific and societal relevance will be briefly touched upon, specifically in relation to climate change and the effect of the shipping industry on it. Subsequently, the following sections discuss the different types of marine power plants and fuels of the past, present, and future; including noteworthy characteristics. After that, waste heat recovery will be introduced, followed by an overview of common sources of waste heat and different waste heat recovery systems. Chapter 3 contains an evaluation applied to the previously discussed marine power plants, marine fuels, waste heat sources, and waste heat recovery systems to determine a promising scope of research. Finally, in chapter 4, the aforementioned scope of research will be used and a case study will be specified; this will be followed by the problem statement as well as the planned approach & methodology.

The second part of this study contains the process-oriented approach to evaluate different waste heat recovery options for the presented case study. This is done through a stepwise structure through which a number of waste heat recovery technologies are modelled, evaluated, and omitted if necessary. Chapter 5 contains the first step in which the group of promising waste heat recovery technologies, as obtained at the end of chapter 3, is further reduced to match application to the case study, and their designs are specified. In chapter 6, the selection of waste heat recovery technologies is compared based on their performance regarding their thermodynamic efficiency; this is done through the description and creation of first law thermodynamic models, and the subsequent evaluation of the results. Next, chapter 7 contains the third step of the evaluation regarding the size of the waste heat recovery technologies, which specifically focuses on heat exchangers by further extending the thermodynamic models with heat transfer calculations. This chapter also presents relevant sizing considerations regarding turbomachinery and other components.

In chapter 8, the final parameter of the evaluation is presented: the economics. In this chapter, the waste heat recovery technologies are broken down into their main components, namely heat exchangers and turbomachinery, and component costs are determined as a basis to compare the economics of the different technologies. Finally, in chapter 9, summaries of the results are provided and the final conclusions are presented, followed by recommendations for further research.

2

Background

This chapter provides a comprehensive overview on marine propulsion in terms of power plants and fuels, as well as on waste heat generation and recovery. In the first section of this chapter, the issue of climate change and its connection to the maritime sector is discussed to present the societal relevance of the topic. In the second section, several types of marine power plants will be explained regarding relevant operational aspects and their classification. In the third section, various marine fuels will be presented and discussed with respect to, amongst others, their characteristics, production pathways, and application. In the final section, an overview of the waste heat generated by the aforementioned marine power plants is presented; additionally, a number of waste heat recovery systems are discussed and finally summarised in an overview containing relevant characteristics.

2.1. Climate change

The global temperature is rising due to the increasing concentration of a number of anthropogenic pollutants in the atmosphere. The most impactful of these pollutants are carbon dioxide (CO₂), methane, and nitrous oxide, which account for 66%, 16%, and 7%, of the effect on global warming respectively [11]. Other harmful pollutants include nitrogen oxides (NO_x), and sulfur oxides (SO_x). Apart from methane, which mainly results from natural gas leaks and livestock industry, the aforementioned pollutants are predominantly the result of conversion processes, such as combustion, in which substances containing carbon, nitrogen, and/or sulfur react with oxygen.

In light of the devastating effects of climate change, such as rising sea levels and extreme weather conditions, 196 parties reached a consensus at the 2015 United Nations Climate Change Conference and adopted the Paris Agreement. The goal of the Paris Agreement is to limit the global temperature rise, with respect to the pre-industrial temperature, to a maximum of 2 degrees Celsius [49]; this should be achieved reducing GHG emissions and becoming climate neutral by the second half of this century.

Through the combustion of fossil fuels, the energy sector is responsible for the bulk of emissions; this includes energy used in the maritime transportation industry, and to achieve climate goals, it will have to transition to more sustainable energy.

2.1.1. Shipping industry

Many emissions are caused by the maritime transport sector, and although marine engines have relatively high efficiencies, roughly 3% of all global emissions are the result of this sector [31]. Reaching climate goals will involve the implementation of new marine propulsion systems able to run on cleaner fuels. However, there are many barriers to overcome as alternatives are often underdeveloped, too complex, too expensive, or lacking necessary infrastructure.

Like many institutions the IMO has introduced regulations to mitigate the impact of shipping on the climate and environment, with the goal to have the sector reduce GHG emissions compared to 2008 levels with 50% by 2050 [31]. In pursuit of the reduction of GHG emissions, the IMO has introduced thresholds regarding engine efficiency for new marine vessels to uphold. To limit emissions of harmful pollutants such as NO_x and SO_x, the IMO continues to set higher standards for the maritime transport sector to comply with. In addition to these regulations, the International Convention for the Prevention

of Pollution from Ships (MARPOL) has designated certain emission control areas to limit environmental pollution of SO_x, NO_x, and particulate matter (PM) [21].

Most of the active marine vessels currently operate on large diesel engines running on HFOs. The reason for this is the low cost of HFO, high energy density, and widespread availability. In addition, marine diesel engines have relatively high efficiencies [29]. However, with regards to the energy transition, companies within the marine sector are becoming increasingly interested in alternative prime movers and fuels. This has resulted in vessels operating on cleaner fuels such as liquefied natural gas (LNG) and methanol, as well as increased research and development of even cleaner alternatives such as fuel cells and zero-emission fuels [78]. Unfortunately, many of these alternatives are not applicable yet or have barriers preventing implementation.

One of these barriers is the large power requirement, and thus high fuel consumption, of marine vessels. Many marine vessels travel long distances without refuelling, which provides complications for alternatives such as batteries since these often can not provide enough energy for a long voyage [44]. Additionally, alternative fuels often have lower energy densities compared to HFOs, which is undesirable due to the limited storage capabilities of marine vessels and could require significant modifications to compensate.

Another barrier is cost, which is a driving factor for the use of HFOs. Acquiring new vessels, or retrofitting current ones, that are equipped with more advanced power plants and operate on alternative fuels, requires high capital expenditure. Many vessels and their power plants are not at the end of their life cycle and could still operate for quite some time [37]; therefore, it is often financially desirable to continue business as usual until they are fully depreciated. The main reasons most alternative fuels are significantly more expensive than common fuel oils are because of their limited and complex production and transportation, as well as their relatively low energy density [130].

Finally, because the demand for alternative fuels is still low, there are limited ports with suitable bunkering infrastructure to supply possible alternatives, which makes the fuels in turn less attractive [138]. The result is somewhat of a paradox; for as long as demand is low, so will be the willingness to build bunkering infrastructure, which will disincentivize marine vessel operators to switch to alternative fuels. To mitigate this final problem along with emission reductions, inroads have been made by the invention of dual-fuel engines providing fuel flexibility; these engines typically operate on HFOs and another (cleaner) fuel such as LNG or methanol [138].

2.2. Marine power plants

There are several types of power plants for the propulsion of marine vessels; over the course of history the choice of marine engine has changed significantly. The four overarching classes of power plants discussed here are turbines, reciprocating engines, full-electric and assisted-drive. In which full-electric power plants consist of batteries and fuel cells as those directly provide electricity without an additional generator, and assisted-drive is considered as renewable energy technologies that are typically not suitable to be the sole means of propulsion. A selection of marine power plants applied historically, currently, and potentially in the future, is described here.

2.2.1. Turbines

Turbine power plants are continuous internal/external combustion engines, and are based on the principle of expanding gases through (a series) of blades attached to a shaft. The moving gases, either steam or combustion gases, act on the blades to produce rotational shaft power. In general, turbine powered vessels are not very common, and find their application in naval vessels and some commercial transport vessels. The disadvantages of turbines are due to their high shaft speeds which need to be lowered to obtain efficient propeller speeds; therefore, they require large gearboxes as well as having poor efficiency at low power output [96]. Turbines are therefore commonly used in combination with another type of engine [29].

Steam turbine

As an external combustion engine, the steam turbine was historically widely used, powered by the burning of coal to create steam; it was later also powered by the burning of other fuels and nuclear energy. There are several types of steam turbine with varying applications, they can be categorised as a condensing, back-pressure, reheat, and extraction steam turbine; for simplicity, this research will

only consider condensing steam turbines. Steam turbines present advantages regarding their high power output, size, low noise and vibration, and ease of maintenance; regardless, steam turbines are currently relatively uncommon for main propulsion apart from some applications in LNG carriers and nuclear powered naval vessels [59]. The main advantage of steam turbines is the option to use polluting and corrosive fuels; however a disadvantage is that load change can only occur relatively slowly [96].

Gas turbine

In contrast to steam turbines, gas turbines are of the internal combustion type, and burn a fuel/air mixture after which the combustion gases are expanded to produce power. Internal gas turbines are the most common type of turbine for marine application, and are used in naval vessels and increasingly in large passenger vessels [29]. Gas turbines have several advantages, one of which is that they allow for a fast change of the load level to produce large amounts of power. Additionally, they have high power density, fuel flexibility, ease of maintenance and robustness due to simplicity, and they have the possibility of being swapped out instead of requiring time-consuming repairs [29]. However, in addition to the aforementioned disadvantage regarding the poor efficiency at low load levels of turbines, gas turbines require relatively clean and expensive fuels [96]. Naval vessels mainly equip gas turbines for their ability to provide fast load changes and high speeds due to their high specific power. Similarly, while passenger vessels primarily apply them for their high speed applications, they also often equip them to be used in areas where emissions have to be reduced.

2.2.2. Reciprocating engine

The class of reciprocating engines used in marine applications is currently comprised of the internal combustion engine, and the Stirling engine. Both engines are based on the combustion of fuel driving reciprocating pistons to generate power. However, they have widely different designs, operating principles, and application.

Internal combustion engine (ICE)

Reciprocating internal combustion engines are subdivided into spark-ignition engines, commonly referred to as petrol engines, and compression-ignition engines, also known as diesel engines. The diesel engine is the most commonly used prime mover in the maritime transport sector, and nearly all commercial vessels are equipped with this type of engine. The main reason for its popularity is that this type of engine can run on relatively inexpensive fuels with high energy densities. Additionally, these engines have the advantage of high thermal efficiencies in the range of 50%, combined with (increasing) fuel flexibility [29]. Marine diesel engines have a low speed two-stroke variant and higher speed four-stroke variant; the two-stroke variant is typically the dominant choice for large ocean going vessels. Compared to the four-stroke variant, the advantages of the two-stroke engine are its high efficiency, its low maintenance requirement, and the reduced need for a transmission system as direct drive without a gearbox is possible due to the low shaft speeds. The four-stroke engine is typically used in smaller vessels that require higher shaft speeds for manoeuvring purposes; the main advantage of this variant is its compactness and higher power-to-weight ratio.

Stirling engine

Unlike the reciprocating internal combustion engine, the Stirling engine is of the external (closed system) combustion type, which allows for the use of a wide variety of fuels, including ones that could be damaging to the engine internals. Stirling engines operate using the expansion and compression of a working medium between a hot and cold source respectively. Their marine application is limited and Stirling engines are mainly found in naval submarine vessels for air-independent propulsion, benefiting from seawater as the cold source, and because of its low noise and vibration generation [116].

2.2.3. Full-electric

In recent years more attention has been given to alternative ways to power marine vessels, mainly with respect to emission reductions. Full-electric marine power plants are one of the alternatives, and are based on chemical energy being converted into electricity; however, there is currently little application. Depending on the origin of their fuel or electricity, the following marine power plants have the possibility of being zero-emission. It should be noted that full-electric propulsion in this study does not refer to electric motors powered by diesel generators, but refers to the application of charged batteries and fuel cells.

Batteries

Batteries are a commonly used energy storage device, with increasing application in road transportation. In the marine sector, lead-acid batteries have been traditionally used for backup power, and due to the development of lithium-ion (Li-ion) batteries these types are becoming increasingly applied. Batteries being used as the main power source can find their application in smaller vessels, vessels that travel relatively short distances, or vessels that have the possibility of recharging frequently. Examples of this are inland shipping, ferries, and small specialized ships. However, batteries are unsuitable as the main power source for vessels undergoing long voyages because they lack the ability to deliver the required power [134]. Batteries are often used in a hybrid combination with generators, either to allow running of the generators at a more efficient operating point or because the use of batteries permits vessels to operate in emission control areas. If the electricity stored in the battery has been produced from renewable sources, this technology classifies as zero-emission.

Fuel cells

There are several types of fuel cells, all of which are based on the principle of redox reactions that produce electricity [66]. Unlike batteries, fuel cells are continuously fed with a fuel and oxidizing component, flowing along two electrodes: the anode and cathode. As ions from the fuel or oxidizing component move from one electrode to the other through the electrolyte, electrons flow through a circuit which generates an electric current. Fuel cells are often categorized by the used electrolyte, and typically have different operating temperatures [48]. A common fuel and oxidizing component for fuel cells are hydrogen and oxygen respectively, producing only water as a result, making it a zero-emission technology as long as green hydrogen is used. Additionally, certain types of fuel cells can have efficiencies of 60%, and produce little to no noise [128]. The technology has proven suitable for road transportation and has substantial application in space travel; however, there have been only few applications of fuel cells as marine power plants, mostly in small vessels and naval submarines [128]. While hydrogen is the most common fuel for fuel cells, other alternatives containing hydrogen, such as ammonia, can be applied as well; however, fuel reforming may be required. In such instances, a fuel cell with a high operating temperature, such as a solid oxide fuel cell (SOFC), can be advantageous. Because of their zero-emission potential there is increasing interest in fuel cells and some projects are underway, perhaps most notably the Viking Energy, which is to run on a 2 MW ammonia-fed SOFC [34].

The most common types of fuel cells are briefly discussed regarding their efficiency, operating temperature, power density and output, or their respective application. The alkaline fuel cell (AFC) is suitable for application in several industries due to its low production cost and relatively high efficiency [48]; however, its low power output makes it unsuitable for large marine applications. Additionally, the electrolytes of an AFC can be poisoned by CO_2 , resulting in the necessity of applying CO_2 -free fuels and oxidants [48]. The polymer electrolyte membrane fuel cell (PEMFC) has a low and high-temperature version, the latter of which will be touched upon later. The low-temperature PEMFC has an operating temperature of 50-100 °C, presents with advantageous power output and has found application in the automotive industry [128] [48]. The phosphoric acid fuel cell (PAFC), which operates at temperatures near 200 °C, has shown higher power outputs than the AFC [48], but low power densities and durability issues; therefore, it has yet to find marine application [128]. High-temperature PEMFCs have been developed by combining the technology of the aforementioned low-temperature PEMFC and PAFC to increase power density while operating at temperatures similar to PAFCs [20] [128]. The aforementioned fuel cell types all present with relatively low operating temperatures of less than 200°C; consequently, these low temperatures make them advantageous regarding startup times. The high-temperature fuel cells (HT-FC) consist of the molten carbonate fuel cell (MCFC) and the previously mentioned SOFC, which operate at temperatures of 650-700 °C and 500-1000 °C respectively [128]. These two types of fuel cells are suitable for large power outputs at high efficiencies, and have the benefit of being capable of the direct internal reforming (DIR) of fuels; additionally, these fuel cells have a significant potential for waste heat recovery due to their high operating temperatures, which stands to increase their efficiencies even further [128]. However, HT-FCs are currently still associated with high cost, low power density, slower startup, and difficulties regarding powering down [128] [48]. A schematic of an example SOFC operating on hydrogen is provided in figure 2.1, most other fuel cells operate in a somewhat similar manner.

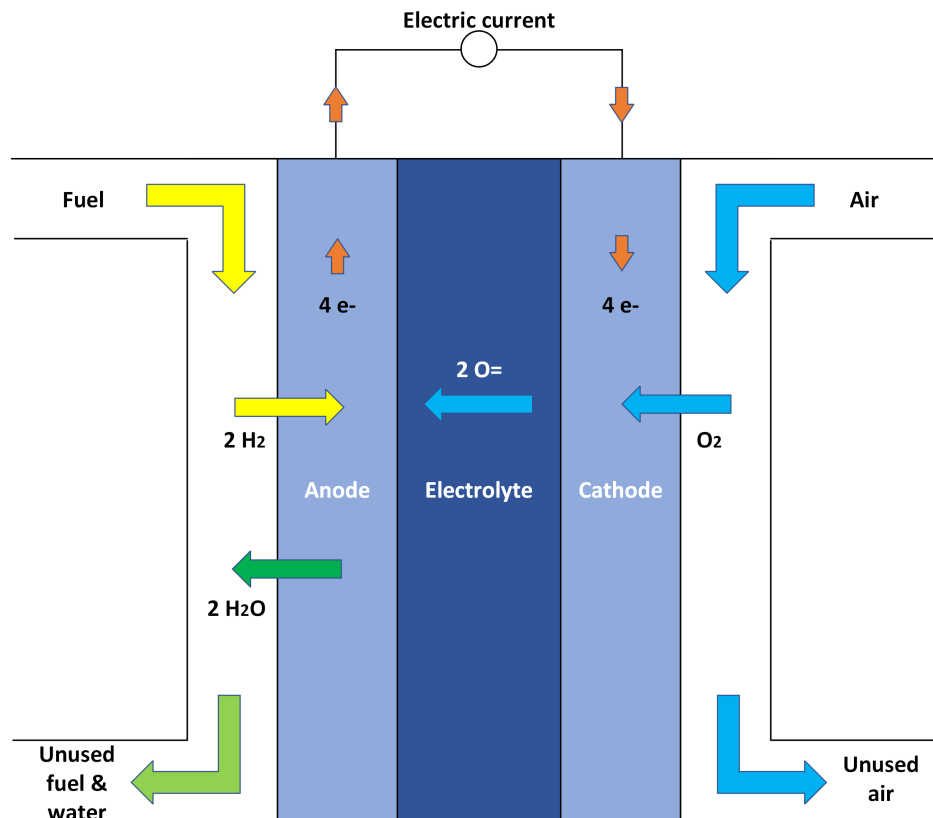


Figure 2.1: A schematic of an SOFC and its operation

2.2.4. Assisted drive

Renewable energy sources, such as wind, wave, and solar power, can be used in the propulsion of a vessel and allow for zero-emission propulsion; the technologies used for this type of propulsion will be classified as "assisted drive" due to their limited suitability for main propulsion. Since these power suppliers are dependent on renewable energy sources which are not always present for harvesting energy, assisted drive systems will most likely have to be used in combination with another type of marine power plant, such as ICEs. Of the three aforementioned renewable energy sources, solar and wind power are described below, while wave energy has been omitted due to it being relatively underdeveloped compared to the other energy sources.

Solar power

The first common renewable energy source is solar power; using photovoltaic cells to harvest energy from the sun, electricity can be generated to provide propulsion. Since the required area of photovoltaic cells needed to generate sufficient power typically surpasses the available space on a vessel, and vessels often have to operate at night or when it is cloudy, this type of power generation will have to be part of a hybrid system.

Wind power

The second renewable energy source is wind power and has worldwide application in energy production with the use of wind turbines. To harvest wind power in marine propulsion applications there are several possibilities such as wing sails, kite sails, and Flettner rotors [83]. Like solar power, these applications are dependent on the presence of sufficient wind speeds, and vessels will require additional power generation systems.

Figure 2.2 provides an overview of marine power plants and their fuel consumption classification. Stirling engines are not present in this overview, and are categorised as "Conventional fuel-consuming".

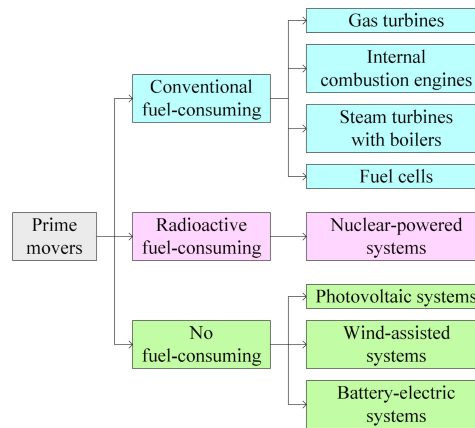


Figure 2.2: Overview of marine power plants, obtained from Xing et al. [138].

2.3. Marine fuels

Marine vessels have operated, and currently operate, on several types of fuel; from highly polluting coal to hydrogen, which only has water as a reaction product. To achieve climate goals and follow regulations, the marine industry will have to continue to operate on new and cleaner fuels. While the influence of a fuel on the waste heat production of a power plant is limited, different fuels do have widely varying characteristics that influence storage, operation, and engine efficiency; therefore, their general application and properties are touched upon. The classes of marine fuels discussed in this section encompass most fuels that are currently used, and a number of fuels that are expected to play a role in the coming years; however, not all marine fuels are discussed.

2.3.1. Marine fuel oils

Crude oil, or petroleum, is at the basis of many fuels, which are produced through refining processes. To be used as marine fuel, certain parameters are to be met, such as sulfur content, density, viscosity, and flammability or combustibility. However, sometimes direct crude oils come close to meeting these parameters, which means they can be slightly adjusted to be used as marine fuel. Marine fuel oils and their subclasses are used in internal combustion engines.

Heavy fuel oil (HFO)

Typically, crude oil is refined into other fuels to meet the aforementioned parameters. One of these refined fuels is the class of HFO, or residual fuel oil, which is the fuel of choice for most commercial vessels. Since regulations regarding sulfur content have been getting increasingly stringent, fuel oils are often differentiated by their maximum sulfur content. As of 2015 in MARPOL designated emission control areas, the use of fuels with a maximum sulfur content of 0.1% is required, and as of 2020 the maximum allowable sulfur content in fuels used outside of the emission control areas is 0.5% [21].

Blends and distillates

To comply with emission and sulfur content regulations, HFOs or residual fuel oils often get blended with other fuels or distillates. Distillates are the result of evaporated components of crude oil distillation being condensed. When a fuel oil blend consists predominantly of HFO and a small amount of distillates, it is commonly referred to as intermediate fuel oil; when it is mainly consisting of distillates and a relatively small amount of HFO it is referred to as marine diesel oil. Blends that consist entirely of distillates are categorized as marine gas oil [123].

2.3.2. Natural gas

An increasingly popular alternative to petroleum-based fuels is natural gas, which predominantly consists of methane and stands to significantly reduce CO₂, NO_x, SO_x, and PM emissions [120]. However, the combustion process currently results in the emission of methane, which is called methane slip; as methane is a stronger GHG than CO₂, there are questions of the benefit of natural gas as a marine fuel. Natural gas as a marine fuel can be stored as a liquid, also known as LNG, or as a gas, known

as compressed natural gas [30]. LNG storage requires cryogenic conditions of approximately $-162\text{ }^{\circ}\text{C}$ at atmospheric pressure [108], while compressed storage requires a pressure of approximately 250 bar [30]. Natural gas can be applied as fuel in turbines, reciprocating engines, and fuel cells. When used as a fuel in compression-ignition combustion engines, natural gas requires the aid of some pilot fuel as it has a relatively poor ignition character due to its low cetane number [52]. Additionally, marine engines on LNG carriers can be fueled using the so-called boil-off gas [30].

2.3.3. Biofuels

Biofuels are the class of fuels derived from biomass and even though their use emits carbon, they are often seen as potentially carbon neutral fuels since CO_2 was absorbed during the growth of the biomass [78]. The subdivision of biofuels can be done through the classification of their level of "generation"; namely first, second, and third [64]. First-generation biofuels are typically produced from edible feedstock, second-generation biofuels are mainly produced from non-edible feedstock, and third-generation biofuels are made from algal biomass or possibly from CO_2 sources [67]. Commonly, biofuels can be used both as primary fuels and drop-in fuels in several engine types, although in certain cases some engine modification is required. Since there are many different types of biofuel, a small selection will be discussed below.

First-generation

Two examples of first-generation biofuels are straight vegetable oil and biodiesel. The former is made from vegetable oils, and can be directly used in diesel engines that underwent slight modification [85]. Biodiesel can be made from vegetable oils as well as from animal fats, and has undergone a process called transesterification [75]. The resulting biodiesel is commonly referred to as fatty acid methyl esters, and while biodiesel performs better as a fuel than the aforementioned straight vegetable oil, it is still not entirely compatible with currently applied diesel engines [44].

Second-generation

Besides occurring naturally underground, natural gas can be produced synthetically from biomass sources [63]. This type of second-generation biofuel is known under various names such as bio-synthetic natural gas and biomethane. Biomethane is produced by improving the quality of biogas, mainly through CO_2 removal [62]; it can be applied the same way as other natural gas (see section 2.3.2). Another type of second-generation biofuel is hydrotreated vegetable oil which has vegetable oils as biomass source; it is produced by the introduction of hydrogen in a process called hydrotreating, and can be used in unmodified diesel engines [114].

Third-generation

A relatively underdeveloped biofuel is fuel derived from algae, also known as algal biofuel [64] [83]. This type of biofuel is produced through the extraction of lipids from algae, after which the lipids undergo a transesterification process, making it similar to biodiesel [67].

Other synthetic biofuels

Like natural gas, there are a number of other fuels that can be produced synthetically from biomass. Examples are ethanol, methanol, dimethyl ether (DME), and other fuels such as hydrogen; the first of which is a first-generation biofuel, while the last three are second-generation biofuels [64]. These fuels will be discussed in section 2.3.5 as they are not necessarily produced from biomass.

2.3.4. Zero-carbon fuels

Regarding emissions it would be ideal to power marine vessels with fuels that contain no carbon, and that are produced through green production processes. Unfortunately there is limited production of zero-carbon fuels, most of which are produced from fossil fuels instead of green alternatives [78].

Hydrogen

Hydrogen is considered as an ideal alternative marine fuel as it has a zero-emission potential and a high gravimetric energy density; however, it displays poor volumetric energy density because of its very low density [79]. The characteristics of hydrogen make storage complex as it has to be stored cryogenically as a liquid at temperatures in the vicinity of $-252\text{ }^{\circ}\text{C}$, or highly compressed as a gas

at approximately 800 bar [144]. The storage requirements of hydrogen result in increased size and weight of the storage system, diminishing the benefit of the high gravimetric energy density. Hydrogen can be produced from fossil fuels through steam reforming, from biomass, and through electrolysis [56]; the first of which would still make it polluting, the second pathway could be potentially carbon neutral, while the last process would result in fully green hydrogen provided renewable energy is used. Hydrogen could find application in several marine power plants such as internal combustion engines (including turbines) and fuel cells [79]. As of yet there are limited vessels operating on hydrogen, with the exception of some small fuel cell-powered ships.

Ammonia

Another fuel that is seen as a potentially green alternative marine fuel is ammonia, and there is growing interest combined with some projects to realise ammonia powered vessels [34]. As ammonia does not contain any carbon, using it as a fuel would result in no carbon emissions; however, due to its nitrogen content it could produce some harmful NO_x pollution [78]. One disadvantage of ammonia is its toxicity, and while it has been transported (for agricultural purposes) for decades, it does require additional caution when used as a fuel [79]. Compared to hydrogen, ammonia has a higher volumetric energy density and storage is much easier as it is a liquid at around -34 °C and ambient pressure, or with a pressure of 10 bar at ambient temperatures; however, ammonia does have a much lower gravimetric energy density [78]. The production pathways of ammonia are similar to those of hydrogen as it is made by combining hydrogen and nitrogen [90]; therefore, it could be a green marine fuel requiring only one additional production step compared to hydrogen. Ammonia has the potential to find its application in most marine power plants, including ICEs and fuel cells [140].

Zero-carbon hydrogen carriers

Besides the aforementioned direct use as fuel, ammonia can be used as a zero-carbon hydrogen carrier in (for example) a fuel cell before or in which the ammonia would undergo a cracking process. Ammonia is not the only possible zero-carbon hydrogen carrier, with hydrogen having the possibility to be stored in other compositions such as hydrides and boranes [26]. Typically, these types of hydrogen carriers require an additional process to obtain pure hydrogen for use. While there are several zero-carbon hydrogen carriers, for simplicity, only ammonia will be considered in this review.

Nuclear

A well known zero-emission power generation technology is nuclear power, which generates steam to drive a turbine. Its marine application is predominantly present in naval vessels as it has high initial costs and is subject to additional safety regulations; its main benefits are being air-independent, requiring infrequent refuelling, and the ability to reach high power outputs [95] [46].

2.3.5. Other fuels

As the classification of fuels often depends on production pathways, in this section a number of fuels will be discussed that can either be produced in several ways, or fall outside common fuel classes. Additionally, two alternative fuel production processes will be briefly touched upon to further demonstrate the wide variety in production pathways.

Liquefied petroleum gas (LPG)

LPG is similar to LNG, except it mainly consists of propane and butane instead of methane [138]. In contrast to LNG, LPG has better ease of storage and handling, requiring a pressure of around 8 bar at atmospheric temperatures to be liquefied [6]; however, LPG does pose additional risks regarding flammability and its higher density in case of spills [16]. Research has shown that LPG as a fuel could reduce CO₂, NO_x, SO_x, and PM significantly; additionally, unlike LNG having polluting methane slip, LPG does not produce such unwanted polluting fuel slip [16]. Because of the low cetane number and high octane number of LPG, it can best be applied in spark-ignition engines, or dual-fuel engines [6]. LPG is commonly produced as a by-product of certain fuel production and refinery processes; it can also be made through alternative production processes such as from biomass [16] [124]. Its application is thus far limited to a small number of vessels but it has the benefit of an existing infrastructure because of its widespread application in other industries [16].

Alcohols

Two potential fuels for the marine sector are ethanol and methanol as they display significant reductions in emissions; however, their lower energy density requires larger storage volumes [138] [94]. Both ethanol and methanol are produced on a large global scale for various applications, which provides them with the benefit of an existing infrastructure. While ethanol is predominantly produced from biomass feedstock through fermentation, methanol is mainly produced through steam reformation of coal and gas, but can be produced renewably from biomass, CO₂, and hydrogen [78] [94]. Methanol has found some application in both spark-ignition and compression-ignition marine engines, but poses risks regarding toxicity and flammability [44]; additionally, both ethanol and methanol have corrosive properties [94]. While ethanol has been used in blends for road transportation purposes, it has yet to find application in marine engines [138]. Even though both alcohols could be applied in fuel cells [68], in this research they will be assumed to merely serve as fuel in ICE applications.

Dimethyl ether (DME)

DME has seen increasing interest in recent years and found some application as a potential transport fuel, mainly because it shows significant decreases of emissions compared to fossil fuels [76]. Regarding storage, DME liquefies around 5 bar at atmospheric temperatures and presents equal ease of storage compared to LPG, but more complex than alcohols [76] [138]. DME is primarily derived from methanol, therefore having the same production pathway including an extra dehydration step, or DME can be produced from syngas directly; depending on the origin of the methanol or syngas, DME can be produced as a biofuel [138]. DME has a much higher cetane number than alcohols and is suitable for compression-ignition engines; it can also be applied in other power plants such as fuel cells [84].

Figure 2.3 provides an overview of the volumetric and gravimetric energy densities of various marine fuels; most, but not all, of the fuels discussed in this chapter are included.

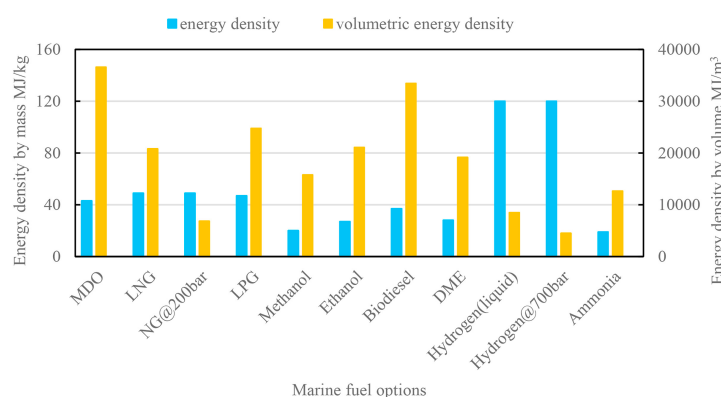


Figure 2.3: Overview of the energy densities for different marine fuels, obtained from Xing et al. [138].

Coal

Historically, coal was a widely used marine fuel to drive steam turbines; however, its high emissions and the transition of marine vessels to ICEs and HFOs left coal with extremely limited marine application.

Alternative production pathways

While many fuels are produced through oil refinery, distillation, and reforming processes, several fuels can be produced alternatively; two such processes are discussed here in short. The Fischer-Tropsch process is one of these production methods and is used to convert hydrogen and carbon monoxide into several types of hydrocarbons. The feedstocks for Fischer-Tropsch fuels are mainly produced through the gasification of coal, natural gas, but also biomass [40]. Power-to-x is another fuel production process and is used to create a wide variety of fuels using electricity. This process produces hydrogen, which can subsequently be used to produce other fuels, including hydrocarbons [135]; depending on the origin of the electricity, this process can result in cleaner (or even green) fuels.

Figure 2.4 provides an overview of possible marine fuels, including production pathways and characteristics, for ICEs and fuel cells; these fuels could also find application in other marine power plants. The most relevant, but not all of the aforementioned fuels are included.

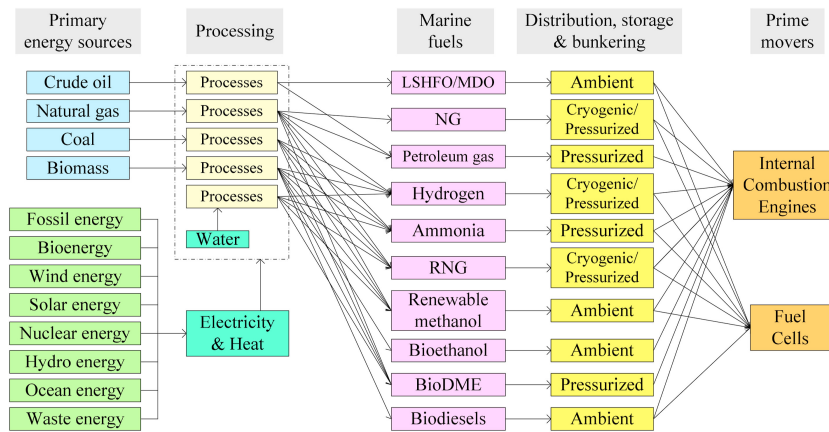


Figure 2.4: Overview of possible marine fuels and some of their characteristics, obtained from Xing et al. [138].

2.4. Waste heat recovery

Power plants are used to convert some form of energy, such as chemical energy, into mechanical energy; however, this conversion is never 100% efficient and typically produces large amounts of heat. This heat, often referred to as waste heat, is generally discarded towards the surroundings. As higher efficiencies are desirable, waste heat recovery technologies have been widely researched and applied, including in marine power plants. This section provides an overview of the most common waste heat sources in marine power plants, their waste heat potential specified through waste heat distribution and temperature, and a number of waste heat recovery systems. Not all marine power plants are considered for waste heat recovery; batteries and assisted drive technologies fall within this category. While batteries do generate some heat, they require low operating temperatures of approximately 20-55 °C and 25-45 °C for Li-ion batteries and lead-acid batteries respectively [61] [92]; therefore, their waste heat recovery potential is limited and will not be considered. Assisted drive technologies, such as sails, produce no waste heat and while other technologies, such as Flettner rotors, might produce some heat through friction, this amount is assumed insufficient for waste heat recovery; therefore, waste heat recovery of these technologies is not considered.

2.4.1. Waste heat sources

Different power plants have varying efficiencies, and the produced waste heat is unevenly distributed over several waste heat sources at different temperatures. The additional energy that can be recovered from a power plant through waste heat recovery is directly dependent on the amount of energy expelled as waste heat and its temperature. A number of waste heat sources available for waste heat recovery are discussed here, related to the power plants from section 2.2 and their energy potential in the form of waste heat distribution and temperature.

Exhaust

Most of the power plants discussed in section 2.2 expel a large part of their waste heat through the exhaust system. The amount of energy contained in and the temperature of the waste heat expelled through the exhaust of a power plant mainly depends on the type of power plant and its efficiency; however, it is also largely dependent on other factors, such as the applied type of fuel and air-fuel ratio.

Steam turbines present in various forms depending on their application; however, for simplicity, only condensing steam turbines, in which the maximum energy content of the steam is extracted, are assumed. In such a condensing steam turbine the exhaust temperature is around 30 °C; as such, there is little possibility for external waste heat recovery. In the steam turbines of a nuclear power plant, nearly 60% of all energy is lost through the steam condenser [41].

Gas turbines, in contrast to steam turbines, expel 95% of the energy that is not converted into mechanical energy through the exhaust system [131]; the exhaust gas temperatures are typically around 500-600 °C [59]. Due to the large waste heat flow and relatively high temperature, gas turbine exhaust gases are well suited for waste heat recovery.

Marine ICEs, which are typically large two-stroke diesel engines, present relatively high efficiencies;

however, still around half of all energy contained in the fuel is not converted into mechanical energy and is expelled as waste heat. According to Singh et al., a reference case of a large two-stroke marine diesel engine with an efficiency of 49.3% presents with 25.5% of all energy supplied being expelled through the exhaust [111]; the energy distribution of the reference case is shown in figure 2.5. Exhaust gas temperatures are typically in the range of 200-500 °C depending on engine type, wherein two-stroke engines produce exhaust gas temperatures in the lower part of the range and four-stroke engines in the higher part [111]. To prevent corrosion and buildup in the aftertreatment equipment, exhaust gas temperatures should not fall below a certain limit, decreasing the waste heat recovery potential; however, as the main cause of the aforementioned issues relates to sulfur content, future alternative fuels might not present this problem, subsequently allowing for increased waste heat recovery [111].

Fuel cells present in widely varying types, especially regarding their operating temperatures. For MCFCs and SOFCs, which are both HT-FCs, most of the waste heat is expelled through the exhaust by applying excess air along the cathode side [129] [128]. Due to the high operating temperatures of 650-700 °C for MCFCs, and 500-1000 °C for SOFCs, the waste heat recovery potential is high [128].

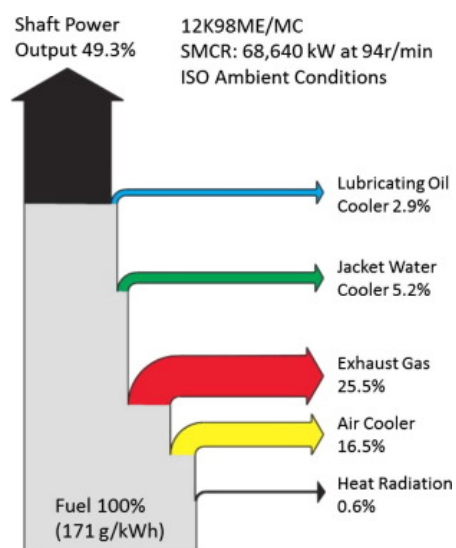


Figure 2.5: Sankey diagram of the energy distribution for a MAN 12K98ME/MC marine two-stroke diesel engine, obtained from Singh et al. [111].

Charge Air Cooling (CAC)

Reciprocating ICEs make use of compressed and cooled charge air for optimized combustion as well as for scavenging, which is a commonly used process to drive out exhaust gases from the combustion chamber while simultaneously lowering the piston temperature. Due to compression, the temperature of the air increases significantly, after which it is cooled before being supplied to the engine. The heat that is extracted through this cooling process creates a potential application for waste heat recovery [9]. Regarding the aforementioned marine diesel engine, 16.5% of all energy is lost as waste heat through CAC, with a temperature of 100-160 °C [111]. While the temperature of the charge air decreases significantly at low engine loads [143], utilisation of this waste heat source can prove advantageous [81].

Engine/jacket cooling (water)

Various marine power plants operate at a high temperature and are fitted with a cooling system in order to prevent undesirable operating conditions, or even reduced engine integrity. Such a cooling system, which is typically operated with air or water, absorbs heat from the engine (or jacket) and therefore presents an opportunity for waste heat recovery.

Again considering the marine diesel engine, 5.2% of all energy is expelled through the jacket cooling of the engine, with a waste heat temperature of 70-125 °C [111].

Stirling engines are external combustion engines, which do not produce exhaust gases themselves, and most of the energy losses occur in the regenerator due to regenerator inefficiency [121]. As engine

performance is determined by the temperature difference between the hot and cold source, it is desired to keep this temperature difference as large as possible; therefore, heat transferred to the cold source should be removed. The temperatures of the heat flows are dependent on the operation of the Stirling engine and the external combustion process; Babaelahi et al. used the specifications of the GPU-3 Stirling engine with temperatures of approximately 704 °C and 15 °C for the hot and cold source respectively [8]. As found by Babaelahi et al., around 35% of the heat addition is rejected by the cold source cooling at temperatures ranging from approximately 82 to 187 °C depending on crank angle [8].

Unlike HT-FCs, the exhaust stream of low-temperature fuel cells (LT-FC) rejects little of the heat that needs to be removed, and most of the heat must be removed using a cooling system [58]; depending on fuel cell efficiency and operating temperature, this is nearly 40% of all energy [10]. Typically, LT-FCs operate around 50-200 °C [48], which makes their waste heat recovery potential limited.

Lubrication oils

Engines that contain moving parts require lubrication oils to decrease friction, and therefore wear; in this process, the lubrication oils absorb some heat generated by the moving parts. While there is waste heat available in lubrication oils, the temperatures are quite low, and because lubrication oils should not be supplied to the engine at too low temperatures, their waste heat recovery potential is limited.

Steam and gas turbines expel nearly all of the waste heat through the exhaust, while only a small amount of generated heat is transferred to the lubrication oils. The amount of heat in the lubrication oils is only a few percent of all waste heat, and the lubrication oil temperatures are generally quite low in the range of 65-90 °C [145] [35]. Depending on the type of bearings and turbine size, the losses due to friction in a gas turbine are in the range of 0.1-4% [131]; these values are assumed to be similar for steam turbines.

For the large marine diesel engine, 2.9% of all energy is lost through the lubrication oil and its cooling [111]. As per the MAN K98ME-C6 engine specifications, lubrication oil temperatures are assumed not to exceed 70 °C [22].

The percentage of energy lost as waste heat to lubrication oils in a Stirling engine is low (<2%) and at temperatures of <90 °C; these values are approximated by assuming values similar to those of ICEs and turbines.

Radiation

Objects expel energy towards their surroundings through radiation, where higher temperatures of the source object result in more energy being expelled as radiation; this energy can be recovered if desired and sufficient energy is available. However, since the amount of heat lost through radiation is generally significantly less than through the aforementioned sources, it is often not economical to apply waste heat recovery to radiation. For example, from the large marine diesel engine only 0.6% of all energy is expelled through radiation [111]; as such, the waste heat recovery potential is very limited and will not be considered further. While diesel engines can be considered as low temperature sources, in contrast to other power plants such as turbines or SOFCs which operate at higher temperatures, relatively small waste heat losses through radiation are assumed for the other marine power plants and will therefore be omitted as well.

2.4.2. Overview of waste heat sources

Table 2.1 contains an overview of marine power plants and their respective waste heat recovery potential per source regarding waste heat percentage and temperature; the waste heat percentage, which depends on power plant efficiency, either concerns the distribution of all energy supplied by the fuel, or the percentage of the waste heat alone such as for the gas turbine exhaust. Regarding waste heat recovery potential, it is assumed that the influence of the supplied fuel is negligible compared to other factors such as power plant efficiency; additionally, radiation has been nearly completely omitted due to low waste heat recovery potential.

Table 2.1: Overview marine power plants and waste heat sources

Marine power plant	Waste heat source	Waste heat percentage	Waste heat temperature ^a
Steam turbine	Exhaust	~60% of all energy	~30 °C
	Lubrication oils	0.1-4% of all energy	< 90 °C
	Radiation	NA	NA
Gas turbine	Exhaust	95% of energy losses	500-600 °C
	Lubrication oils	0.1-4% of all energy	< 90 °C
	Radiation	NA	NA
Internal combustion engine	Exhaust	25.5% of all energy	200-500 °C
	CAC	16.5% of all energy	100-160 °C
	Jacket cooling	5.2% of all energy	70-125 °C
	Lubrication oils	2.9% of all energy	< 70 °C
	Radiation	0.6% of all energy	NA
Stirling engine	Cooler	35% of all energy	~80-190 °C
	Lubrication oils	< 2% of all energy	< 90 °C
	Radiation	NA	NA
Fuel cells	Exhaust	HT-FC: ~40% of all energy	500-1000 °C
	Jacket cooling	LT-FC: ~40% of all energy	50-200 °C ^b
	Radiation	NA	NA

^aWaste heat source temperature ranges can be categorised as low (<230 °C), medium (230-650 °C), and high (>650 °C) [119].

^bIt should be noted that the waste heat temperatures for both HT-FCs and LT-FCs are their respective operating temperatures, actual rejected waste heat temperatures are often lower.

2.4.3. Waste heat recovery systems

There is a wide variety of waste heat recovery methods of which several are discussed here. These systems have been selected based on their potential to directly generate mechanical and/or electrical power. Systems that do not directly produce power have been omitted, this includes burners, boilers, economisers, preheaters, heat exchangers, heat pipes, heat pumps, and (vapour absorption) refrigeration systems. Additionally, processes that use waste heat recovery to produce other substances, such as systems for hydrogen electrolysis and desalination, have been omitted as well.

Bottoming power cycles

Power cycles convert heat into mechanical work, the simplest ones typically consist of a compression and expansion process, while some have an additional heating and/or cooling step. When applied to current marine engines, bottoming power cycles allow for increased power plant efficiency in the range of 4-15%, but are divided regarding suitable waste heat temperatures, size, and cost [143]. Typical power cycles are the Rankine Cycle (RC), Kalina Cycle (KC), Brayton Cycle (BC), and Stirling Cycle (SC).

Of the RC-based systems, the Steam Rankine Cycle (SRC) is one of the most common bottoming power cycles applied in multiple industries, it is often combined with gas turbines in combined power production. SRC is best suited for waste heat recovery in a waste heat temperature range of 350-500 °C [111]; however, SRC systems can be operated on waste heat temperatures as low as 250 °C, limited by the vapour pressure of water, and as high as 700 °C, considering material and technological limitations [77]. When applied to current marine diesel engines, SRC systems can improve plant output with 4-8%, but generally display disadvantages due to their large size and medium cost [143].

An alternative to the SRC is the Organic Rankine Cycle (ORC), it operates using the same cycle as an SRC but it has an organic working medium typically with a low boiling point to be applied in low-grade waste heat recovery. ORC systems for current marine diesel engine waste heat recovery can improve power plant efficiency by 5-15% [143], with some research simulations even showing possible improvements of up to 20% [115]. The ORC system is applicable for waste heat temperatures between approximately 90 °C and 470 °C [111]. Compared to SRC systems, ORC systems present

with medium size but higher cost; additionally, ORC systems can make use of waste heat from multiple sources separately or combined [143].

In a Supercritical Rankine Cycle (SCRC), the working medium is supplied with a pressure above its critical pressure prior to entering the boiler in which the working medium is evaporated from the liquid state into the vapour phase directly. In contrast to an SRC or ORC system, the supercritical pressure allows the working medium to skip the two-phase region and present improved thermal matching with the waste heat, therefore increasing efficiency relative to SRC and ORC systems by approximately 5-13% and 3% respectively [111]. The waste heat temperature range suitable for SCRC systems depends heavily on the working medium; temperatures and pressures exceeding 374 °C and 220.6 bar respectively are required for steam to become supercritical, while these values are significantly lower for CO₂ with a critical point at 31 °C and 73.8 bar. For organic working media the waste heat temperature range is similar to that of ORC systems [111]. While the layout of an SCRC is similar to subcritical RCs, SCRC systems require significantly larger heat exchange surfaces and therefore increased size and cost; however, this is not the case for SCRC systems with CO₂ as the working medium [82].

Regarding the aforementioned RC-based systems, a schematic of a simple RC system is shown in figure 2.6a.

The KC is another modification of the RC and uses a mixture as the working medium; a commonly used mixture is water and ammonia, but other combinations are possible. The mixture consists of fluids with different boiling points, allowing for a better thermal match [89]; in addition, KC systems show improvements of 5-8% for current marine engines [143]. This type of cycle has increased system complexity due to additional components compared to other RCs; a simple KC additionally consists of recuperators, mixers, valves, and a separator [111]. The KC is suited for a waste heat temperature range of 200-500 °C [111]. Because of the additional equipment required in KC systems, these systems are accompanied by increased size and cost [143]; a schematic of a simple KC is shown in figure 2.6b.

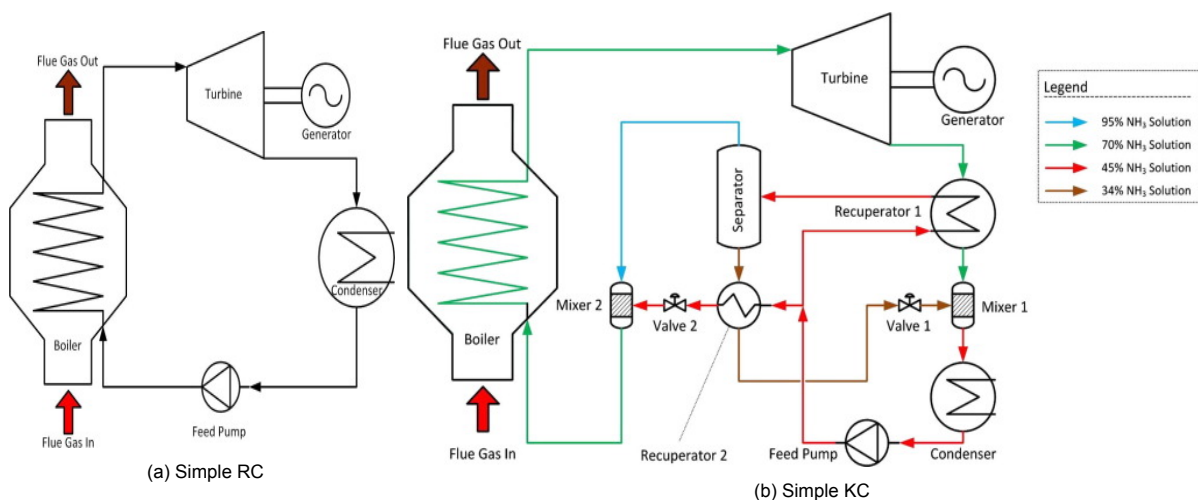


Figure 2.6: Example schematics of a simple RC and KC, obtained from Singh et al. [111]. The KC applies additional recuperators, mixers and a separator to reuse remaining heat and reject heat more efficiently from the system at the expense of increased size and complexity.

The BC can be either an open or closed system and operates on a gaseous medium, an open BC has the benefit that it can operate without requiring heat exchangers to cool the working medium after expansion [89]. A schematic of a simple open air BC is shown in figure 2.7a; a closed BC has a similar layout in which the working medium does not leave the system and is cooled prior to the compressor. When operated on air, an open BC can be referred to as an air bottoming cycle; a closed BC is typically operated on other working gases such as nitrogen, helium, or (supercritical) CO₂ [141]. In a BC, the working medium is subsequently compressed and expanded, where the turbine is fixed to the same shaft as the compressor to deliver the compressor power. The reduced equipment requirements for BC

systems means they are relatively small in size [136], and depending on the working medium they also present with low cost [113]. However, because BCs operate on a gaseous medium, they are mainly suitable for high-temperature waste heat recovery [136]. Turbine inlet temperatures of around 700 °C are common when operated on supercritical CO₂ (sCO₂) [106], with a wider range being possible; in contrast, for air BCs, temperatures typically exceed 1000 °C [106]. According to Hossain et al., a work-optimized basic sCO₂ BC for the waste heat recovery of a 17.55 MW marine engine could produce an additional 1000.96 kW of power at a waste heat temperature of 373 °C, which is an improvement of 5.7% [50]. When observing the results of Hossain et al., the work-optimized basic sCO₂ BC appears to produce approximately 2200 kW at a waste heat temperature of 600 °C, which corresponds to an improvement of ~12.5% [50].

(Supercritical/transcritical) CO₂ power cycles are closed systems and are commonly operated as an RC (transcritical) or BC (supercritical) [143]. While CO₂ power cycles are best operated at a waste heat temperature range of 240-600 °C [143], for waste heat temperatures of up to 850 °C, sCO₂ cycles can be used [77]. CO₂ based power cycles are advantageous when it comes to size and can improve current marine engine output with 8-11%, but do display downsides regarding cost requirements [143].

The SC, also known as Stirling engine, operates on a closed system with alternating compression and expansion fixed to a heat source and sink; it is mainly suitable for recovering waste heat with temperatures in excess of 300 °C [24]. Since a Stirling engine is a closed system it can be operated on several working media, the choice of which is dependent on the amount of waste heat available and its temperature; helium is very common, but other media such as air, nitrogen, and hydrogen are possible as well [24] [19]. Stirling engines for waste heat recovery are advantageous due to their wide operating temperature range and small size, combined with ease of maintenance [19]; however, especially when operated on helium or hydrogen, the cost becomes significantly higher [45]. In figure 2.7b, a schematic of an SC is shown. Hirata et al. discussed a Stirling engine for waste heat recovery of a large marine vessel and came to an ideal efficiency of approximately 3.5% (of main engine power) for exhaust gas temperatures of 400 °C [45]. Rokni investigated an SOFC-Stirling engine combined plant and found the efficiency to increase by 6.1-7.1% with respect to a standalone SOFC plant [99].

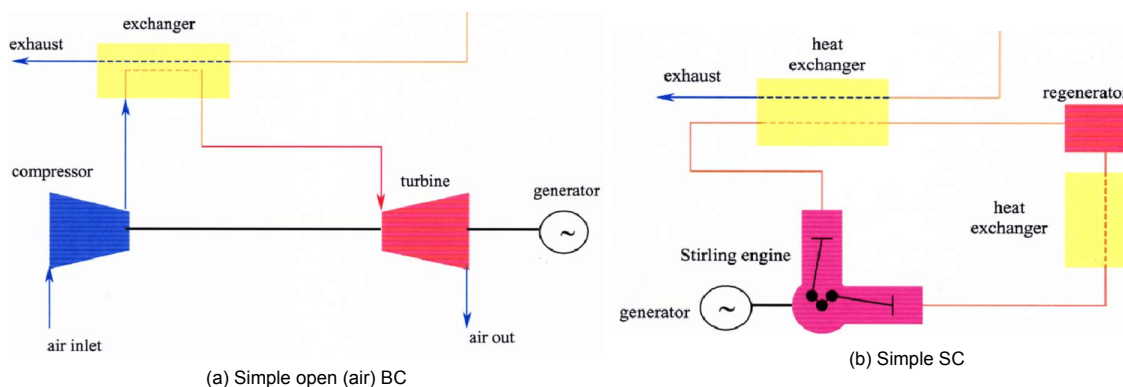


Figure 2.7: Example schematics of a simple BC and SC, obtained from Poullikkas [93] (modified).

Power turbine (PT)

Powered by waste heat, PTs can directly supply generated power to an engine output shaft to increase efficiency, this is also known as turbocompounding. The PT can be placed directly in the exhaust stream as an exhaust gas turbine, converting some of the high pressure exhaust energy into mechanical work; it may also be applied in series or parallel with a turbocharger. Even though PT systems are significantly small in size and low in cost, they show low efficiency improvements of 3-5% when applied to current marine engines, as well as requiring high engine loads and high waste heat temperatures for operation [143]. A schematic of an exhaust PT for waste heat recovery is shown in figure 2.8; the system can also be fitted directly to the engine exhaust in case the engine is not turbocharged. As engine exhausts typically have a lower temperature limit of 200 °C, this is assumed to be the minimum waste heat temperature.

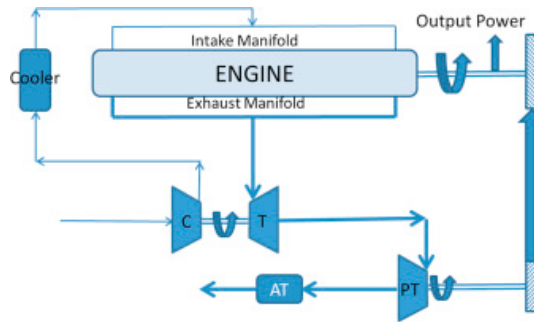


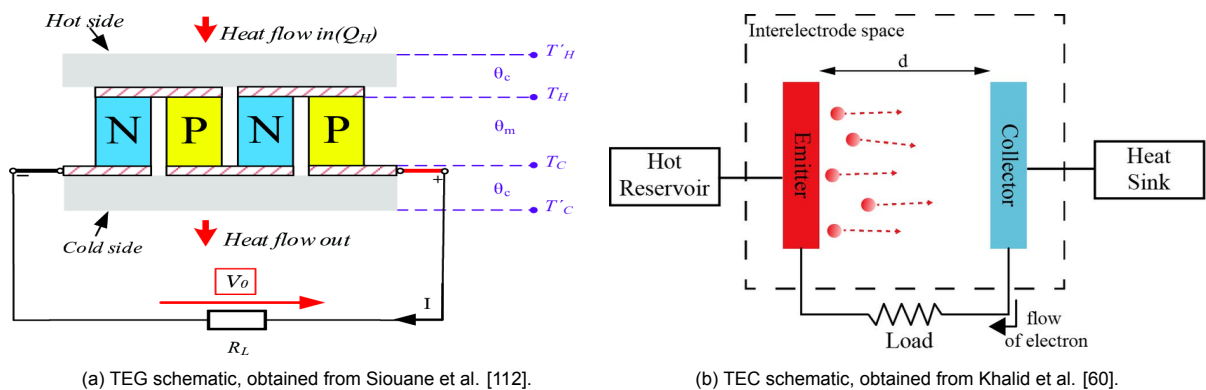
Figure 2.8: Example of a conventional turbocharged system with turbocompounding for an ICE, obtained from Aghaali et al. [2].

Direct electrical conversion devices

The class of direct electrical conversion devices convert mechanical energy or heat directly into electricity. While these devices are compact in size, they often present disadvantages regarding efficiencies, cost, and application [55]; nonetheless, thermoelectric, piezoelectric, thermionic, and thermophotovoltaic generators will be briefly discussed here.

Thermoelectric generators (TEG) produce electricity due to the Seebeck effect, in which a temperature gradient between two different semiconducting surfaces results in an electrical current [57]; a schematic of a TEG module is shown in figure 2.9a. These devices have seen little application yet due to their relatively low efficiency, allowing for approximately 2-5% in fuel savings from diesel engines [109]. Additionally, TEGs historically present with high cost [72]; however, inroads have been made to increase efficiency using nanotechnology [57]. TEG systems for waste heat recovery are suitable for waste heat temperatures of 150-500 °C and present advantages regarding reliability and lack of moving parts [111]. Additionally, TEG systems are fully scalable and therefore have few barriers regarding size [109].

Similar to TEGs, thermionic energy converters (TEC) also produce an electrical current due to temperature differences; however, these devices operate on the principle of electron emissions between two electrodes across an inter-electrode space containing either a vacuum or a vapour [60]. While TECs are scalable and compact devices [132], they are associated with high cost [137]. One electrode is heated which cause it to emit electrons, while the other electrode is held at a low temperature and receives the electrons [60]; a schematic of a TEC module is shown in figure 2.9b. TECs are mainly applicable in high temperature systems of around 1000 °C and show low efficiencies, although advancements to improve this technology are being investigated [55] [57]. Research on TEC systems for low temperature waste heat has been conducted, but efficiencies are still limited [71]. Thermal efficiencies in the range of 10-20% have been achieved [110]; additionally, due to TECs having advantageous power densities, complete system power densities can be increased by up to 33% [51]; however, no power output improvement relative to a main engine could be provided.



(a) TEG schematic, obtained from Siouane et al. [112].

(b) TEC schematic, obtained from Khalid et al. [60].

Figure 2.9: Example schematics of a TEG and TEC module.

Piezoelectric generators (PEG) are comprised of materials that produce electricity when undergoing a deformation [101]; the deformations can be caused by vibrations of moving parts or flows. For waste heat recovery applications, and specifically for flows, PEGs consist of thin-film membranes [57]. These devices present very low efficiencies of approximately 1%, high cost, and present complications regarding durability and reliability [27] [57]; a schematic of a PEG is shown in figure 2.10a. PEGs find their application in small power output systems [101], and are suitable for low temperatures in the range of 100-150 °C [55].

Thermophotovoltaic (TPV) generators produce electricity from radiation, and consist of an emitter which produces electromagnetic radiation when heated, a filter, and a photovoltaic cell which converts the electromagnetic radiation into an electrical current [7]; a schematic of a TPV generator is shown in figure 2.10b. The radiation produced by the emitter is highly dependent on the temperature of the emitter, as it is scaled to the fourth power of the temperature [32]; heat source temperatures of 1000-1500 °C are best suited for the use of TPV generators [125], and they are therefore often found in industrial high-temperature processes. Since TPV generators require high-temperature heat sources, there has been conducted little to no research on TPV generators for waste heat recovery of propulsion systems; however, for industrial waste heat recovery, electrical efficiencies of 6-19% are achievable [12]. TPV generators can display significant efficiencies dependent on the photovoltaic cells used; the cost of the system depends on the type of photovoltaic cell used. To prevent loss of efficiency by the photovoltaic cell heating up, specific (costly) materials such as semiconductors should be employed [32].

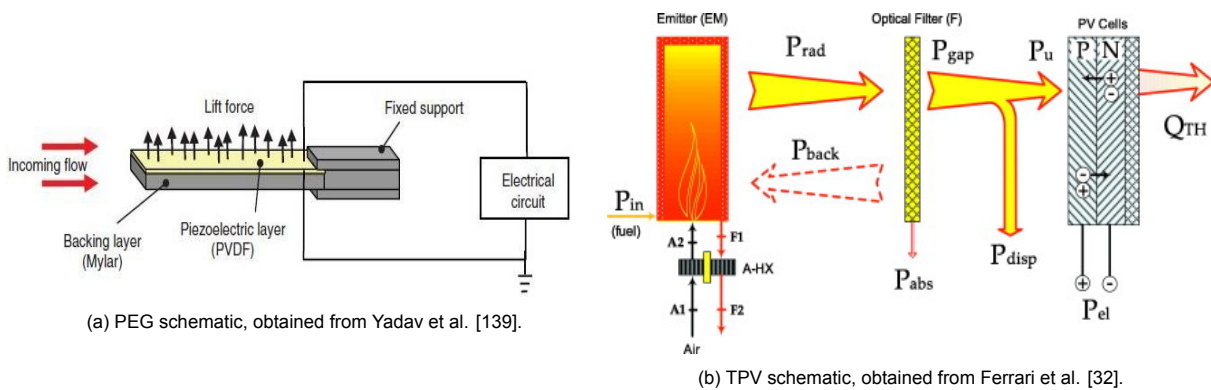


Figure 2.10: Example schematics of a PEG and TPV module.

2.4.4. Overview of waste heat recovery systems

Table 2.2 shows an overview of the aforementioned waste heat recovery systems regarding their size, cost, working media, and typical operating temperature range.

Table 2.2: An overview of waste heat recovery systems and their characteristics.

Waste heat recovery system	Specific size	Specific cost	Working medium	Temperature
SRC	Large	Medium	Water	350-500 °C ^a
ORC	Medium	High	Variable	90-470 °C
SCRC	Large	High	Variable	~90-470 °C
KC	Large	High	Water-NH ₃	200-500 °C
BC	Small	Low ^b	Variable	~700 °C & ^c > 1000 °C
CO ₂ cycle	Small	Medium	CO ₂	240-600 °C
SC	Small	High	Helium etc.	> 300 °C
PT	Very small	Very low	Exhaust gas	> 200 °C
TEG	Small	High	Semiconducting materials	150-500 °C
TEC	Small	High	Vacuum or vapour	~1000 °C
PEG	Small	High	Thin-film membrane	100-150 °C
TPV	Small	Medium	NA ^d	1000-1500 °C

^aThe maximum temperature range is approximately 250-700 °C [77].

^bWhen applied as an air BC, other working media such as sCO₂ can present with higher costs.

^cFor an sCO₂ and air BC, respectively [106].

^dWhile not technically a working medium, variances do occur in the type of photovoltaic cell used.

3

The future of marine propulsion

Potential future scenarios for the maritime industry, regarding power plants and fuels, and their suitable options for waste heat recovery, are plenty. In this chapter, an estimation of promising and high potential marine power plants and fuels, as well as waste heat sources and waste heat recovery systems, will be made through an evaluation based on relevant selection criteria. The purpose of this evaluation is to refine and filter the different components of marine propulsion and waste heat recovery, which will allow for a well-substantiated research area to be determined in the next chapter. First, the selection criteria will be briefly explained after which each component is discussed and evaluated separately; finally, a preliminary scope for the subsequent research will be presented.

3.1. Marine power plant evaluation

Power plant efficiency has been leading for the choice of marine propulsion system, which is why large two-stroke diesel engines with efficiencies around 50% have become the dominant marine power plant in large ocean-going vessels; therefore, this is adopted as the first selection criterion. The second selection criterion is the measure of application of a marine power plant; this regards both current application and the likelihood of future application. The latter is estimated based on perceived public and scientific interest; however, the likelihood of future application is inherently uncertain and therefore difficult to estimate.

Steam and gas turbines, without additional cycles, present moderate to low efficiencies respectively, and are especially disadvantageous at low load levels [96]. Mainly as a result of their limited efficiency, turbines find relatively little application in the maritime industry, which is assumed to remain that way as they have been around for a significant amount of time without sufficiently competing with ICEs. In contrast to turbines, ICEs currently dominate the maritime industry due to their relatively high efficiencies [29]; however, while they will likely continue to find significant application in the future, they might experience a decrease as the energy transition progresses. Stirling engines require external combustion, and despite presenting decent efficiencies themselves, the external combustion process causes the overall system efficiency to decrease; in addition, they can be associated with disadvantages regarding cost and life span [116]. As marine prime movers Stirling engines have found little application, which is assumed to go unchanged.

Belonging to a different category, batteries are energy storage devices which, while displaying high charging efficiencies, do not present a conversion efficiency. They currently find limited application as primary marine power plants due to barriers regarding low power capacity [134]; however, increased application for supporting power is likely. Not operating on any fuel in the general sense, whether batteries present with clean propulsion depends on the origin of the stored electricity. Fuel cells can be seen as continuous batteries, and as they are not limited by the Carnot efficiency, they can present with even higher efficiencies than ICEs [128]. While current application of fuel cells is severely limited, interest in these power plants has seen an increase and they can be considered as a likely candidate in the future of marine propulsion.

Due to low power outputs and weather dependencies, assisted drive technologies are not considered to be suitable prime movers for marine vessels; however, they may find increased application to improve fuel economy. Assisted drive is considered green and does not operate on any fuel in the general sense.

3.2. Marine fuel evaluation

Alternative (green) marine fuels are being increasingly investigated in response to climate change and emission regulations; therefore, the first selection criterion for marine fuels are its associated emissions. The second criterion is the application of fuels in marine power plants, both currently and in the future; this criterion includes to some extent climate impact, cost, and ease-of-use related to storage, distribution, bunkering, and safety. Similar to the application criterion of marine power plants, the likelihood of future application is inherently uncertain and difficult to estimate.

Fuel oils and their use are causing a lot of negative emissions of CO₂, SO_x, NO_x, and PM, which is why the maritime industry is investigating the use of alternative fuels. Currently, fuel oils are the dominant choice for marine application due to their low cost and advantageous ease-of-use, which is likely to remain for quite some time. However, the pursuit of climate change mitigation will undoubtedly result in the decreased appreciation of fuel oils. A relatively recent development in marine fuels is the move away from fuel oils through the application of (liquefied) natural gas, which has the benefit of showing decreased emissions compared to fuel oils [120]; however, it does result in methane slip, which is a very potent GHG. Furthermore, while natural gas has a higher cost than fuel oils in addition to having moderate ease-of-use due to storage complexities, the cost is still significantly lower than alternative fuels such as synthetic and zero-carbon fuels. Finally, natural gas has seen an increase in application recently which is expected to continue to a certain extent; however, similar to fuel oils, natural gas still presents with negative emissions and does not fit well into a climate neutral future.

Whether a fuel is in fact carbon-neutral depends on the life cycle of the fuel, including production, transport, and use. To be an actual carbon-neutral fuel, the well-to-wake net carbon emissions should be zero. Biofuels are commonly considered to be carbon-neutral and therefore advantageous regarding emissions [78]; additionally, depending on the type of biofuel, they can be applied to most fuel-consuming power plants. When compared to their fossil-fuel counterparts, biofuels are more expensive due to their more complex production, but they present with similar ease-of-use. Several manufacturers have developed marine ICEs that can operate on biofuels as (drop-in) fuel; however, while future application is expected, it has yet to occur on a large scale [44].

In contrast to the aforementioned fuels, zero-carbon fuels result in no CO₂ emissions, and are therefore considered as desirable future marine fuels; while hydrogen and ammonia produce no carbon emissions on board, their application may still result in harmful NO_x emissions. Apart from nuclear energy, which is exclusively applied in steam turbines, zero-carbon fuels are commonly associated with application in fuel cells [79]; however, other options such as hydrogen fuelled turbines and ICEs are being investigated as well. The main downside of zero-carbon fuels is their high cost, although for hydrogen and ammonia this is expected to decrease with increased production and application. Additionally, zero-carbon fuels have decreased ease-of-use [78]; amongst the barriers are the storage complexity of hydrogen, the toxicity of ammonia, and nuclear energy being inherently controversial. As a zero-carbon fuel, nuclear energy has seen naval applications, but large scale future application is uncertain, in contrast to hydrogen and ammonia which have seen little to no marine application, but are expected to see a significant increase.

Compared to natural gas, LPG shows some increase in emissions, slightly decreased cost, and increased ease-of-use regarding storage; however, bunkering, safety, and distribution require some attention [6] [16]. Current application of LPG is limited, and while it is expected to increase in the near future, similar to LNG, its negative climate impact makes it an undesirable fuel in a climate neutral future. Similarly, methanol and ethanol present with comparable emissions as those of natural gas and LPG, but are currently associated with higher costs and decreased ease-of-use [44] [94]. These fuels have experienced little application, but are considered as possible transitioning (drop-in) fuels and will therefore see a potential increase in application; however, their application in the (far) future is expected to be limited due to their climate impact. DME has emissions comparable to those of methanol, but does present with a slight decreased ease-of-use regarding storage, as well as increased cost since

it is commonly produced from methanol [138]. Application of DME as a marine fuel is virtually non-existent, and while it is often considered a suitable and significantly cleaner fuel, its future application is assumed similar to other fuels such as methanol. While the aforementioned fuels could potentially be produced synthetically or as a biofuel, which would allow them to be classified as carbon-neutral depending on the life cycle of the fuel, they are not considered as such unless stated otherwise.

Finally, while coal was historically a common marine fuel, due to its climate impact it no longer is and will be assumed to remain without application. As a fuel however, it is associated with low costs and advantageous ease-of-use.

3.3. Waste heat source evaluation

Marine power plants have various waste heat sources which expel wasted energy at different quantities and in different forms. The amount of waste heat and the possible extraction of said waste heat is summarised as the potential, which is the first criterion in the selection of waste heat sources. The second criterion is the temperature of the waste heat, which determines in part the available energy that can be recovered and its ease of extraction.

In several power plants, most of the waste heat is expelled through the exhaust, both in quantity and temperature range; this applies to steam and gas turbines, ICEs, and HT-FCs. As provided previously in table 2.1, HT-FCs expel waste heat through the exhaust at the highest temperatures, followed by gas turbines, then ICEs, and finally steam turbines. Although steam turbines, specifically those of the condensing type, expel most of the waste heat through the exhaust [41], temperatures are very low and unsuitable for waste heat recovery.

Scavenging, and thus CAC, is only applied in ICEs, but accounts for a significant amount of waste heat [111]; however, the waste heat temperatures are low and the waste heat recovery potential is limited. Engine (jacket) cooling is required in ICEs, Stirling engines, and LT-FCs; for Stirling engines and LT-FCs this accounts for the main body of waste heat, while for ICEs it only accounts for a few percent. Typical waste heat temperatures of engine cooling are low, but as the process is commonly conducted through heat exchangers and cooling liquids, there is some waste heat recovery potential.

Lubrication oils applied in power plants with moving parts often require cooling; therefore, steam and gas turbines, ICEs, and Stirling engines lose energy through this type of waste heat. The percentage of the energy, with respect to the amount of energy converted by the entire fuel consumption process, expelled as waste heat through the cooling of the lubrication oils, is low, as well as the waste heat temperatures; therefore, the waste heat recovery potential is very limited. Finally, while nearly all marine power plants, apart from assisted drive technologies, expel waste heat through radiation, the amount of waste heat is thus far limited that recovery is considered uneconomical.

The aforementioned characteristics and specifics of the waste heat sources were more extensively discussed in section 2.4.1.

3.4. Waste heat recovery system evaluation

When it comes to the selection of a waste heat recovery system, an important factor is the efficiency improvement that a system can provide; therefore, this is the first selection criterion for the choice of waste heat recovery system. Spatial planning is an important factor in the design of marine vessels, as it is desired to have a much space as possible for the transportation of goods or other equipment, in addition to keeping the weight limited; therefore, the second selection criterion for waste heat recovery systems is their associated size. Waste heat recovery is typically applied to improve efficiency and decrease fuel consumption, with a view to decrease cost and/or emissions; therefore, cost is the final selection criterion used to evaluate whether a waste heat recovery system is economical to apply. The following discussion and remarks are based on the literature reviewed and summarised in section 2.4.3.

Power cycles show varying levels of power output improvements with respect to standalone main engine output, this percentage can get as high as 15% when applied to current marine diesel engines [143]. Due to equipment size, SRCs, SCRCs, and KCs are commonly large, while ORCs can be considered medium sized, and BCs, CO₂ cycles, and SCs can be more compact; it should be noted that the size is a result of the equipment requirements which are, amongst others, dependent on cycle configuration and the working medium. Most power cycles are relatively expensive, such as ORCs,

SCRCs, KCs, and SCs; other cycles such as SRCs, and CO₂ cycles, can present with medium cost, while BCs can present with relatively low cost requirements depending on the working medium.

PTs display relatively low improvements for current marine engines of 3-5% compared to main engine output, and require a significant waste heat flow; however, since they operate directly on exhaust gases and typically have little added equipment, they are small in size and low in cost. Finally, direct electrical conversion devices find little application in marine waste heat recovery; amongst others, this is due to the low power output improvements of only a few percent and high associated costs. The main benefit of direct electrical conversion devices is that they are singular and modular, because of which they can be relatively small depending on the amount and distribution of the energy to be recovered and are easily scalable.

3.4.1. Waste heat recovery system variations & dependencies

Waste heat recovery systems are often presented with a wide range of variations to improve their efficiency; amongst others, these variations include equipment choice, added cycles and modifications, and the state of the working medium. Other aspects that influences the functioning of a waste heat recovery system are the operating conditions, such as ambient conditions and the amount of waste heat and its temperature, which are related to the type of marine power plant and engine power output. The configuration and operating conditions of a waste heat recovery system influences efficiency, cost, size, and more; however, for simplicity, only the basic forms of waste heat recovery systems have been discussed, and no specific operating conditions have been assumed.

3.5. Overview of evaluation

Table 3.1 contains a complete overview of the conducted evaluation of power plants, fuels, waste heat sources, and waste heat recovery systems. Each of these four is followed by the selection criteria used to filter out combinations that present limited future application and potential. The colouring denotes the (dis)advantages of the different components as summarised in this chapter, where red corresponds to scoring poorly, yellow to scoring moderately, and green to scoring satisfactorily.

Table 3.1: Overview of the evaluation of marine power plants, marine fuels, waste heat sources, and waste heat recovery systems. Here, red=poorly, yellow=moderately, and green=satisfactorily.

Power plant	Efficiency	Application ^a	
Steam turbine			
Gas turbine			
ICE			
Stirling engine			
Batteries	NA ^b		
Fuel cells			^c
Assisted drive	NA ^d		
Fuel ^e	Emissions	Application ^f	
Fuel oils			
Natural gas			
Biofuels	^g		
Zero-carbon fuels			
LPG			
Alcohols			
DME			
Coal			
Waste heat source	Potential ^h	Temperature	
Exhaust			
CAC			
Engine cooling	ⁱ		
Lubrication oils			
Radiation			NA ^j
Waste heat recovery system	Improvement	Size	Cost
Power cycles		Variable	Variable
Power turbines			
Direct Electrical Conversion Devices		^k	

^aRegarding current and/or future application; additional considerations, such as operational characteristics, may be involved.

^bBatteries present with conversion efficiencies, which are not assumed a comparable measure to conversion efficiencies.

^cThe application of fuel cells in marine propulsion is currently very limited; however, they are being increasingly investigated as future marine power plants.

^dAssisted drive technologies are commonly measured by their improvement related to the decreased requirement of main engine output; however, this is not assumed a comparable measure to conversion efficiency.

^eNG, LPG, alcohols, and DME are assumed to be produced from fossil feedstock.

^fRegarding current and future application; additionally, climate impact and ease-of-use regarding storage, distribution, bunkering, and safety, have been considered as well.

^gWhen assumed to be fully carbon-neutral (well-to-wake).

^hWith respect to the amount of energy in the waste heat and the expected ease of extraction.

ⁱThe amount of energy is dependent on the type of power plant; however, engine cooling is considered consistent and dense.

^jThe amount of energy radiated depends on the temperature of the body, which differs substantially per power plant; therefore, the temperature of this waste heat source is omitted.

^kThese devices being modular and therefore scalable, the system size depends on amount of heat to be recovered.

3.6. Scope of research

To determine a relevant scope for the subsequent research, this section summarises the previous evaluations followed by a choice of power plants, fuels, waste heat sources and recovery systems, which have presented with high potential for marine application.

Steam and gas turbines, and Stirling engines have relatively low efficiencies, and currently limited application as marine power plants; as the efficiencies and marine application of these power plants are assumed to go unchanged, these power plants are omitted from further investigation. While batteries can be considered green depending on the origin of the electricity, they are excluded from the remainder of this research due to current barriers regarding power capacity, which limits their application as the prime source of power. Assisted drive technologies are also unsuitable to become main propulsion systems, and can therefore be omitted. Additionally, both batteries and assisted drive technologies present very limited waste heat recovery potential. The conclusion is that ICEs and fuel cells will both play a large role in marine propulsion, both in the near as well as further future. While ICEs are the dominant choice of power plant at the moment, which is expected to remain that way for the coming years, the growing interest in fuel cells as marine power plants speaks for its high future potential. The downside of fuel cells is that they, and their fuels (such as hydrogen), are currently expensive compared to ICEs operating on fuel oils; however, the cost of fuel cells and alternative fuels is expected to decrease. Due to their high efficiency and zero-emission potential, and the aforementioned points of interest, fuel cells will be the focus of this research. In addition, compared to ICEs and other common power plants, fuel cells as marine power plants and their potential for waste heat recovery has been investigated significantly less.

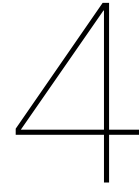
Fuel oils are currently dominating marine propulsion, and while this is expected to remain the case in the near future, the maritime industry is likely to transition to carbon-neutral or even zero-carbon fuels. This is due to the fact that fuel oils are associated with high emissions, which makes long term application undesirable from a climate mitigation perspective; therefore, these fuels are excluded from further research. Natural gas, LPG, alcohols, and DME, when produced from fossil fuels, are cleaner than fuel oils but still cause undesirable emissions, in addition to being more expensive than fuel oils. While these fuels can be expected to find increased application and are good options for the transition towards the cleaner biofuels and eventually to zero-carbon fuels, due to their emissions they are excluded from further research as well. Carbon-neutral biofuels and zero-carbon fuels, such as hydrogen and ammonia are the most sustainable option. Between the two classes, the latter has recently received significant interest as potential future marine fuels, partially regarding their fuel cell application; therefore, these will receive further attention. Nuclear energy, while being zero-carbon, is a very expensive and politically challenging fuel, it is therefore excluded due to its unlikely future application. Coal has high emissions and while it found wide application historically, it is expected to find no future application; therefore, it is omitted from further consideration.

It can be concluded that exhaust gases, CAC, and engine cooling are the sources that allow for maximum waste heat recovery; however, it should be noted that CAC is only applicable in ICEs. Between exhaust gases and engine cooling, the source of waste heat that allows for maximum waste heat recovery depends on the related power plant; when looking at fuel cells, LT-FCs can be optimized by recovering engine cooling waste heat, while for HT-FCs this should be done using exhaust waste heat. Lubrication oils and radiation present with limited waste heat in terms of quantity and temperature; therefore, these sources of waste heat are considered uneconomical and will be omitted.

Of the waste heat recovery systems, power cycles can present superior improvement over PTs and direct electrical conversion devices; however, the size and cost of power cycles is highly dependent on the chosen power cycle. A PT can be a suitable waste heat recovery system if small improvements are acceptable and small size and low cost are desired. Both power cycles and PTs can be applied to HT-FCs, while only power cycles can provide waste heat recovery from LT-FCs. Direct electrical conversion devices perform the worst due to them showing very small improvements while being high in cost; additionally, while they are modular, system sizes can be large depending on the number of modules required for sufficient waste heat recovery. Research to improve the efficiency and associated cost of direct electrical conversion devices is ongoing; however, these waste heat recovery systems are currently inferior to power cycles and the PT, and are henceforth excluded from this research.

3.6.1. Summary

The results of the evaluation point towards the high future potential of fuel cells, especially when considering efficiencies, these types of power plants are unparalleled. Combined with zero-carbon fuels such as hydrogen or ammonia, fuel cells would allow for clean marine propulsion and support climate change mitigation efforts. Waste heat recovery can be applied to increase system efficiency, which may result in physical benefits such as improved power density, as well as economical benefits. Depending on the type of fuel cell, waste heat recovery should be applied to exhaust gases or engine cooling; the most suitable waste heat recovery systems for this purpose are power cycles and the PT. In the next chapter, these results will be used to determine a specific case study to be further researched.



Research objective

In the previous chapters, this study has provided a general overview of historical, current, and future marine propulsion and the possibilities with respect to waste heat recovery. It serves as both an extensive summary of the various components and their characteristics, as well as a guide to relevant considerations regarding marine propulsion and waste heat recovery. Additionally, it forms the basis from which a promising area of waste heat recovery in marine applications can be determined to investigate further. In this chapter, first the problem statement will be described, and a case study is chosen which is considered to be a potential future marine power plant. Subsequently, the research questions to be answered are presented followed by the methodology to approach the investigation on the topic of waste heat recovery. The subsequent chapters will focus on evaluating the application of waste heat recovery to the case study.

4.1. Problem statement

The future of marine propulsion is uncertain, and while the mitigation of climate change demands a change of the status quo, it is not clear which marine power plants and fuels will dominate. One possibility is a transition of ICEs towards fuel cells, specifically SOFCs, supplied with a zero-carbon fuel such as ammonia. However, fuel cells and alternative fuels are significantly more expensive than ICEs and fuel oils, which is why the latter still dominate the industry. The costs associated with alternative fuels currently present a barrier; therefore, waste heat recovery can provide incentive for faster transition towards cleaner alternatives by increasing system efficiency of a marine power plant, resulting in improved fuel economy and a decrease in operational expenses. However, in marine applications, specifically those of a smaller vessels, spatial considerations are highly relevant, and besides system efficiency and cost, the size associated with additional systems such as those for waste heat recovery is a limiting factor.

Therefore, to determine the benefit of applying waste heat recovery to a case study, a number of parameters are relevant. Firstly, the efficiency of the waste heat recovery system, which translates to decreased fuel consumption and cost. Secondly, the size of the system, which as previously mentioned is an important consideration, especially in marine applications. And thirdly, the cost of the system, which in combination with the cost savings resulting from decreased fuel consumption ultimately determines its economic feasibility.

4.2. Case study

The previous chapter evaluated the potential of marine power plants for the future, and while it is not certain whether fuel cells will become common marine power plants, interest and research into this possibility have been increasing. Therefore, to investigate waste heat recovery in future marine applications, a case study of a vessel powered by a fuel cell system will be applied. To further specify the case study, the choice is made to select the power output of the fuel cell system, which will later on allow for an approximation of the amount of waste heat available. While power plants in marine vessels present with a wide range of power outputs of up to tens of megawatts, fuel cell systems capable of

this power output are uncommon; therefore, a relatively low power output of approximately 2 MW is chosen to encompass the first class of vessels likely to be equipped with fuel cells.

Out of the various types of fuel cells, MCFCs, PEMFCs and SOFCs have experienced the most attention for marine application. Of these, PEMFCs have superior transient capabilities compared to the HT-FCs; however, HT-FCs, and especially SOFCs, show increased efficiency and their high operating temperature creates a better waste heat recovery potential than that of PEMFCs. Due to its superior efficiency and higher waste heat recovery potential, an SOFC is chosen as the marine power plant for this case study. SOFCs expel nearly all waste heat through the exhaust, and as such, this is the only waste heat source which will be investigated in this study. The aforementioned fuel cell power output of 2 MW will not be applied as a direct input parameter in the subsequent investigation; however, it will be used to estimate the SOFC exhaust gas mass flow rate, which will be further explained later on.

Another benefit of SOFCs is that they can be operated on several fuels, including carbon-based fuels; however, with respect to climate mitigation policies, the most desirable fuels would be hydrogen and ammonia. The latter of which presents with a higher volumetric energy density and thus lower storage volume requirements, allowing for longer sailing times; in addition, the required storage conditions of ammonia are superior to those of hydrogen. Finally, while ammonia can be cracked prior to entering the fuel cell, the high operating temperatures of SOFCs would even allow a direct supply followed by internal decomposition. In this study, the influence of the type of fuel on the waste heat recovery will not be considered; however, (direct) ammonia SOFCs are considered to be highly promising future marine power plants.

To summarise, this research will be conducted at the hand of a case study for a marine vessel fitted with a solid oxide fuel cell system capable of delivering approximately 2 MW of power output.

4.2.1. In literature

There have been interesting studies into the application of SOFCs in marine applications, as well as the waste heat recovery of SOFCs.

Regarding marine applications, van Biert et al. [128] investigated the potential of fuel cells in marine vessels, and concluded amongst others that SOFCs are better suited than PEMFCs when longer refuelling intervals are required. And an optimization of the component sizing of a natural gas fuelled SOFC, gas engine, and battery for marine propulsion, conducted by Haseltalab et al. [42], displayed significant fuel consumption reductions through the application of the SOFC. Finally, a natural gas fuelled combined SOFC-ICE marine power plant was developed and evaluated by Sapra et al. [104].

Regarding the waste heat recovery of SOFCs, Schöffner et al. [106] investigated a sCO₂ Brayton bottoming cycle for a methane fed SOFC. And Al-Hamed et al. [4] investigated combined waste heat recovery for a large direct ammonia SOFC in electric rail transportation, which resulted in significant system efficiencies.

There has also been some research into waste heat recovery of marine SOFCs, with Ghirardo et al. [36] having studied the application of waste heat recovery to a methanol fed SOFC for auxiliary marine power production. And similar investigations of waste heat recovery cascades for a natural gas fuelled SOFC for marine applications were conducted by Ouyang et al. [87] [88].

From literature it is evident SOFCs can prove an interesting alternative marine power plant and allow for increased efficiencies through waste heat recovery; however, no research has been found applying a case study to investigate various possibilities in the waste heat recovery of a large marine SOFC as the main propulsion system.

4.3. Research questions

To structure the investigation of waste heat recovery when applied to a vessel powered by an SOFC, a main research question and supporting sub-research questions have been designed. Combining the answers to the sub-research questions will provide the overarching answer to the main research question.

4.3.1. Main research question

The following main research question is presented to summarise the goal of this study, which is to conduct a thermo-economic evaluation of waste heat recovery technologies for future high-temperature marine SOFCs:

- *"How can a process-oriented approach be developed and executed to evaluate the efficiency, size, and cost of various waste heat recovery technologies when applied to a marine vessel powered by a 2MW SOFC?"*

4.3.2. Sub-research questions

Throughout the research, various sub-questions will be answered, this will subsequently result in answering the main research question. The sub-research questions are as follows:

- *"Which waste heat recovery technologies are most likely to present with high suitability for application in a marine SOFC?"*
- *"What is the efficiency of the waste heat recovery technologies when applied to the case study?"*
- *"How do the waste heat recovery technologies perform regarding spatial considerations?"*
- *"How do the waste heat recovery technologies compare from an economic point of view?"*

4.4. Planned approach & methodology

In this section, the approach and methodology to answering the main research question is presented. The research will be conducted according to a number of steps, through which each sub-question will be answered, eventually providing a solution to the main research question.

The first step is to determine an initial selection of waste heat recovery technologies suitable for application to the case study. This selection follows from the results of the previous chapter, as well as general considerations regarding operating temperatures, system sizes, and costs commonly associated with the various technologies. The second step is to evaluate the selected waste heat recovery systems based on their thermal performance. The thermal performance will be measured by the theoretical efficiency of each system when applied to the case study. To obtain this, the thermodynamic behaviour of each system will be modelled after which the efficiency of the various systems will be compared against one another and if deemed appropriate, poorly performing systems will be omitted.

The third step is to conduct an analysis to compare the remaining systems based on their respective size. This analysis will consist of quantified comparisons of heat exchanger sizes, as well as qualitative comparisons regarding the size of other components. The models created during the second step will be extended with heat transfer area calculations, which will simultaneously result in the power output of each waste heat recovery system, to be subsequently used to express the size and cost of the systems per unit electric power produced. The fourth step is to evaluate the cost associated with the various waste heat recovery systems. This evaluation will be conducted through component cost estimations and the relative comparison between the different systems. The final step is to evaluate the results of the efficiency, size, and cost analyses to explore the suitability of the different waste heat recovery systems.

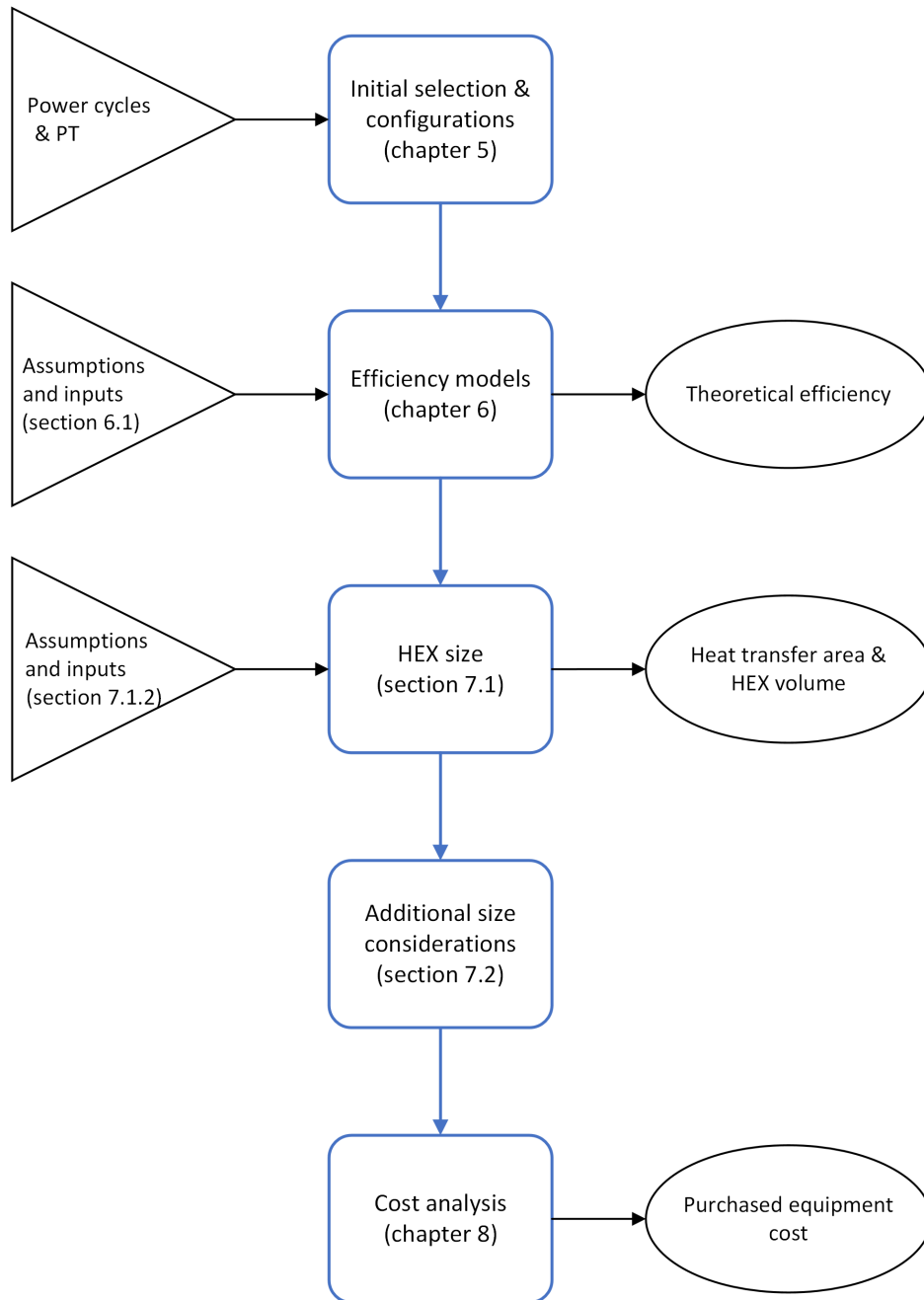


Figure 4.1: Applied process steps to answer each individual sub-research question.

5

System characteristics, selection, and design

The technologies which were concluded in section 3.6 to be promising for the waste heat recovery of future marine propulsion systems consisted of power cycles and the PT. In this chapter, a more narrow selection of suitable waste heat recovery technologies for SOFCs will be specified to undergo the different evaluations regarding efficiency, size, and cost. Starting from the power cycles and the PT, this chapter will result in several possible waste heat recovery systems and working media, and their various configurations.

5.1. Initial selection

To identify the waste heat recovery systems to be evaluated more closely, and to exclude other systems from further investigation, specifications are made regarding the working media of the systems, as well as by applying additional considerations and constraints. The PT and each type of power cycle with their applicable working media is first subjected to a brief evaluation based on relevant operational characteristics such as typical operating temperatures, and commonly applied considerations regarding system sizes and costs. Finally, various operating regimes associated with power cycles are described, and the basic designs of the resulting waste heat recovery systems are presented.

The RC-based systems can operate on several working media such as water, CO₂ and many different organic substances; however, organic substances are typically unsuitable for the high waste heat temperatures associated with SOFCs. While research into ORCs for high-temperature applications has been conducted, the maximum temperatures are still well below those of typical SOFC operating temperatures [65]; therefore, organic compounds, and thus ORCs, will be omitted from this research. The KC typically operates on a water-ammonia mixture, and similar to cycles operating on organic compounds, the KC matches low-temperature to medium-temperature heat sources well, while being less suitable for higher temperatures such as those associated with SOFCs [142]. Additionally, as the KC is comprised of significantly more components than other cycles and commonly associated with large sizes, it is omitted henceforth [142].

While BC-based systems can be operated on several gaseous media such as air, CO₂, helium, and nitrogen, the choice is made to focus on the first two for the remainder of this research. The reason a choice is made for BC systems with air as the working medium is due to them having both found significant application and being suitable for high-temperature waste heat sources. CO₂ BCs are chosen as they are also suitable for high temperatures and despite having found only limited practical application, interest in applying CO₂ as a working medium has seen a significant increase.

The SC is associated with very high costs compared to alternatives such as steam and gas turbines, and it finds very limited practical application even though interest regarding concentrated solar systems has been present for a significant amount of time [117]. While the SC is suitable for high-temperature

waste heat, such as from an SOFC, it will not be considered in this study due to the aforementioned barriers and the complexity of the engine [13].

Besides power cycles, the PT was in section 3.6 also concluded to be a promising waste heat recovery technology; however, application of a directly coupled PT would require pressurizing the SOFC system. To allow for a more narrow and balanced comparison, only indirectly coupled waste heat recovery systems will be considered, and the directly coupled PT will be henceforth omitted.

Thermodynamic power cycles can be differentiated based on their operating regime, which depends on the conditions of the fluid during the cycle with respect to the critical point. The operating regimes of thermodynamic cycles are referred to by the terms "subcritical", "transcritical", and "supercritical", and to be consistent in their meaning, the following definitions will be assumed for the remainder of this study.

A subcritical cycle is assumed to operate entirely below the critical pressure of the working medium, while a supercritical cycle is henceforth defined to operate entirely above the critical pressure of the working medium. Lastly, a transcritical cycle is assumed to operate partially below, and partially above the critical pressure, where the main heat addition process takes place above the critical pressure, and the heat rejection process below the critical pressure.

While there are many possibilities regarding the operating regime of the remaining cycles, a few are chosen as to reduce the size of the final selection.

The RC-based systems applying water will be solely investigated as a subcritical cycle, also referred to as the common SRC, and a transcritical steam Rankine cycle (TCSRC); due to the high critical pressure of water, no supercritical SRC will be investigated. Additionally, while SRC and TCSRC systems are limited regarding the operating temperatures due to material considerations, it is for the moment assumed that future developments might allow operation of (TC)SRCs at higher temperatures than currently applied; therefore, these systems will still be considered in this study. Besides the SRC and TCSRC, an RC-based system operating on CO₂ will be investigated as a transcritical Rankine cycle (TCRC). In all of the aforementioned RC-based systems, the temperature of the fluid exiting the condenser will be below its critical temperature, while the temperature of the fluid in other stages of the cycle may exceed the critical temperature.

The BC-based systems which will be investigated are the subcritical air BC, and the CO₂ supercritical Brayton cycle (SBC); both cycles are taken to operate entirely above the critical temperature of the respective working medium.

An overview of the initial selection of waste heat recovery systems is shown in table 5.1.

Table 5.1: The waste heat recovery systems to be investigated and their respective working media.

Waste heat recovery system	Working medium
SRC	Water
TCSRC	Water
TCRC	CO ₂
BC	Air
SBC	CO ₂

5.2. System configurations

The systems from table 5.1 can be applied in their simplest form, henceforth referred to as the basic configuration, or be applied with various modifications. This section will first briefly describe the basic configurations, after which a number of commonly implemented modifications are presented. At the end, an overview of all configurations to be investigated further is provided.

5.2.1. The basic configurations

This section describes the basic configuration associated with the power cycles from table 5.1; the basic configuration is the simplest possible design of a power cycle, and forms the starting point from which a cycle can be modified.

fluid has at this point already experienced a temperature rise, it is cooled back down through another cold source heat exchanger, called the intercooler, before being compressed in the high-pressure compressor (HPC) to reach the final pressure. As intercooling is designed to reduce the work required for compression, it is deemed unsuitable for application in RC-based systems as the compression process is applied to a liquid, which typically sees only a small temperature increase during compression, and already requires relatively little work compared to gas compression processes. A PFD of a cycle with intercooling is shown in figure 5.2b.

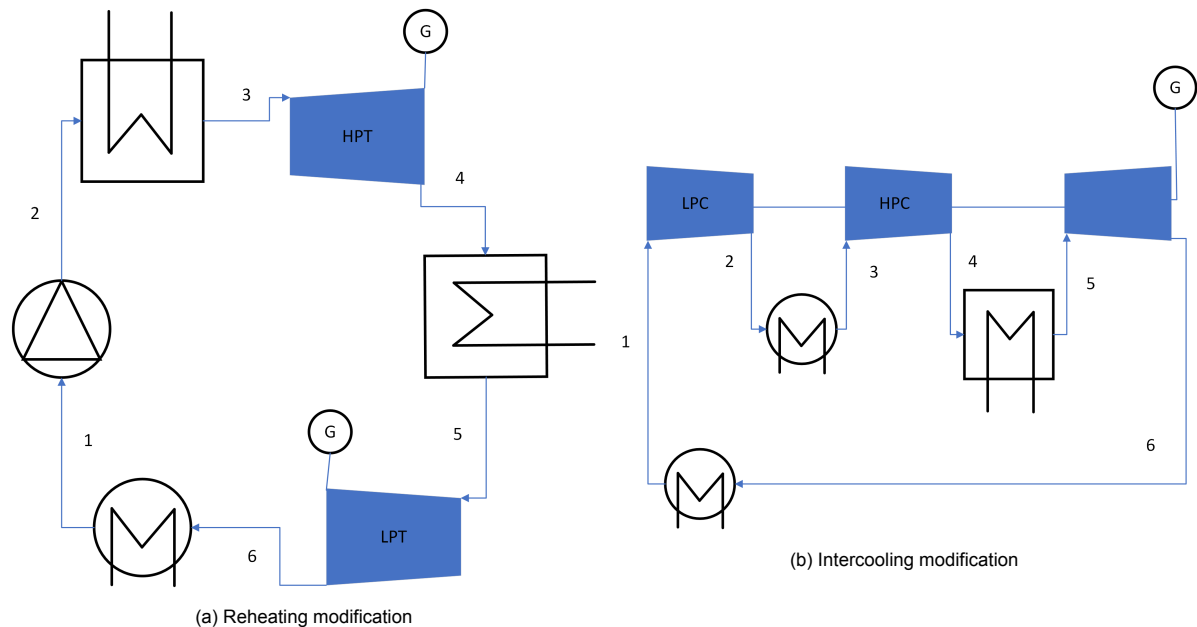


Figure 5.2: The PFDs of the reheating and intercooling modifications.

Recuperation

The third modification is recuperation, which is often applied when the fluid exiting the expander still has a relatively high temperature compared to the temperature of the fluid exiting the compressor. This modification is designed to not waste energy by expelling it unnecessarily from the cycle. Recuperation requires the implementation of an additional heat exchanger to pass the remaining heat from the stream exiting the expander to the stream exiting the compressor. Unlike reheating and intercooling, recuperation does not increase the net power output of the cycle, but rather decreases the net heat input to the cycle, since using the heat left over after expansion decreases the required heat input from the hot source heat addition process. As the heat of the fluid after expansion in the SRC and TCSRC is typically only slightly higher than that of the fluid after compression, recuperation will only be considered for the BC systems and the CO₂ TCRC. A PFD of a cycle with recuperation is shown in figure 5.3a.

Regeneration

Similar to recuperation, the modification of a cycle with regeneration is applied to decrease the net heat input of the cycle. Regeneration is solely applied in SRCs and TCSRCs and requires an additional pump and heat exchanger or mixer; the two pumps are referred to as a low-temperature pump (LTP) and a high-temperature pump (HTP). In regeneration, part of the vapour is extracted at an intermediate pressure during the expansion process, while the rest of the vapour is fully expanded. The latter part of the flow is then condensed during the cooling process, and subsequently pumped by the LTP to the same pressure as the previously extracted vapour. The flow from the LTP then enters the additional heat exchanger where it is mixed with the extracted vapour; in this study, the mixing occurs in an open feedwater heater (FWH) during which the extracted vapour is condensed. The combined (liquid) flow is brought to the final pressure by the HTP, after which it undergoes the heat addition process before once again entering the expander. A PFD of a cycle with regeneration is shown in figure 5.3b.

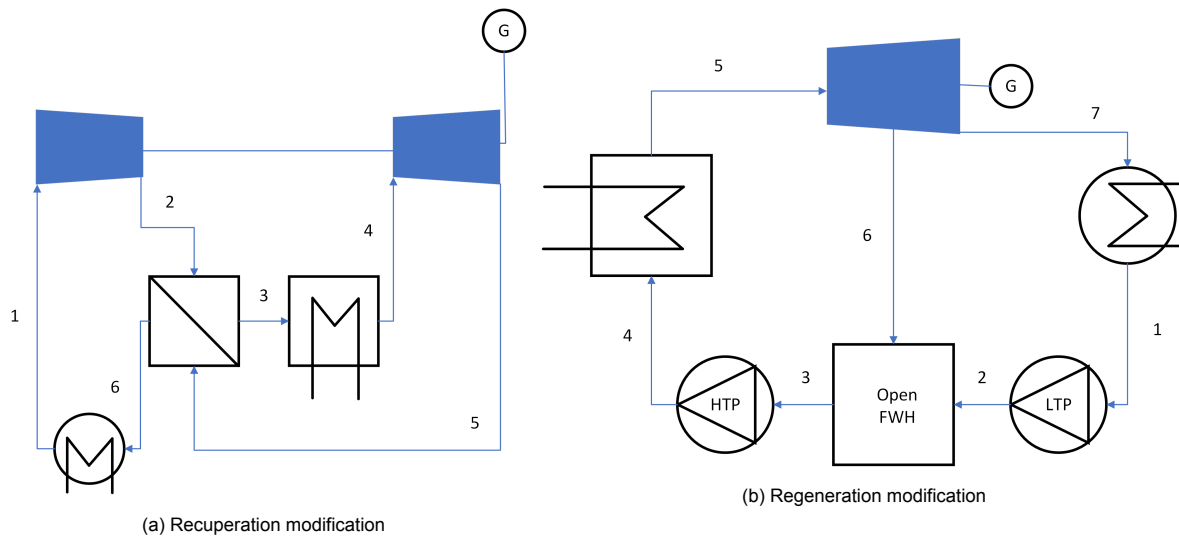


Figure 5.3: The PFDs of the recuperation and regeneration modifications.

Recompression

The final commonly implemented modification to be considered in this study is recompression, which, similar to recuperation and regeneration, reduces the amount of useful heat rejected from the cycle and therefore decreases the net heat input. This is achieved by reusing the heat left after expansion, as well as by reducing the flow through the cold source heat exchanger, effectively reducing the heat expelled during the cooling process. Recompression is a configuration that can only be applied when the fluid is in a gaseous state, and requires two additional heat exchangers operating as recuperators and an additional compressor. As with recuperation, instead of expelling the heat after expansion from the system, the fluid is passed through a recuperator, the so-called high-temperature recuperator (HTR), to transfer heat to the fluid before it undergoes the final heat addition process. The fluid is then passed through another recuperator called the low-temperature recuperator (LTR), this time transferring heat to the fluid exiting the compressor classified as the low-temperature compressor (LTC). Finally, the flow is split in two after the LTR, from which one stream enters the cold source heat exchanger, to be cooled and subsequently fully compressed in the LTC, while the second flow enters the additional compressor, or high-temperature compressor (HTC), to be immediately fully compressed. After the flows exiting the LTR and HTC are recombined, the fluid is passed to the aforementioned HTR from which it will undergo the final heat addition and expansion process.

While recompression is typically only applied in the CO₂ SBC, it can also be applied in a CO₂ TCRC, in which case the aforementioned LTC can be considered a pump as well, due to the fluid initially being in a liquid state. A PFD of a cycle with recompression is shown in figure 5.4.

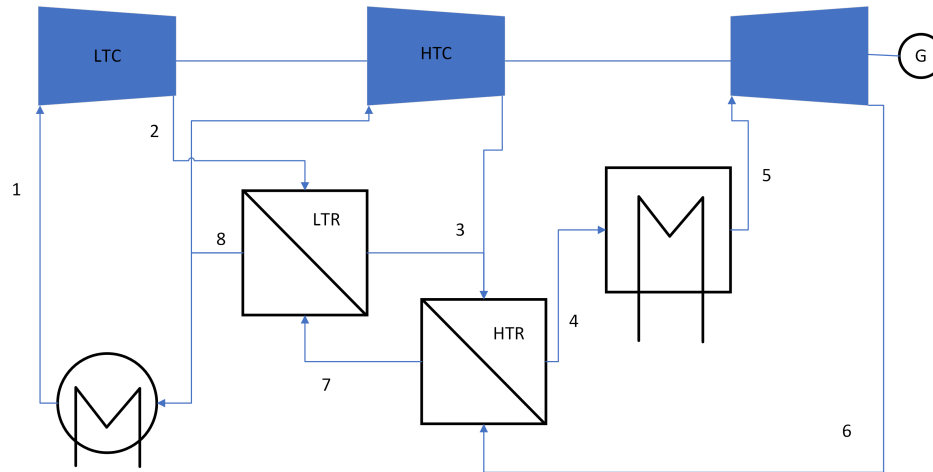


Figure 5.4: Recompression modification

To summarise, in SRCs and TCSRCs, only reheating and regeneration are commonly applied modifications. While TCRCs operating on CO₂ are typically not applied with regeneration, they can be modified with recuperation and recompression. SBCs can be modified with all configurations except for regeneration as this involves phase transition through vapour and liquid mixing; the BC will be considered to have the same configurations as the SBC, with the exception of recompression. These configurations can be applied solely or combined together, and as such, an overview of possible combinations is created and shown in table 5.2.

Table 5.2: An overview of the waste heat recovery systems, media, and configurations to be subjected to evaluations regarding efficiency, size, and cost.

Waste heat recovery system & medium / Configuration	SRC Water	TCSRC Water	TCRC CO ₂	BC Air	SBC CO ₂
Basic	x	x	x	x	x
Reheating	x	x	x	x	x
Intercooling				x	x
Recuperation			x	x	x
Recompression			x		x
Regeneration	x	x			
Reheating & intercooling				x	x
Reheating & recuperation			x	x	x
Reheating & recompression			x		x
Reheating & regeneration	x	x			
Intercooling & recuperation				x	x
Intercooling & recompression					x
Reheating, intercooling & recuperation				x	x
Reheating, intercooling & recompression					x

6

Efficiency of configurations

The previous chapter provided an extensive list of power cycles that could be applied in the example case study. These power cycles have varying characteristics and their performance should be evaluated; this is done through the creation of thermodynamic models which will determine their theoretical efficiency when applied to the case study. In this chapter, the assumptions relevant to the models will be discussed first, after which the relevant thermodynamics are described; this will be done for two configurations, which together encompass all possible modifications to the basic configuration. To make sure the thermodynamic models created are correct, a validation is applied in section 6.3 which compares the results of the models to the results from other studies. Finally, in section 6.4, the theoretical efficiencies of all the cycles and configurations are compared for a range of operating pressures and temperatures, which will lead to the exclusion of any underperforming configurations.

The configurations from table 5.2 are modelled based on first law thermodynamics using Python v3.8.10 and CoolProp v6.4.1.

6.1. Assumptions

As a starting point, and to further specify the conditions around both the example case study and the design of the configurations, a number of initial assumptions are made to be applied in the thermodynamic models:

- The temperature of the hot source service fluid (SOFC exhaust) is chosen to be 850 °C, which is within the range of operating temperatures currently associated with SOFCs as found and described in section 2.2.3. A similar temperature was applied by Schöffler et al. [106].
- The inlet temperature of the cold source service fluid (seawater) is chosen to be 15 °C, as seawater temperatures are often in the range of 0 °C to 30 °C [98]. It should be noted that standard water is used for obtaining the fluid properties in CoolProp as its data regarding seawater is relatively limited.
- The minimum allowable temperature difference (ΔT_{HEX}) between the flows entering and exiting a heat exchanger is set at 15 °C. A similar value for the minimum allowable temperature difference was used by Schöffler et al. [106].
- The minimum temperature of the system T_{min} is defined as the temperature of the fluid exiting the cooler or condenser depending on the type of cycle. This value is set at 30 °C and follows from the summation of the previously fixed cold source service fluid temperature and the minimum allowable temperature difference. An exception is made for the SBC where it is set to 32 °C as the critical temperature of CO₂ is 31.1 °C.
- The maximum temperature of the system T_{max} , also referred to as the turbine inlet temperature (TIT), is defined as the temperature of the fluid entering the expander; this value is set to 800 °C, which is chosen sufficiently below the aforementioned 850 °C of the SOFC exhaust temperature.

- The temperatures of the fluid after intercooling and reheating are assumed the same as T_{min} and T_{max} respectively.
- The minimum pressure of the system P_{min} is defined as the pressure of the fluid exiting the main cooler; this parameter is only applied as an input in the BC and SBC and is different for both cycles.
- The maximum pressure of the system P_{max} is defined as the pressure of the fluid exiting the final compressor or pump depending on the type of cycle; this value differs per cycle. For the BC configurations and the CO₂ TCRC configurations, the value of P_{max} follows from the main cooler/condenser exit pressure and a pressure ratio $PR = 3$. The same pressure ratio was applied by Sánchez et al. for both an air BC and a CO₂ SBC [118].
- In all RC models, the absent input parameter P_{min} is replaced by the vapour quality (x) at the condenser outlet, which is set as 0.0 to be a saturated liquid. Similarly, the stream exiting an open FWH is also assumed to be a saturated liquid. These assumptions are commonly applied to RC-based systems.
- Mixing is assumed ideal, experiencing no pressure drop, with the enthalpy of mixing being zero. This same assumption was applied by Schöffler [105].
- Pressure drops: all heat exchangers are subjected to a 2% pressure drop ($\Delta P = 0.98$) as applied by Sánchez et al. [118]. An exception is made for open FWHs for regeneration, which apply mixing and are therefore assumed to have no pressure drop.
- The pressure ratios for the stages of intercooling and reheating are set equal when ignoring the pressure drop of the intermediate heat exchanger; similarly for regeneration, the extraction pressure is set to have the same pressure as after the first pump, which is again based on equal pressure ratios between the two pumping stages. This assumption has been subjected to a verification, which is described and discussed in appendix A.1.
- Compressor/pump and turbine isentropic efficiencies are assumed constant and set to $\eta_C = 0.8$ and $\eta_T = 0.9$, respectively. The same values of the isentropic efficiencies were applied by Schöffler et al. [106].
- The temperature differences between the flows entering and exiting a recuperator follow from a heat balance of the flows while setting the minimum allowable temperature difference (ΔT_{HEX}) of 15 °C. In cycles containing recompression, the temperature difference between the cold flow entering the LTR and the hot flow exiting the LTR is fixed at the aforementioned ΔT_{HEX} , while the flow fractions after the split are compensated to achieve a balance between the heat flows. These balances were similarly applied by Schöffler [105].
- All cycles are assumed closed for modelling purposes.
- Generator efficiency is assumed to be constant and fixed at 95%. The same value for the efficiency of the generator was used by Schöffler et al. [106].

6.2. Thermodynamics

To describe the applied method, two configurations from table 5.2 will be explained in detail along with their relevant thermodynamic model development. The first model to be described is the combined reheating, intercooling & recompression BC, which will contain thermodynamics on recuperation as well; the second model to be described is the regenerative RC. These two models combined encompass all possible modifications of the basic configuration and their associated thermodynamic operation. Figures 6.1 and 6.3 show the respective PFDs of the aforementioned configurations.

6.2.1. Combined reheating, intercooling & recompression BC

The combined reheating, intercooling & recompression BC contains several of the modifications as described in section 5.2.2. Compared to the basic configuration of the BC, this cycle has an additional cooler and compressor for the intercooling part, an extra heater and turbine for the reheating part,

and an added compressor and recuperators to provide the recompression part. The points (or nodes) before and after each component are numbered, which describes the beginning and end of a process, such as compression. This section walks through each of these processes by providing the relevant thermodynamic equations required to obtain the fluid conditions at each point.

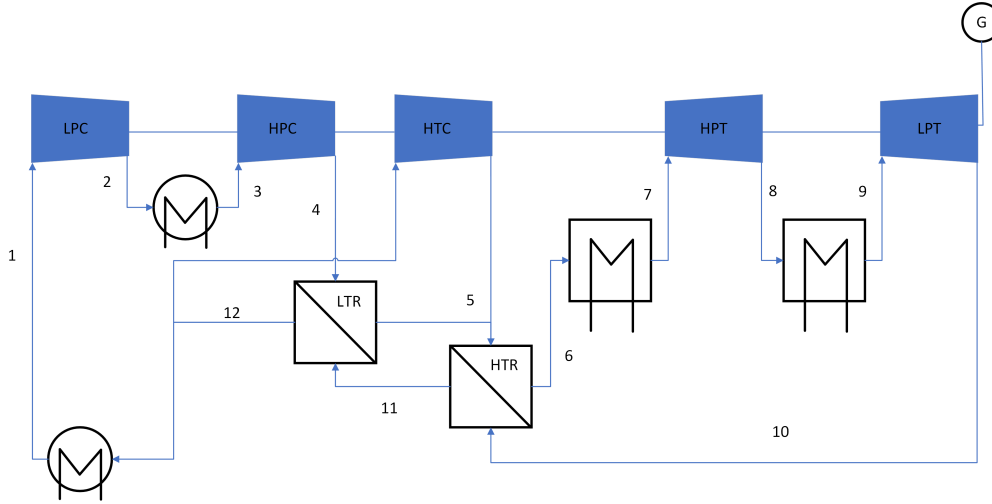


Figure 6.1: Combined reheating, intercooling & recompression BC

The values for the specific enthalpy (h) and entropy (s) at each point are determined using CoolProp. The first point in the PFD is determined by setting T_{min} and P_{min} . The fluid conditions at the second point follow from the equal pressure ratio assumption from section 6.1 according to

$$P_2 = \sqrt{P_1 * P_{max}}, \quad (6.1)$$

in which $P_{max} = PR * P_{min}$. After setting the specific entropy with ideal compression $s_{2,ise} = s_1$, the value for the specific enthalpy with ideal compression $h_{2,ise}$ is found using CoolProp. The value of h_2 can then be determined by applying

$$h_2 = \frac{h_{2,ise} - h_1}{\eta_c} + h_1, \quad (6.2)$$

after which the remaining fluid conditions can be obtained. Here, η_c is the isentropic efficiency of the compressor. The fluid conditions for the third point are determined by applying the pressure drop across the intercooler as $P_3 = \Delta P * P_2$, and setting $T_3 = T_{min}$. The fourth point is obtained in a similar manner to the second point, but now by setting $P_4 = P_{max}$.

The fifth point is a combining flow, where P_5 is derived from the flow exiting the recuperator using $P_5 = \Delta P * P_4$, and h_5 is derived from the flow exiting the compressor by setting $s_{5,ise} = s_{12}$ and applying the same steps as for the second and fourth point.

The fluid conditions at the sixth point result from a pressure drop across the recuperator through $P_6 = \Delta P * P_5$, and a balance of the heat flows through the recuperator. The latter results in a value of h_6 according to

$$h_6 - h_5 = h_{10} - h_{11}. \quad (6.3)$$

To prevent this returning a value of T_6 above T_{10} , an additional condition is set through ΔT_{HEX} as per the assumptions from section 6.1. If violated, this condition imposes the equation $T_6 = T_{10} - \Delta T_{HEX}$, which is then used to determine h_6 and other fluid properties at this point.

The seventh point follows from a pressure drop across the hot source heat exchanger and $T_7 = T_{max}$. The fluid conditions at the eighth point follow from equal pressure ratios according to

$$P_8 = \sqrt{P_7 * P_{10}}, \quad (6.4)$$

and similar to compressor exit points, after setting $s_{8,ise} = s_7$ and obtaining the value for $h_{8,ise}$. Subsequently, the value of h_8 can be found by applying

$$h_8 = \eta_T * (h_{8,ise} - h_7) + h_7, \quad (6.5)$$

where η_T is the isentropic efficiency of the turbine. The ninth point is obtained similar to the seventh point. The fluid conditions at the tenth point are derived similar to the eighth point, now by setting $P_{10} = P_1/(\Delta P)^3$.

The pressures at the eleventh and twelfth point follow from the pressure drop across the recuperators. The temperature at the eleventh point is obtained by applying the heat balance from equation (6.3) if the aforementioned condition for the sixth point is breached, or through $T_{11} = T_5 + \Delta T_{HEX}$ if not. The temperature at the twelfth point is fixed at $T_{12} = T_4 + \Delta T_{HEX}$ as per the assumptions from section 6.1.

Now that the fluid conditions at all points are determined, the theoretical efficiency (η_{th}) can be derived from the specific net work produced (w_{net}) and the specific heat input (q_{in}) according to

$$\eta_{th} = \frac{w_{net}}{q_{in}}, \quad (6.6)$$

where w_{net} results from the specific work produced by the two turbines, and required by the three compressors. The compressors and turbines are denoted as follows, from left to right in the PFD in figure 6.1: w_{C1} , w_{C2} , w_{C3} , w_{T1} & w_{T2} . To determine these specific work values, first the flow fractions of the split after the twelfth point must be obtained, where $split_{4-5}$ denotes the flow fraction through the points 12-1-2-3-4-5 and $split_{12-5}$ denotes the flow fraction through the HTC. The value of the former is derived by balancing the heat flows in the recuperator through

$$split_{4-5} = \frac{h_{11} - h_{12}}{h_5 - h_4}, \quad (6.7)$$

which allows for the value of the latter to be found using

$$split_{12-5} = 1 - split_{4-5}. \quad (6.8)$$

Now that the flow fractions are determined, the specific work required by the compressors, and produced by the turbines, can be calculated according to

$$w_{C1} = split_{4-5} * (h_1 - h_2), \quad (6.9)$$

$$w_{C2} = split_{4-5} * (h_3 - h_4), \quad (6.10)$$

$$w_{C3} = split_{12-5} * (h_{12} - h_5), \quad (6.11)$$

$$w_{T1} = h_7 - h_8, \quad (6.12)$$

$$\text{and } w_{T2} = h_9 - h_{10}. \quad (6.13)$$

The specific net work produced by the system results from

$$w_{net} = w_{C1} + w_{C2} + w_{C3} + w_{T1} + w_{T2}. \quad (6.14)$$

The specific heat put into the system is the combination of the two flows passing through the heat exchangers between points six and seven, and eight and nine respectively. These specific heat inputs are q_{6-7} and q_{8-9} , and are denoted as q followed by the respective start and end point of the flow. They are obtained by applying

$$q_{6-7} = h_7 - h_6, \quad (6.15)$$

$$q_{8-9} = h_9 - h_8, \quad (6.16)$$

$$\text{and } q_{in} = q_{6-7} + q_{8-9}. \quad (6.17)$$

Figure 6.2 shows the resulting temperature-specific entropy diagram of a combined reheating, inter-cooling, and recompression CO_2 SBC when applying the discussed assumptions and equations. The red curves denote the thermodynamic cycle and fluid flow, while the blue lines denote the locations of recuperation.

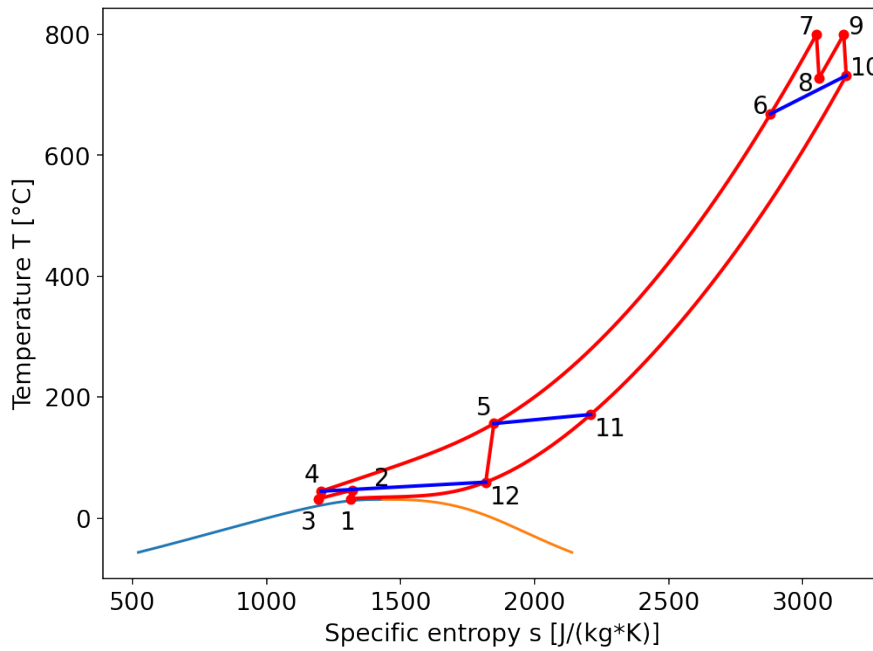


Figure 6.2: T-s diagram of a combined reheating, intercooling & recompression SBC

6.2.2. Regenerative RC

The regenerative RC contains the final modification from section 5.2.2, which is not present in the configuration of the previous section: regeneration. Compared to the basic configuration of the RC, this cycle has an additional pump and heat exchanger, the open FWH. The approach to modelling this configuration is similar to that in the previous section, and some of the processes which are present in both configurations will not be discussed in detail again.

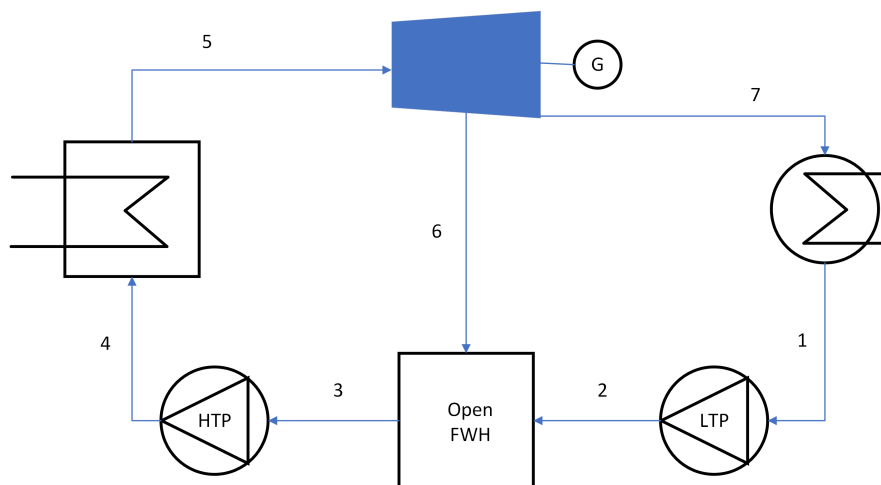


Figure 6.3: Regenerative RC

In the regenerative RC, the first point is determined by setting $T_1 = T_{min}$ and the vapour quality to be $x_1 = 0.0$ to denote a saturated liquid. The fluid conditions after compression at the second point are derived the same way as for the second point of the previously described combined reheating, intercooling & recompression BC.

The third point is determined by again applying a vapour quality $x_3 = 0.0$ for a saturated liquid, and by setting the pressure $P_3 = P_2$, following the assumptions from section 6.1 that the flow exits

the FWH fully saturated and experiences no pressure loss due to mixing. As the fourth point follows a compression process similar to that of the previously described combined reheating, intercooling & recompression BC, the fluid conditions are obtained in the same manner.

At the fifth point, the exit of the hot source heat exchanger, the temperature is set at T_{max} and the flow experiences a pressure drop ΔP . By applying a pressure $P_6 = P_2$ to match the pressure of the cold flow entering the open FWH, as well as by setting $s_{6,ise} = s_5$, the value of $h_{6,ise}$ can be obtained. Subsequently, the specific enthalpy at point six h_6 can be determined using

$$h_6 = \eta_T * (h_{6,ise} - h_5) + h_5, \quad (6.18)$$

after which all the fluid conditions at point six can be obtained. Here, η_T is the isentropic efficiency of the turbine. Finally, the fluid conditions at the seventh point are obtained by setting $P_7 = P_1/\Delta P$, and by applying the turbine exit formulae above in a similar manner.

The theoretical efficiency, net specific work, and specific heat input are determined similar to the previously described combined reheating, intercooling & recompression BC.

The value of w_{net} results from the specific work produced by the turbine and the work required by the two pumps. The pumps are denoted as follows, from left to right in the PFD in figure 6.3: w_{C2} and w_{C1} ; the turbine is split into stages where w_{T1} and w_{T2} denote the high-pressure and low-pressure stage, respectively. To determine these specific work values, the fractions of the flow after the extraction from the turbine must be obtained, where $split_6$ denotes the flow fraction of the extracted vapour and $split_7$ denotes the flow fraction through the condenser. The value of the former is derived by balancing the heat flows in the open FWH using

$$split_6 = \frac{h_3 - h_2}{h_6 - h_2}, \quad (6.19)$$

which allows for the value of the latter to be found through

$$split_7 = 1 - split_6. \quad (6.20)$$

Now that the flow fractions are determined, the specific work required by the pumps, and produced by the two turbine stages, can be calculated according to

$$w_{C1} = split_7 * (h_1 - h_2), \quad (6.21)$$

$$w_{C2} = h_3 - h_4, \quad (6.22)$$

$$w_{T1} = h_5 - h_6, \quad (6.23)$$

$$\text{and } w_{T2} = split_7 * (h_6 - h_7). \quad (6.24)$$

The specific net work produced by the system results from

$$w_{net} = w_{C1} + w_{C2} + w_{T1} + w_{T2}. \quad (6.25)$$

The specific heat put into the system occurs between the fourth and fifth point, and is denoted as q_{4-5} ; it is obtained using

$$q_{in} = q_{4-5} = h_5 - h_4. \quad (6.26)$$

Figure 6.4 shows the resulting temperature-specific entropy diagram of a regenerative SRC when applying the discussed assumptions and equations.

6.3. Validation of models

In this section, a validation is conducted and discussed to verify the correctness of the designed thermodynamic models. As the total number of models is quite high, a small selection of other studies has been used which apply the same cycles and configuration as those in this study. The validation compares the resulting efficiencies of the other studies to those obtained from the models in this study when applying the same inputs. Table 6.1 shows the applied inputs for the models, the output obtained by the respective source and this study, and the results as a difference between the outputs; each row is first denoted by the respective source, cycle, configuration, and working medium.

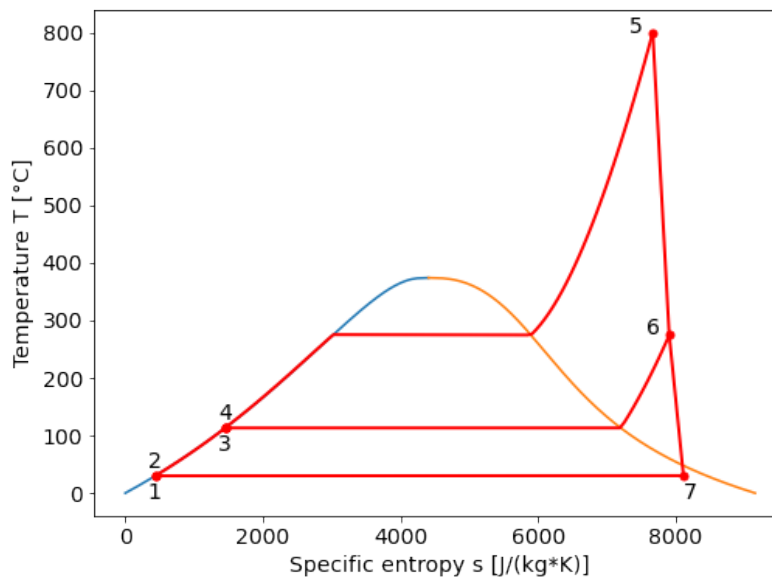


Figure 6.4: T-s diagram of a regenerative SRC

Table 6.1: Comparison of first law models to other studies.

Reference source & input					Output		Result
ΔP	ΔT_{HEX}	η_c / η_T	$T_{min} / T_{max} [^{\circ}C]$	$P_{min} / P_{max} [bar]$	Source $\eta_{th} [\%]$	This study $\eta_{th} [\%]$	$\Delta\eta_{th} [\%]$
Valencia et al. [126], SRC, regeneration, water							
NA	NA	0.85 / 0.9	38.806 / 500	NA / 50	37.42	37.42	0
Sánchez et al. [118], BC, recuperation, air							
0.98	44 & 46.1	0.85 / 0.9	25 / 650	1 / 3	33	33.01	0.03
Adibi et al. [1], BC, reheating-intercooling-recuperation, air							
NA	111.6 & 111.5	0.8 / 0.8	25 & 52.33 / 1000	1 / 9	39.79	40.43	1.61
Schöffler et al. [106], SBC, recuperation, CO ₂							
0.990	10	0.8 / 0.9	32 / 700	80 / 250	43.16	43.22	0.139
Schöffler et al. [106], SBC, recompression, CO ₂							
0.993	15	0.8 / 0.9	32 / 700	80 / 250	49.68	49.72	0.081

While the results between this and the other studies would ideally be identical, small variations do occur. The difference between the results from other studies and this study, as obtained and shown in table 6.1, can to a certain extent be explained based on slight inconsistencies between the models.

Valencia et al. set a value for P_{min} instead of T_{min} , the value for the latter has been taken from their results and it was verified that the value for P_{min} , as applied by Valencia et al. to be 0.07 bar, corresponds to the value obtained by this study [126]. Additionally, Valencia et al. apply an open FWH pressure of 10 bar [126], this same value has been applied to the model for the validation.

Sánchez et al. obtain the temperature differences of 44 °C and 46.1 °C between the flows of the recuperator through a recuperator effectiveness of 0.85 defined as a balance of the temperatures of the fluid across the recuperator [118]. As this study obtains the temperature differences through a heat flow balance and minimum allowable temperature difference, the temperature differences as obtained by Sánchez et al. have been applied as direct inputs to the model for the validation; this might have caused slight inconsistencies due to number rounding. Additionally, Sánchez et al. have modelled an open cycle [118]; since the model in this study was assumed closed as per the assumptions in section 6.1, the effect of the pressure drop for the additional heat exchanger has been corrected for the validation.

Adibi et al. apply a recuperator effectiveness of 0.8 defined as a balance of the temperatures of the fluid across the recuperator, resulting in temperature differences between the flows of 111.6 °C and 111.5 °C; additionally, Adibi et al. have applied an intercooler efficiency of 0.8 resulting in an intercooler exit temperature of 52.33 °C [1]. As this study applies no intercooler efficiency and a heat flow balance with a minimum allowable temperature difference, the three aforementioned temperatures were applied as inputs for the validation; this may have resulted in slight inconsistencies due to number rounding.

Schöffner et al. apply a pressure drop of 0.98 over an entire flow, and relate the pressure drop per heat exchanger to the change in enthalpy [106]. For the validation, a ΔP of approximately 0.990 and 0.993 has been taken per heat exchanger for the recuperation and recompression cycle respectively; however, these are not the exact same values, and slight deviations may have resulted.

As previously mentioned, ideally the results between this and the other studies are identical; however, when considering the order of magnitude of the differences and the described possible explanations for the differences, it is concluded that the models created in this study are valid.

6.4. Comparison

In this section, the comparison of the different cycles and configurations is discussed based on their theoretical efficiency; additionally, in a number of cases, some considerations regarding system complexity and size are introduced as well. Firstly, within each type of cycle an evaluation of the different configurations is conducted, after which the best performing ones are chosen while the rest is eliminated. For the evaluation, P_{max} and T_{max} are varied to include the influence of these parameters on the theoretical efficiency. Secondly, the remaining and best performing configurations of each type of cycle are compared against each other in a similar manner. In all of the following comparisons, the assumptions from section 6.1 are applied, and the individual analyses are conducted using the following approach:

- Firstly, a T_{max} , or TIT, of 800 °C is applied while P_{max} is varied; for each configuration, P_{max} is plotted against the theoretical efficiency.
- Secondly, P_{max} is fixed while T_{max} is varied from 600 to 900 °C, and for each configuration, T_{max} is plotted against the theoretical efficiency.

6.4.1. Comparison of the SRC configurations

For the comparison of the different SRC configurations, first, P_{max} is varied from 30 to 120 bar, after which P_{max} is set at 60 bar while T_{max} is varied; the results are shown in figures 6.5a and 6.5b respectively.

From these graphs, it is clear that the basic configuration of the SRC performs worse than the other configurations when it comes to theoretical efficiency; however, the difference is small and limited to approximately 3%. Additionally, the basic configuration has the fewest components and may prove to be smaller in size; as such, none of the SRC configurations will be discarded.

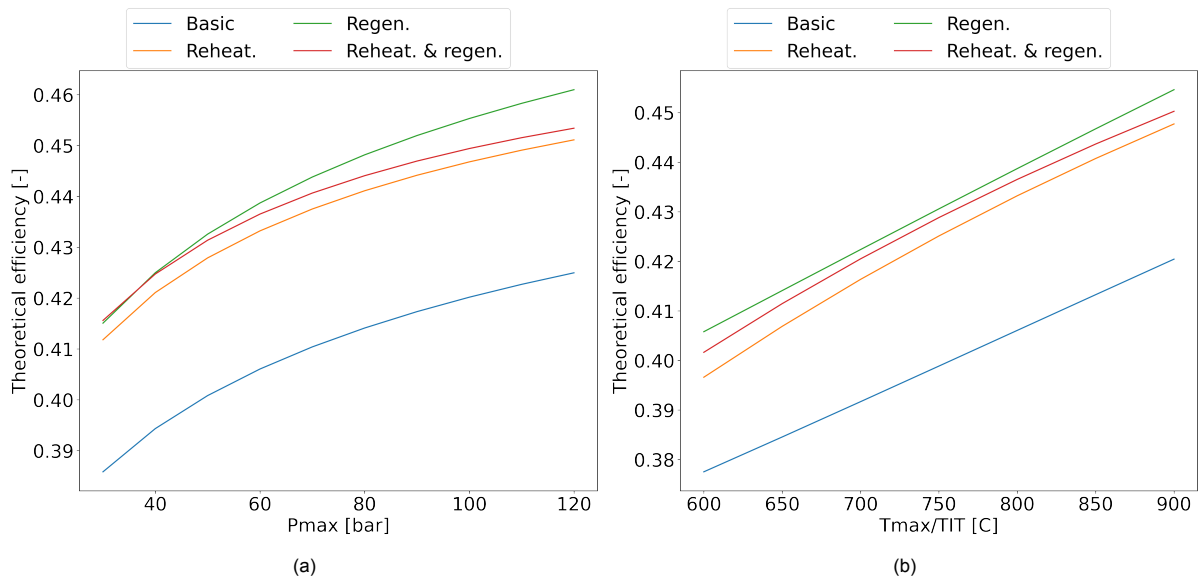


Figure 6.5: Comparison of the theoretical efficiency of different SRC configurations. Where figure (a) is at varying P_{max} , and figure (b) is at varying T_{max} .

6.4.2. Comparison of the TCSRC configurations

For the TCSRC configurations, P_{max} is varied from 225 to 375 bar while T_{max} is fixed, after which P_{max} is set at 300 bar while T_{max} is varied; the results are shown in figures 6.6a and 6.6b respectively.

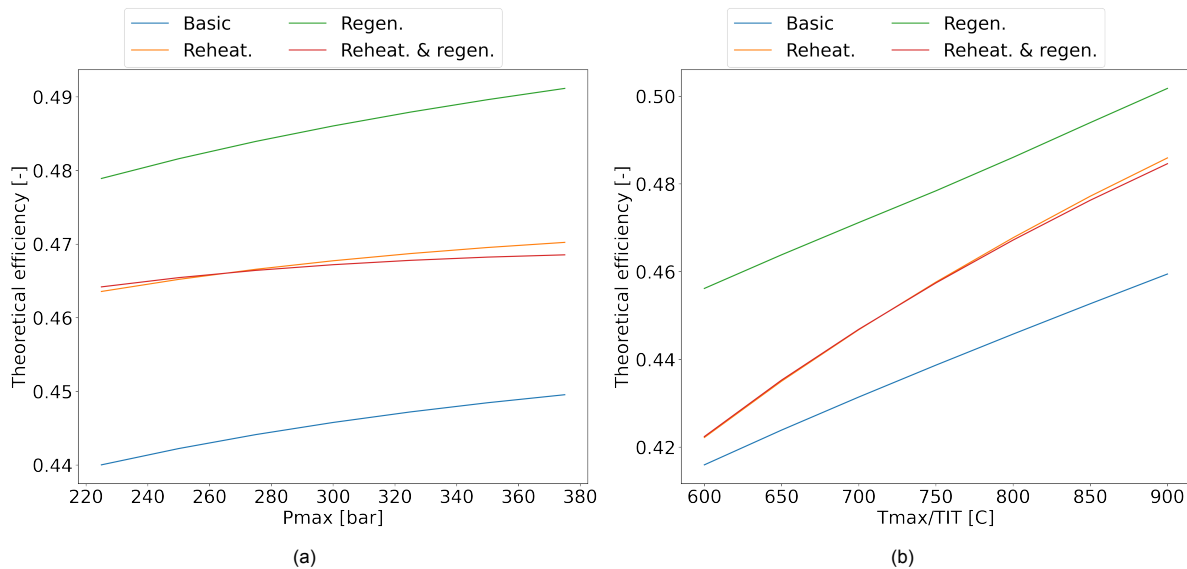


Figure 6.6: Comparison of the theoretical efficiency of different TCSRC configurations. Where figure (a) is at varying P_{max} , and figure (b) is at varying T_{max} .

Similar to the comparison of the SRC configurations, the basic configuration performs worst and the regeneration cycle performs best regarding theoretical efficiency; however, the difference between the two configurations is limited to approximately 4%, and the basic configuration may prove more economical when considering system size. Therefore, no configurations of the TCSRC will be omitted at this point.

6.4.3. Comparison of the CO₂ TCRC configurations

In the TCRC configurations, P_{max} is varied from 135 to 350 bar, after which P_{max} is fixed at approximately 216 bar while T_{max} is varied; the results are shown in figures 6.7a and 6.7b respectively.

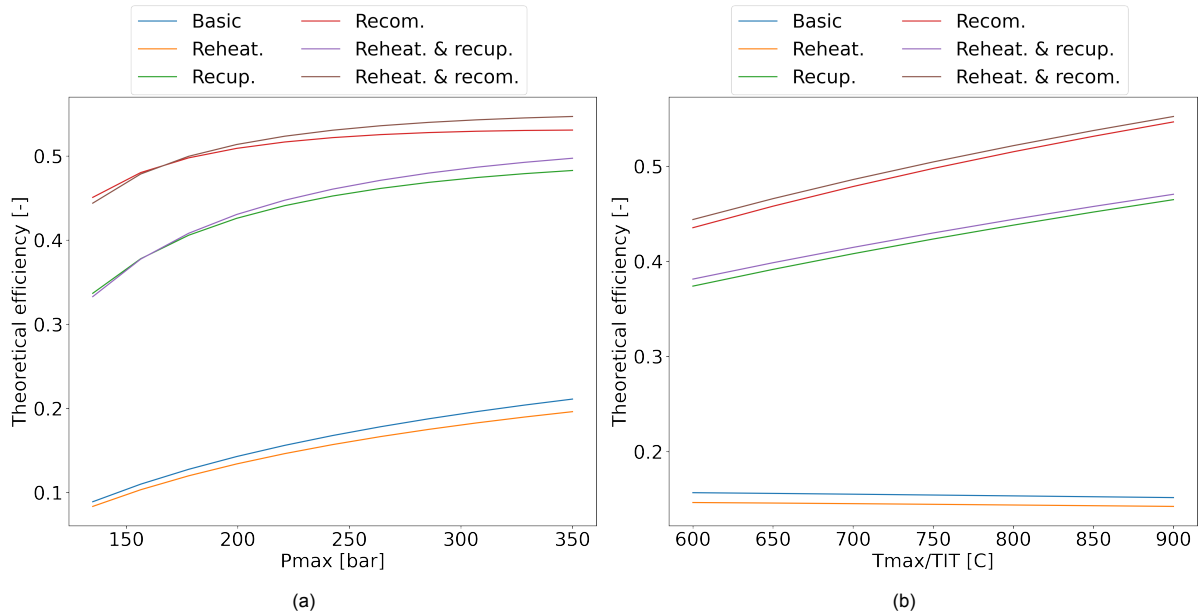


Figure 6.7: Comparison of the theoretical efficiency of different CO₂ TCRC configurations. Where figure (a) is at varying P_{max} , and figure (b) is at varying T_{max} .

Regarding the theoretical efficiency, it can be seen that the configurations with recompression perform best, followed by those with recuperation; finally, the basic and reheating cycle perform significantly worse than the other configurations. Due to the very poor theoretical efficiencies of the basic and reheating configurations compared to the other configurations, these two cycles are eliminated from further investigation. The difference in theoretical efficiency between the standalone recuperation and recompression configurations and their combined reheating counterparts is very small, while the latter are expected to present with a larger system size; therefore, only the standalone recuperation and recompression configurations will receive further attention for the remainder of this study.

6.4.4. Comparison of the air BC configurations

In the comparison of the air BC configurations, P_{max} is varied from 2 to 5 bar, after which P_{max} is set at 3 bar while T_{max} is varied; the results are shown in figures 6.8a and 6.8b respectively.

The basic, reheating, intercooling, and combined reheating & intercooling cycles show the poorest theoretical efficiencies, and, as such, they are eliminated from further investigation. The combined reheating, intercooling & recuperation cycle shows the highest theoretical efficiency. However, the difference compared to the other configurations is limited, and size considerations may prove vital. Therefore, the recuperation cycle, and its reheating and/or intercooling counterparts will be investigated further.

6.4.5. Comparison of the CO₂ SBC configurations

Finally, for the SBC configurations, P_{max} is varied from 150 to 350 bar, after which P_{max} is set at 240 bar while T_{max} is varied; the results are shown in figures 6.9a and 6.9b respectively.

The results from the comparison of the SBC configurations are similar to those of the TCRC, with the difference being mainly the presence of intercooling in the SBC configurations. Regarding the theoretical efficiency, it can be seen that the configurations with recompression perform best, followed by those with recuperation; finally, the remaining cycles perform significantly worse and show very poor theoretical efficiencies. As a result, the basic, reheating, intercooling, and combined reheating & intercooling configurations are omitted from further consideration. Similar to the conclusion of the CO₂ TCRC, only the standalone recuperation and recompression configurations of the CO₂ SBC will receive further attention for the remainder of this study, as these perform comparably to their combined reheating and/or intercooling counterparts, but are expected to have a significantly smaller system size.

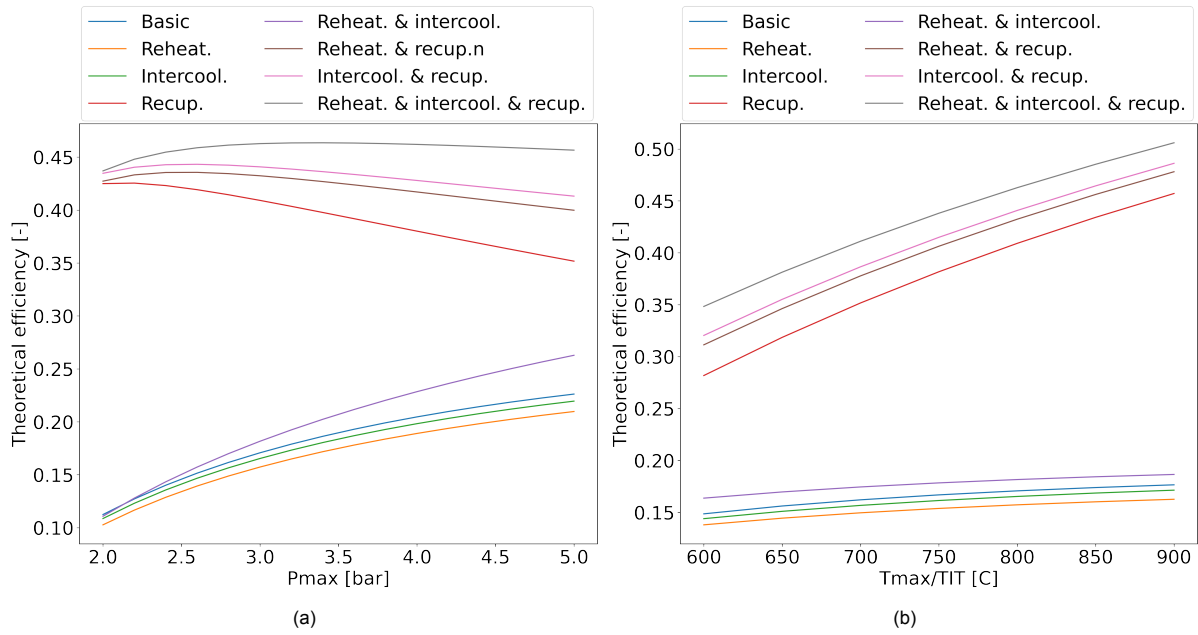


Figure 6.8: Comparison of the theoretical efficiency of different air BC configurations. Where figure (a) is at varying P_{max} , and figure (b) is at varying T_{max} .

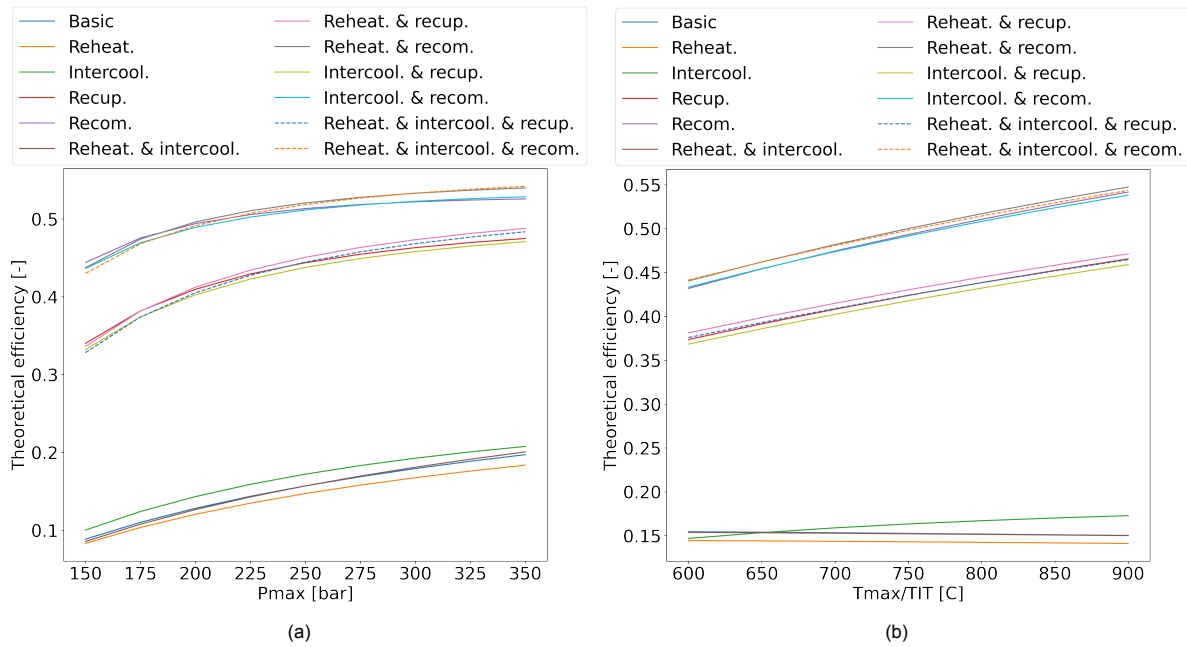


Figure 6.9: Comparison of the theoretical efficiency of different CO₂ SBC configurations. Where figure (a) is at varying P_{max} , and figure (b) is at varying T_{max} .

6.5. Final comparison and conclusions

The different comparisons of the configurations of the SRC, TCSRC, TCRC, BC, and SBC, resulted in the elimination of eighteen cycles, and sixteen remaining cycles to receive further attention. Now, in a similar manner as before, these sixteen cycles will be compared against one another. For each cycle and configuration, first P_{max} is varied while T_{max} is fixed at 800 °C, after which P_{max} is fixed while T_{max} is varied; the results are shown in figures 6.10 and 6.11 respectively. The pressure range and fixed pressure for P_{max} is identical to those previously applied specific to each cycle.

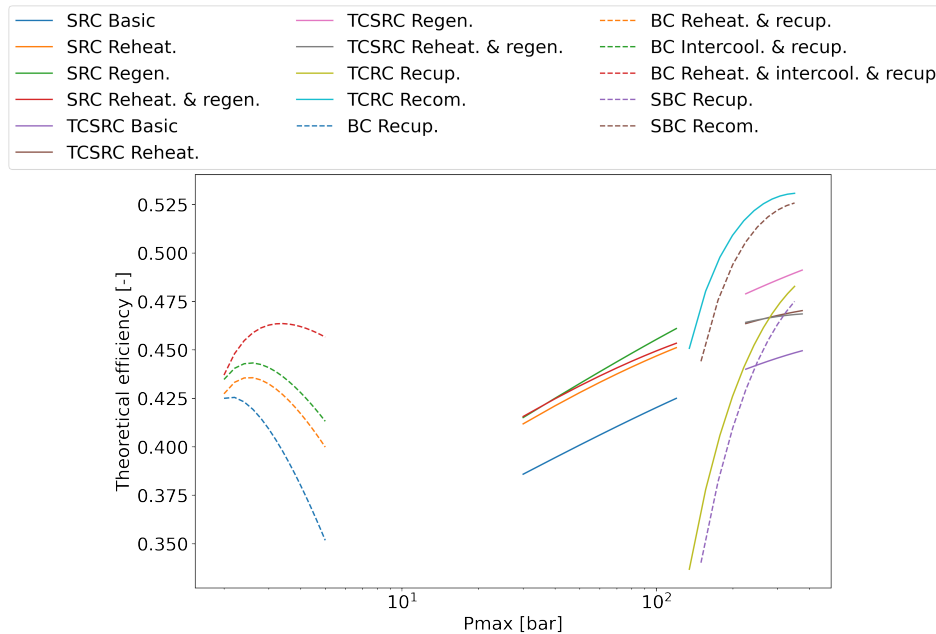


Figure 6.10: Comparison of the theoretical efficiency of the remaining configurations while varying P_{max} .

In figure 6.10 it can be seen that both the recuperation and recompression TCRC perform better regarding theoretical efficiency than their SBC counterparts at the same P_{max} ; however, at the same P_{max} , the TCRC configurations have a larger pressure ratio than the SBC configurations, as well as having a lower T_{min} . As can be seen in figure 6.11, the difference in theoretical efficiency between the TCRC configurations and SBC configurations becomes smaller at the same pressure ratio, while the remaining difference can be in part explained by the lower T_{min} of the TCRC configurations. As this condenser exit temperature is lower for the TCRC configurations than the cooler exit temperature of the SBC, the TCRC configurations are subjected to a larger heat input than those of the SBC, which reduces their theoretical efficiency. However, due to the CO_2 being in the liquid phase when exiting the condenser, the work required by the pump of the TCRC configurations is reduced compared to that of the compressor in the SBC. This results in a higher specific net work for the TCRC configurations, and as such, slightly higher efficiencies compared to those of the SBC configurations are not unexpected. Even though the TCRC configurations present with higher efficiencies, the choice is made not to omit the SBC configurations yet, as the differences are small and size considerations may still prove relevant.

From figure 6.11, it can also be seen that the theoretical efficiency of the SRC and TCSRC configurations are a maximum of 5% apart at a P_{max} of 60 and 300 bar respectively. While the higher pressure of the TCSRC configurations is expected to result in an increase of both size and cost, due to the higher efficiencies, the TCSRC configurations will still be considered until size and cost have been sufficiently analyzed. It can be seen in figure 6.10 that the remaining air BC configurations present with efficiencies comparable to those of the other cycles and configurations, with the main benefit of the former being the low values of P_{max} . Low operating pressures may result in decreased system complexity and cost, as well as requiring reduced safety measures. From figure 6.11 it can be seen that the efficiencies of the BC configurations become especially competitive at values of T_{max} over 800 °C. All of the remaining configurations of the air BC will thus be considered for the following part of this

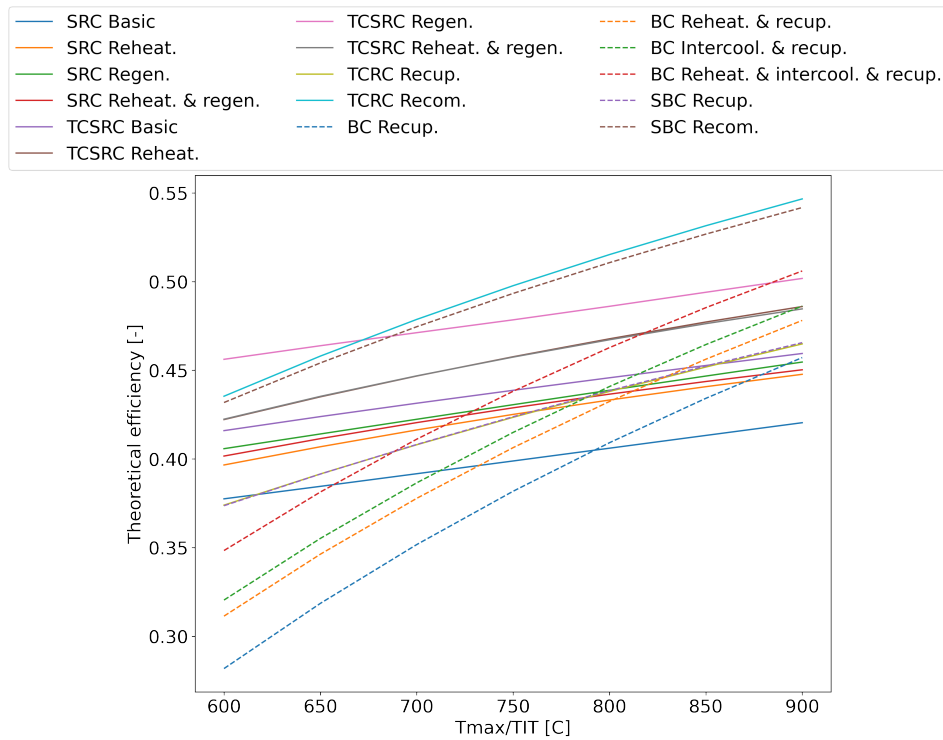


Figure 6.11: Comparison of the theoretical efficiency of the remaining configurations while varying T_{max} .

study. An overview of the remaining configurations which will receive further attention regarding size and cost is provided in table 6.2. In this table, the red marks denote those configurations which have been eliminated based on the results from the previous sections.

Table 6.2: Remaining waste heat recovery configurations.

Waste heat recovery system & medium / Configuration	SRC Water	TCSRC Water	TCRC CO ₂	BC Air	SBC CO ₂
Basic	x	x	x	x	x
Reheating	x	x	x	x	x
Intercooling				x	x
Recuperation			x	x	x
Recompression			x		x
Regeneration	x	x			
Reheating & intercooling				x	x
Reheating & recuperation			x	x	x
Reheating & recompression			x		x
Reheating & regeneration	x	x			
Intercooling & recuperation				x	x
Intercooling & recompression					x
Reheating, intercooling & recuperation				x	x
Reheating, intercooling & recompression					x

7

Size of configurations

The previous chapter provided an overview of efficient power cycles suitable for application in the waste heat recovery of the example case study. While efficiency is a very important parameter in any power conversion system, another important consideration is the size of such a system, especially when it comes to marine applications where space is limited. Therefore, in this chapter, the remaining cycles and configurations are compared based on their system size. While a complete waste heat recovery system consists of many components, the main focus will be on the heat exchangers, and some considerations regarding the size of the turbomachinery will be discussed. First, the size of the heat exchangers will be discussed, which includes the determination of heat transfer coefficients associated with the different heat exchangers in the remaining configurations. To determine the size of the heat exchangers, the models from the previous chapter will be further expanded with heat exchanger models. Using these expanded models, the mass flow rate within each configuration and its power output will be determined, which will finally result in the required heat transfer area and heat exchanger volume. Second, additional size considerations will be discussed, with the focus on the turbomachinery present within each cycle. Finally, conclusions are presented based on the heat exchanger size and the considerations regarding turbomachinery.

7.1. Heat exchanger size

To determine the size of the heat exchangers, the area of heat transfer must be calculated for each heat exchanger in the remaining configurations, which depends largely on the type of heat exchanger applied and its overall heat transfer coefficient. When choosing a type of heat exchanger, it is common practice to base a decision on several parameters, such as temperature, pressure, fluid phase, fouling, size, cost, and ease of maintenance. However, as the remaining 16 configurations have a combined number of 54 heat exchangers, the choice is made to compare all the cycles for two types of heat exchanger. The first heat exchanger type for which the configurations will be evaluated is the printed circuit heat exchanger (PCHE), which is known for being highly efficient and very compact, but is also relatively new and expensive. The second heat exchanger type is the shell and tube heat exchanger (STHE), which is widely used and considered to be a low cost solution; however, this type of heat exchanger is associated with significantly larger sizes than the aforementioned PCHE. For the remainder of this section, only these two types of heat exchanger are assumed, with the exception of open FWHs as these employ direct contact heat transfer through mixing of the fluids.

7.1.1. Overall heat transfer coefficients

As previously mentioned, an important parameter in the calculation of heat transfer areas is the overall heat transfer coefficient, which varies depending on fluid characteristics and conditions, as well as on the type of heat exchanger applied. In this section, the overall heat transfer coefficients are estimated by applying considerations regarding the operating conditions of the different heat exchangers, such as the fluid phases and pressures. These estimations follow from typical values of overall heat transfer coefficients as provided by a manufacturer of PCHEs [43] and literature [25] [122], which are displayed in table 7.1.

Table 7.1: Typical overall heat transfer coefficients of PCHEs and STHEs.

	\bar{U} [$Wm^{-2}K^{-1}$]
PCHE [43]	
LP gas cooler	500-1000
HP gas cooler	1000-4000
Water/water	7000-10000
STHE [25]	
LP gas/LP gas	5-35
HP gas/HP gas	150-500
Liquid/LP gas	15-70
HP gas/liquid	200-400
Liquid/liquid	150-1200
Vapor condenser	300-1200
Steam condenser	1500-4000
STHE [122]	
Water/water	800-1500
Gas/gas	10-50
Gas/water	20-300
Flue gas/steam	30-100
Steam condenser	1000-1500
Vapor condenser	700-1000

As previously mentioned, heat transfer coefficients depend on fluid characteristics and conditions; these include density, viscosity, and heat capacity, amongst others [122]. Of these properties, some considerations regarding the density of the fluids will be given in addition to the values provided in table 7.1 in order to estimate the overall heat transfer coefficients. Fluids with a high density, such as liquids and high pressure fluids, typically have relatively high overall heat transfer coefficients compared to low density fluids, such as low pressure gases. This can also be seen in table 7.1, where the primary differentiation between the overall heat transfer coefficients is a result of the phases and pressures of the fluids.

The condensers in the SRC and TCSRC operate with the same fluids and phases at the same pressures, and the heat transfer coefficients are therefore chosen equal. Regarding the PCHEs, the lower limit of the water/water application is chosen; while for the STHEs, a value of 2000 is chosen as the average of the steam condenser values from table 7.1.

Due to the higher pressure, and the presence of liquid phase, the heat transfer coefficients of the heater in the SRC and TCSRC are assumed higher than those of the reheater. Additionally, the heat transfer coefficient of the heater in the TCSRC is estimated to be higher than that of the heater in the SRC, as it operates at a much higher pressure; this is similarly applied to the reheaters, although the pressure in the reheater of the TCSRC is only slightly higher than that of the SRC. Regarding the PCHEs, it is assumed that the heater and reheater act as LP gas coolers, where the reheater operates at a relatively low pressure of only a few bar; therefore, the lower limit of the LP gas cooler chosen for the reheater of the SRC and an intermediate value of 750 is chosen for the heater of the SRC. For the TCSRC, values of 1000 and 600 are chosen for the heater and reheater respectively.

Regarding the STHEs, a value of 40 is chosen for the reheater of the SRC, which is approximately the average of the LP gas/LP gas, gas/gas, and flue gas/steam values from table 7.1; a slightly higher value is chosen for the reheater of the TCSRC. For the heater of the SRC, a value of 65 is estimated from the value of the reheater as well as through intermediate values of liquid/LP gas and gas/water from table 7.1. Again, the heat transfer coefficient of the heater in the TCSRC is assumed higher than that of the heater in the SRC.

The heat exchangers of the TCRC and SBC operate in the supercritical region, which creates some special circumstances regarding fluid behaviour. When CO_2 is close to or above its critical pressure and temperature, it has a density similar to that of a liquid and as such, heat transfer coefficients in the

supercritical region are estimated to be between those associated with a (HP) gas and those associated with a liquid.

The heat transfer coefficients of the condenser in the TCRC and the cooler in the SBC are taken equal; this assumption is made due to the fact that while the pressure in the cooler of the SBC is higher than that of the condenser in the TCRC, the latter experiences condensation which is typically associated with an increased heat transfer coefficient as well. Regarding the PCHEs, the average of the upper limit of the HP gas cooler and lower limit of the water/water from table 7.1 is taken for the heat transfer coefficient of both the condenser in the TCRC and the cooler in the SBC. Regarding the STHEs, approximately the average of the HP gas/liquid, the liquid/liquid, the two vapor condenser, the water/water, and the gas/water values in table 7.1 is chosen.

The heaters of the TCRC and the SBC operate at lower pressures than the recuperators, and are therefore estimated to have lower heat transfer coefficients. Additionally, due to the slightly higher pressures in the SBC compared to the TCRC, the heat transfer coefficients of the heaters and recuperators of the SBC are estimated to be slightly higher than those of the TCRC. Regarding the PCHEs, a value below the upper limit of the LP gas cooler from table 7.1 is chosen for the heater of the TCRC, and a slightly higher value is chosen for the heater of the SBC due to the higher pressure. Additionally, it is estimated that the heat transfer coefficients of the heaters in the TCRC and SBC are higher than that of the SRC due to the higher pressure in the former two and the behaviour of $s\text{CO}_2$; however, the heat transfer coefficient of the heater in the TCSRC is predicted higher than those of the TCRC and SBC because the pressure of the TCSRC is even greater.

Regarding the STHEs, the heat transfer coefficients of the heaters in the TCRC and SBC follow from the approximate average of the liquid/LP gas, the gas/gas, and the gas/water values from table 7.1, with the coefficient of the SBC being slightly higher. Similar to the heaters, the heat transfer coefficients of the SBC and TCRC are again predicted to be between those of the SRC and TCSRC. For the PCHE recuperators of the TCRC and SBC, an intermediate value of the HP gas cooler in table 7.1 is chosen, where similar to the heaters, the recuperators of the SBC are assumed to have a slightly higher heat transfer coefficient due to the slightly higher pressures. Regarding the STHEs, the heat transfer coefficient for the recuperators are estimated from the average of the HP gas/HP gas, the HP gas/liquid, and the gas/water values from table 7.1.

The pressures in the BC can be considered to be low and as such, the heaters, reheaters, and recuperators are estimated to have the same heat transfer coefficients; similarly, the coolers and intercoolers are also estimated to have the same heat transfer coefficients. Regarding the PCHEs, the lower limit of the LP gas cooler from table 7.1 is chosen for the heaters, reheaters, and recuperators; the upper limit of the LP gas cooler is chosen for the coolers and intercoolers. Regarding the STHEs, the average of the LP gas/LP gas and the gas/gas values in table 7.1 is taken for the heaters, reheaters, and recuperators. For the coolers and intercoolers, the average of the Liquid/LP gas and the gas/water values is chosen. An overview of the applied overall heat transfer coefficients is provided in table 7.2.

Table 7.2: Applied overall heat transfer coefficients for the two types of heat exchanger.

	$\bar{U} [Wm^{-2}K^{-1}]$		
	(Inter)cooler/condenser	Recuperator	(Re)heater
PCHE			
SRC	7000		(500)/750
TCSRC	7000		(600)/1000
TCRC	5500	2500	850
BC	1000	500	500
SBC	5500	2600	900
STHE			
SRC	2000		(40)/65
TCSRC	2000		(50)/85
TCRC	650	250	75
BC	100	25	25
SBC	650	260	80

7.1.2. Modelling

In this section, the approach to calculate the heat transfer area of each heat exchanger is described. First some assumptions regarding the operating conditions of the heat exchangers are presented, followed by the relevant calculations applied in the models of each waste heat recovery configuration.

To provide a clear basis for the comparison of the different cycles and configurations, assumptions regarding the mass flow rate and the inlet and outlet temperatures of the hot source service fluid (cathode exhaust gas) will result in each waste heat recovery system having the same heat input. The assumptions applied in the calculations of the heat transfer area are as follows:

- The hot source service fluid is the cathode exhaust gas from the SOFC, which is assumed to have a standard air composition. The waste heat from the SOFC will be recovered using a heat exchanger on the cathode side outlet, which will contain heated excess air as is common for SOFCs (see section 2.4.1). A visualization of an SOFC is provided in figure 2.1.
- The mass flow rate of the cathode exhaust gas is the same for all waste heat recovery configurations, and taken to be 14 kg/s.⁽¹⁾
- The cold source service fluid is water, and its mass flow rate is dependent on the heat transfer duty.
- As per the assumptions from section 6.1, the inlet temperatures of the hot and cold source service fluids are 850 °C and 15 °C, respectively.
- The outlet temperature of the hot source service fluid from the (re)heaters is fixed at 750 °C + ΔT_{HEX} (= 765 °C), this leaves sufficient heat to allow air and fuel to be preheated to 750 °C, which is required to limit the temperature gradient across the fuel cell and prevent high thermal stress and decreased reaction kinetics [66].
- The inlet pressure of the hot and cold source service fluid is $P_{amb}/\Delta P$, where the ambient pressure P_{amb} is 1.01325 bar.
- Open FWHs employ direct-contact heat transfer, which is associated with high heat transfer rates [122]; therefore, their size compared to other heat exchangers is assumed insignificant and the influence on the heat transfer area and system size is omitted henceforth, unless specified otherwise.
- The previously determined overall heat transfer coefficients are assumed constant. This has been similarly applied by Schöffler [105].
- All of the heat exchangers apply counterflow operation, and the pressure drop over the length of the flow is assumed linear.
- Unless specified otherwise, the assumptions from section 6.1 are still in effect.

The mass flow rate (\dot{m}_p) of each waste heat recovery configuration must be determined to calculate the heat transfer area. The mass flow rate follows from a balance of the heat flows through the (re)heaters. In configurations without reheating, the balance of the heat flows through the heater (H) results in the system mass flow rate by applying

$$\dot{m}_{H,P} = \dot{m}_{H,S} * \frac{h_{H,S,in} - h_{H,S,out}}{h_{H,P,out} - h_{H,P,in}}, \quad (7.1)$$

in which the mass flow rate of the service fluid ($\dot{m}_{H,S}$) is the assumed 14 kg/s.

In configurations applying reheating, a balance must be made which divides the cathode exhaust gas across the two heaters, resulting in the hot side outlet flows of both the heater and reheater having

⁽¹⁾The value of the cathode air mass flow rate follows from a scaling applied to Schöffler [105], where the flue gas from a 380 kW SOFC was determined to have a molar flow rate of 95.29 mol/s. Combined with the case study in this research being a 2 MW SOFC and applying the assumption that the flue gas consists entirely of air, this results in an approximate mass flow rate of 14 kg/s.

the aforementioned fixed temperature of 765 °C. Starting with the heat balance of the heater as in equation (7.1) and that of the reheater (RH) being

$$\begin{aligned} \dot{m}_{RH,P} &= \dot{m}_{RH,S} * \frac{h_{RH,S,in} - h_{RH,S,out}}{h_{RH,P,out} - h_{RH,P,in}}, \\ \text{with } \dot{m}_{RH,P} &= split_{RH} * \dot{m}_{H,P} \\ \text{and } \dot{m}_{RH,S} &= 14 \text{ kg/s} - \dot{m}_{H,S}. \end{aligned} \quad (7.2)$$

Here, $split_{RH}$ equals 1 for configurations in which the process fluid does not experience a flow split before entering the reheater. The specific enthalpies on the process fluid sides have been determined in section 6.2, while the specific enthalpies on the service fluid sides can be determined using Cool-Prop and the previously applied assumptions of the inlet and outlet temperatures and pressures. After rewriting equations (7.1) and (7.2) for $\dot{m}_{H,P}$ and combining them, the mass flow rate of the hot service fluid through the heater and reheater can be obtained by applying

$$\begin{aligned} \dot{m}_{H,S} &= \frac{14 * a}{1 + a}, \\ \text{and } \dot{m}_{RH,S} &= 14 - \frac{14 * a}{1 + a}, \\ \text{in which } a &= \frac{1}{split_{RH}} * \frac{h_{RH,S,in} - h_{RH,S,out}}{h_{RH,P,out} - h_{RH,P,in}} * \frac{h_{H,P,out} - h_{H,P,in}}{h_{H,S,in} - h_{H,S,out}}. \end{aligned} \quad (7.3)$$

Solving these equations will result in the mass flow rate of the hot source service fluid in the heater and reheater. Finally, when inserting the obtained value of $\dot{m}_{H,S}$ into equation (7.1), the mass flow rate (\dot{m}_p) of the waste heat recovery system is determined.

Inserting the obtained mass flow rates of the different configurations into

$$P_e = \dot{m}_p * \frac{W_{net}}{1000} * \eta_{gen} \quad (7.4)$$

will result in the electric power output of each system. Figure 7.1 shows the resulting power outputs of the different configurations; the mass flow rates associated with these power outputs are provided in appendix B, table B.1.

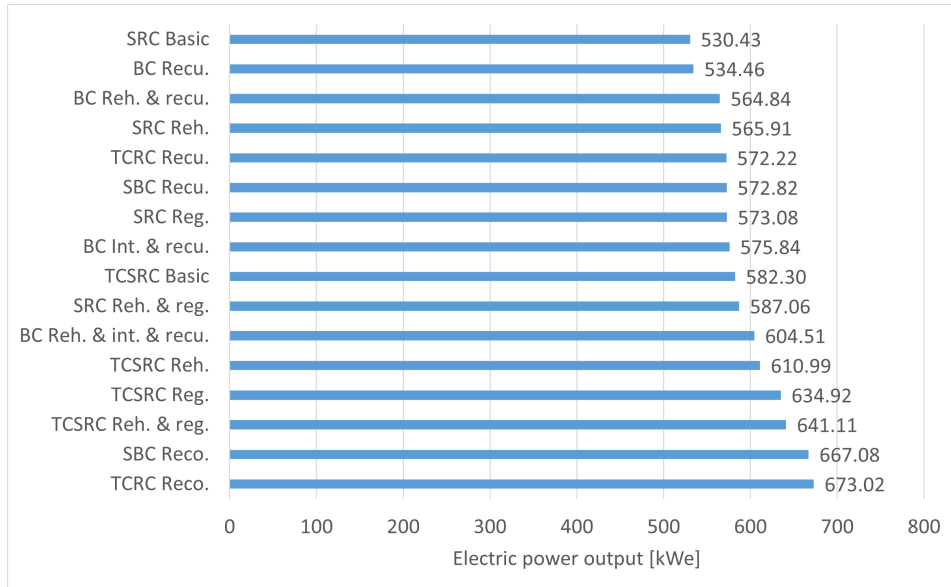


Figure 7.1: The electric power output of the different configurations when applied with the same heat input.

Now that the mass flow rates of the configurations are known, the heat transfer area of each heat exchanger can be calculated.

Two typical approaches to determine the area of heat transfer are the logarithmic mean temperature difference method, and the effectiveness-NTU method [53]; however, both of these approaches assume and require that the fluids have a constant heat capacity, or specific heat. Especially CO₂ in the vicinity of the critical point has a very inconsistent specific heat, and as such, the aforementioned methods will not be used to determine the heat transfer area. Instead, by applying

$$A = \int_0^x \frac{d\dot{Q}}{\bar{U}(T_H(x) - T_C(x))} dx, \quad (7.5)$$

of which the logarithmic mean temperature difference method is the result when assuming constant heat capacity, the influence of varying heat capacities is accounted for [80] [106].

The discretization of this equation results in the flow being split into "blocks" of equal heat transfer, and therefore a linear enthalpy change. The temperature at each point of the flow can now be determined from the pressure and enthalpy at that point; finally, the heat transfer area of each block is calculated and the sum of all the segments results in the total area of heat transfer.

Excluding open FWHs, there are three types of application for the heat exchangers in the remaining configurations, namely heaters, coolers or condensers, and recuperators; the heat transfer area calculations of these three types of application will be briefly discussed.

Firstly, the heat transfer area of the recuperators can be determined from several parameters, of which it is known that the working medium of the cycle is both the process and service fluid, and the previously obtained mass flow rate. The specific enthalpy and pressure at the inlet and outlet on both the hot and cold side are known following the first law models from section 6.2. As previously mentioned, the heat transfer duty is split into equal segments ($\Delta\dot{Q}$), and the specific enthalpy and pressure at each point of the process and service fluid flow follow from a linear change across the flow. Using these, the temperature of both flows at every point can be obtained, and by applying the discretized form of equation (7.5), the area of each segment and resulting total area of heat transfer can be determined.

The area of a (re)heater is determined similarly to that of a recuperator, as the specific enthalpies and pressures at the inlet and outlet on the process and service side are known.

For the coolers and condenser, again a similar approach is taken to that of a heater, with the main difference being the mass flow rate of the service fluid depending on the heat duty. To solve this problem, first an initial value for the mass flow rate of the service fluid is assumed and verified to be insufficient to support the cooling load. Subsequently, by applying

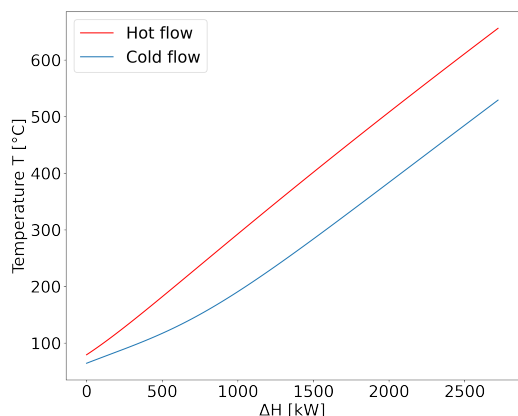
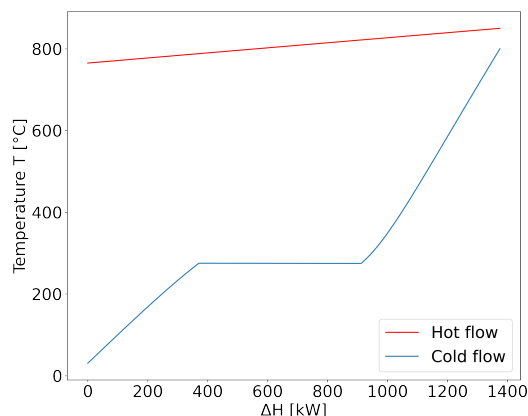
$$h_{S,out} = \dot{m}_P * \frac{h_{P,in} - h_{P,out}}{\dot{m}_S} + h_{S,in}, \quad (7.6)$$

an initial value for the specific enthalpy of the service fluid at the outlet of the heat exchanger is determined.

To obtain the actual value of the mass flow rate of the service fluid, an iteration is conducted which holds the condition of ΔT_{HEX} being 15 degrees. When this condition is breached, the point of occurrence in the service fluid is assigned a new temperature and subsequently obtained specific enthalpy; using the rewritten form of equation (7.6) at that specific point, a new mass flow rate can be determined. Again, the specific enthalpy of the service fluid at the outlet is determined through equation (7.6), and the iteration is executed until the condition is no longer breached; this results in the mass flow rate of the service fluid being sufficient to support the heat duty, while the temperature difference between the hot and cold fluid at each point in the heat exchanger does not drop below the previously assumed value for ΔT_{HEX} of 15 °C.

In configurations experiencing a flow split, the mass flow rate of the process fluid through certain heat exchangers is dissimilar from the overall system mass flow rate; as such, the mass flow rate of the process fluid in such an affected heat exchanger is multiplied by the corresponding flow split.

Figures 7.2a, 7.2b, and 7.2c show the temperature-enthalpy change diagrams of the hot and cold flows through the recuperator of the CO₂ TCRC, the heater of the basic SRC, and the cooler of the CO₂ SBC, respectively; these plots are obtained by applying the discussed assumptions and calculations for the case regarding the PCHE-type.

(a) Recuperator of the recuperation CO₂ TCRC

(b) Heater of the basic SRC

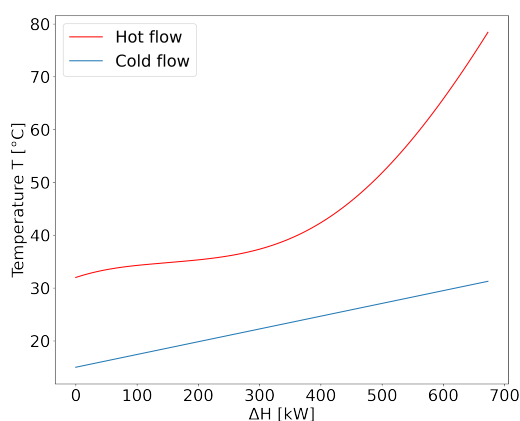
(c) Cooler of the recompression CO₂ SBC

Figure 7.2: Temperature-enthalpy change diagram examples of the three application types for the PCHEs

7.1.3. Results & conclusions

In this section, the results from the models extended with the heat transfer calculations are discussed.

The results of the heat transfer area calculations for both the case applying PCHEs and the one applying STHes are provided in figures 7.3 and 7.4, respectively. From these results it is evident that in both cases the heat transfer areas of the (TC)SRC configurations are smallest, followed by the considerably larger heat transfer areas of the CO₂-based cycles. The largest area of heat transfer is required by the air BC configurations, which is significantly larger than the heat transfer areas of the other cycles and configurations, and predominantly due to the share of the recuperators.

While the area of heat transfer relates in part to the size of the heat exchangers, it does not define the size; therefore, the volume of the heat exchangers has been determined as well. This is done by applying a value for the heat transfer area per unit volume of heat exchanger, which depends not only on the type of heat exchanger, but also on the pressure within the heat exchanger. In practice, these values differ per heat exchanger and the associated pressure; however, for simplicity, some generalizations are made.

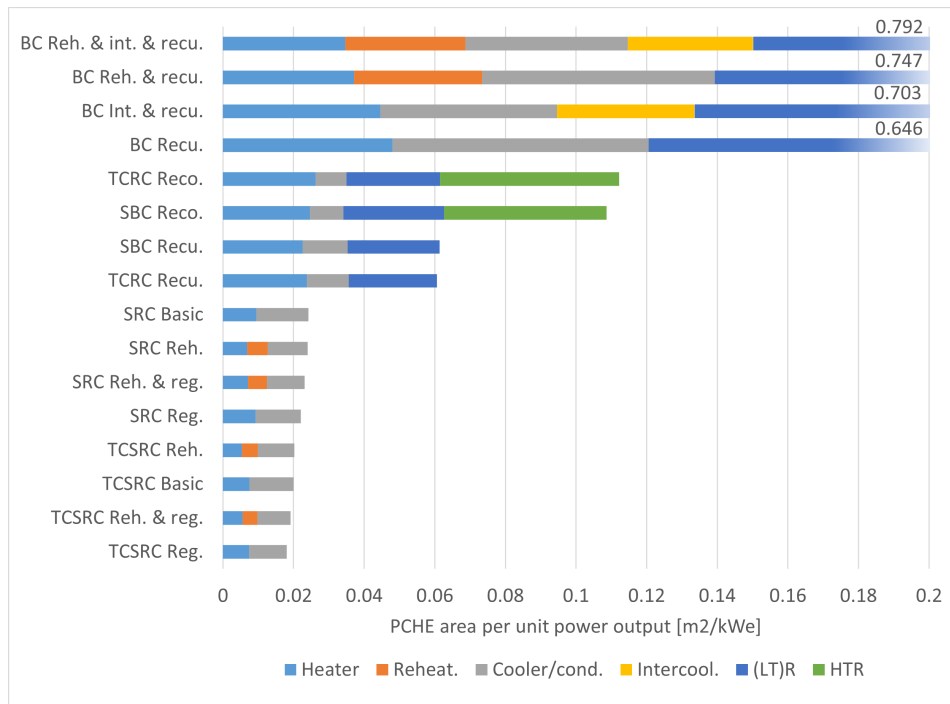


Figure 7.3: Resulting heat transfer area per unit electric power produced for all PCHEs in each configuration.

Firstly, the heaters and condensers of both the SRC and TCSRC configurations contribute roughly the same amount of heat transfer area to the total, as such, the area per unit volume is estimated for a pressure between that of the heaters and condensers of both cycles, respectively. Secondly, the main contribution to the heat transfer area of the TCRC and SBC configurations is due to the recuperators and heaters, which operate within the same pressure range; therefore, one value for the area per unit volume of the heat exchangers has been assumed for the TCRC and SBC, based on the respective pressures of the recuperators and heaters. Finally, all the heat exchangers of the air BC configurations operate within the same pressure range, and as such, one single value for the area per unit volume is assumed.

Two typical values of the area per unit volume are obtained from the manufacturer of the PCHEs [43], namely $1300 \text{ m}^2/\text{m}^3$ at 100 bar, and $650 \text{ m}^2/\text{m}^3$ at 500 bar. For the PCHEs of the SRC, the area-to-volume ratio is estimated to be $1400 \text{ m}^2/\text{m}^3$, while a ratio of $1200 \text{ m}^2/\text{m}^3$ is chosen for the TCSRC; these values are approximated by comparing the average pressures of the SRC and TCSRC to the 100 bar specified by the manufacturer.

As previously mentioned, the estimation of the area-to-volume ratio of the heat exchangers in the TCRC and SBC is based on the pressures within the recuperators and heaters. As such, the PCHEs of the TCRC and SBC are subjected to a ratio of $1100 \text{ m}^2/\text{m}^3$ and $1050 \text{ m}^2/\text{m}^3$, respectively. Finally, the total volume of the PCHEs of the BC configurations has been determined through an area-to-volume ratio of $1450 \text{ m}^2/\text{m}^3$.

For STHEs, the heat transfer area per unit volume of the heat exchanger lies in the range of $50\text{--}100 \text{ m}^2/\text{m}^3$, and while no corresponding pressures are specified, operating conditions ranging from pressures of over 1000 bar to a high vacuum are mentioned [107]. As such, the upper limit of $100 \text{ m}^2/\text{m}^3$ is assumed to correspond to 0.01 bar, and the lower limit of $50 \text{ m}^2/\text{m}^3$ is assumed to correspond to 1000 bar; applying a simple extrapolation this would amount to a decrease of $0.05 \text{ m}^2/\text{m}^3$ per 1 bar of increased pressure.

When applying the aforementioned assumptions, this results in area-to-volume ratios of 98.5, 92.5, 89.25, 88, and 99.9, for the STHEs of the SRC, TCSRC, TCRC, SBC, and BC, respectively. While these ratios are rough estimations, and might present differently in practice, it is assumed sufficient for the purpose of comparison.

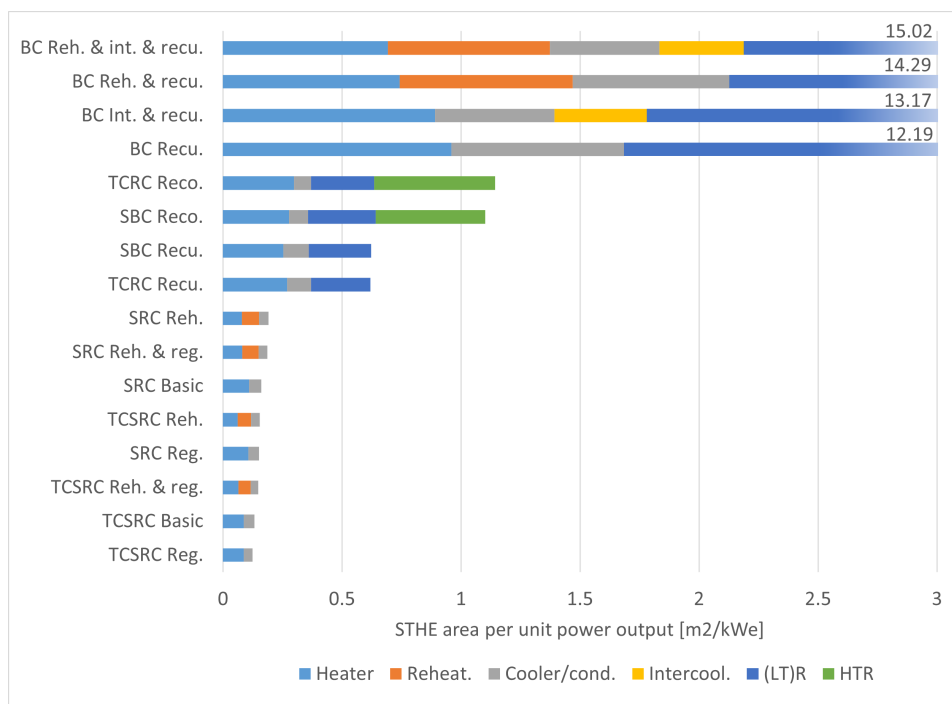


Figure 7.4: Resulting heat transfer area per unit electric power produced for all STHEs in each configuration.

The total resulting volumes associated with the heat transfer areas of the case applying PCHES and the one applying STHEs are provided in appendix B, table B.2. The first observation is that in the case PCHES are applied, the size of the heat exchangers regarding their volume becomes relatively small, and when taking into account the possible size of other components present in such power cycles, the contribution of the heat exchangers might only have a limited influence on the total system volume. However, when comparing the different cycles and configurations, there are still relatively large differences between the (TC)SRC configurations, the CO₂-based cycles, and the air BC configurations. When looking at the case applying STHEs, it can be concluded that especially the air BC configurations present with undesirable volumes.

Important notes

Following the models and the resulting heat exchanger sizes associated with the different configurations, a number of points regarding important considerations will be touched upon in this section.

First, the results displayed in table B.2 follow from a number of assumptions as described in section 7.1.2; one of which was that the mass flow rate of the cold source service fluid is dependent on the heat duty, and is obtained by imposing the minimum temperature difference (ΔT_{HEX}) in the heat exchanger. However, this assumption causes an issue to arise in the condensers of the RC-based configurations as the mass flow rate of the cooling water becomes very high. This is the result of the combination of T_{min} being set at 30 °C, the cooling water temperature assumed to be 15 °C, and the aforementioned ΔT_{HEX} , which is still taken at 15 °C; these factors together require the supply of a very high mass flow rate of cooling water to support the heat duty. The obtained mass flow rates of the cooling water in the condensers range from 178.93 kg/s in the recompression TCRC, to 554.07 kg/s in the basic SRC. This is clearly unlikely to be achieved and a less than satisfactory result; however, it should be noted that in practice, through slight variations of parameters such as T_{min} , ΔT_{HEX} , or the cooling water inlet temperature, the mass flow rate of the cooling water can be significantly reduced while only slightly affecting the system efficiency or total area of heat transfer. Therefore, the negative impact of such high mass flow rates in the condensers of the RC-based configurations will not be considered at this time.

Second, while in reality the pressure drop varies per heat exchanger application, it is outside the

scope of this research to account for different pressure drops and the assumption from section 6.1 still stands.

Similarly, the overall heat transfer coefficients may be more accurately determined; however, it falls outside the scope of the present research for this to be considered in detail; this applies to the heat transfer area per unit volume ratios as well, which are estimated for the sole purpose to approximate and compare the size of the different configurations.

Finally, the value of the mass flow rate of the hot source cathode exhaust exiting the SOFC system is estimated using the research from Schöffler [105]; however, it is considered out of scope to determine the detailed electrochemical operation of the SOFC system to obtain a more accurate value of the exhaust gas mass flow rate.

7.2. Additional size considerations

The sizes of the heat exchangers presented in the previous section provide valuable insights into the variations between the different configurations. However, knowing the size of the heat exchangers is not sufficient to draw conclusions regarding the total system size of the configurations, especially when taking into consideration that there might be significant differences in the size of other components. Therefore, this section will discuss other relevant size considerations that should be taken into account when comparing different power cycles.

Besides heat exchangers, power cycles such as those investigated in this study have a number of other components in common; consisting of turbomachinery, gearboxes, generators, piping, and control systems, to name a few. When looking at the example of an 8 MW CO₂ waste heat recovery module in figure 7.5, it can clearly be seen that such systems are highly complex, and consist of far more components than those displayed in the PFDs provided throughout this paper to show its functioning. Unfortunately, there is hardly any concrete information or data available to calculate the exact size of all components, and thus it is difficult to determine the combined total volume of a power cycle. Due to the lack of a detailed sizing method, some basic sizing considerations are discussed with the focus on turbomachinery, as these components are expected to show the largest variations between the different cycles. Furthermore, it is suggested to investigate the detailed sizing of components as a topic for future research.



Figure 7.5: Echogen's 8 MW CO₂ RC-based waste heat recovery module EPS100 [28].

When discussing turbomachinery, it is common to express its size in the work required or produced; however, due to the cycles investigated in this study having different turbomachinery setups and work-

ing fluids, power does not translate well to the dimensions of the turbomachinery. It is therefore decided to focus on some other parameters that influence the size of a turbomachine as well.

Firstly, the working fluid, and specifically its properties, have a large impact on the required size of a turbomachine. Where high density fluids allow for small turbomachinery, and low density fluids require larger turbomachinery [17]. Secondly, the size depends significantly on the type of turbomachine applied, this includes the distinction between different flow configurations and the number of stages required, which is subsequently related to the pressure ratio of the turbomachine, amongst others [39]. Combining the power requirement or power output with these two additional parameters allows for some estimations to be made regarding the comparison of the size of the turbomachinery in the different cycles.

7.2.1. Turbines

The first type of turbomachinery components to be investigated are the turbines, which will be discussed regarding the aforementioned parameters. To determine the delivered work of each turbine, the equation of the specific work, as previously provided in section 6.2, can be multiplied with the mass flow rate of the working fluid through the turbine. The delivered work is the smallest for the turbines of the SRC and TCSRC configurations, followed by those of the CO₂ TCRC and SBC configurations, and is significantly larger for the air BC configurations.

Regarding the working fluid, the density plays a significant role, and as a result, the relatively high density of sCO₂ compared to steam and air results in smaller size requirements for the turbines of the TCRC and SBC configurations.

The number of stages is, amongst others, dependent on the pressure ratio; the turbine(s) of the TCSRC configurations have the largest pressure ratio, followed by those of the SRC configurations, finally the turbines of the TCRC, SBC, and BC configurations all have approximately the same low pressure ratio.

7.2.2. Compressors & pumps

The comparison of the compressors and pumps is slightly different since the former only operate on a gaseous medium and the latter on a liquid; however, some conclusions can still be drawn.

Firstly, similar to the turbines, the required power is lowest for the SRC and TCSRC, followed by the CO₂ TCRC and SBC, and is the largest for the air BC; additionally, due to pumps operating on a liquid, they are often smaller than compressors. It should be noted that the compressors of the TCRC configurations experience both liquid CO₂ and sCO₂, and while both liquid and supercritical CO₂ have a quite high density, the density of water is still higher, which is in favour of the SRC and TCSRC.

Since pumps and compressors operate in different regimes, it is difficult to compare them based on the number of stages; however, the pressure ratio across the pump/compressor is still relevant, and the TCRC, SBC, and BC configurations operate on a significantly smaller pressure ratio than the SRC and TCSRC configurations.

7.2.3. Turbomachinery in literature

While there has been conducted little research into the exact sizing of turbomachinery, a few studies have been found to provide general remarks and claims regarding the size of turbomachinery and the comparison of its application in different cycles. In this section, the comparative remarks made by these studies are acknowledged in support of the conclusions to be drawn regarding system sizes.

The most frequent remark made on the size between sCO₂ cycles and steam cycles is that the turbomachinery of the former can be as much as ten times smaller than that of the latter. This claim has been made by Ahn et al. [3], who reviewed sCO₂ cycles and assigned that scaling factor to the turbomachinery size due to the higher density of sCO₂, and therefore its decreased volumetric flow rate. In addition, Ahn et al. [3] remarked that the overall system size of an sCO₂ power system could be four times smaller compared to an SRC system, and further found the size per MW of power for steam, air, and CO₂ systems to be 22, 9, and 4 m², respectively. Multiple other studies also applied the aforementioned sizing factor between the turbomachinery of an sCO₂ and steam cycle, such as that conducted by Li et al. [70], who investigated a large coal-fired sCO₂ power plant, and Noaman et al. [86], according to which a steam turbine with ten to fifteen stages would translate to an sCO₂ turbine of

approximately four stages, with again the higher density and lower volumetric flow rate being pointed out as the dominant factor.

A few other studies that draw similar conclusions were conducted by Ishiyama et al. [54], in which a rough component volume calculation results in the turbomachinery size of an sCO₂ system to be approximately 40% of a comparable steam turbine, and Persichilli et al. [91], where the footprint of an sCO₂ power plant is estimated to be under 2/3rds of an equivalent steam power plant. However, even larger differences were put forth by Dostal [23], who compared the turbines of a steam, helium, and sCO₂ nuclear power plant.

While only limited research on the exact size of turbomachines has been found, some sources do provide quantified sizing for the turbomachinery of sCO₂ cycles; unfortunately, this has not been the case for air and steam cycles. For example, Brun et al. [17] put forth that an sCO₂ power cycle with an output of 1 MWe would have a compressor diameter of almost 10 cm, which was likewise described by Biondi [14]. A similar size range was put forth by Fleming et al. [33], where the turbomachinery of sCO₂ cycles in the 0.3-3.0 MWe power range would be of the single stage radial type and can be associated with rotational speeds of 75000-30000 rpm and diameters of 5-14 cm.

As can be seen in figure 7.6, a single stage turbine of an sCO₂ power cycle with an electric power output below 1 MW would have shaft speeds above 100000 rpm and diameters below 10 cm.⁽²⁾

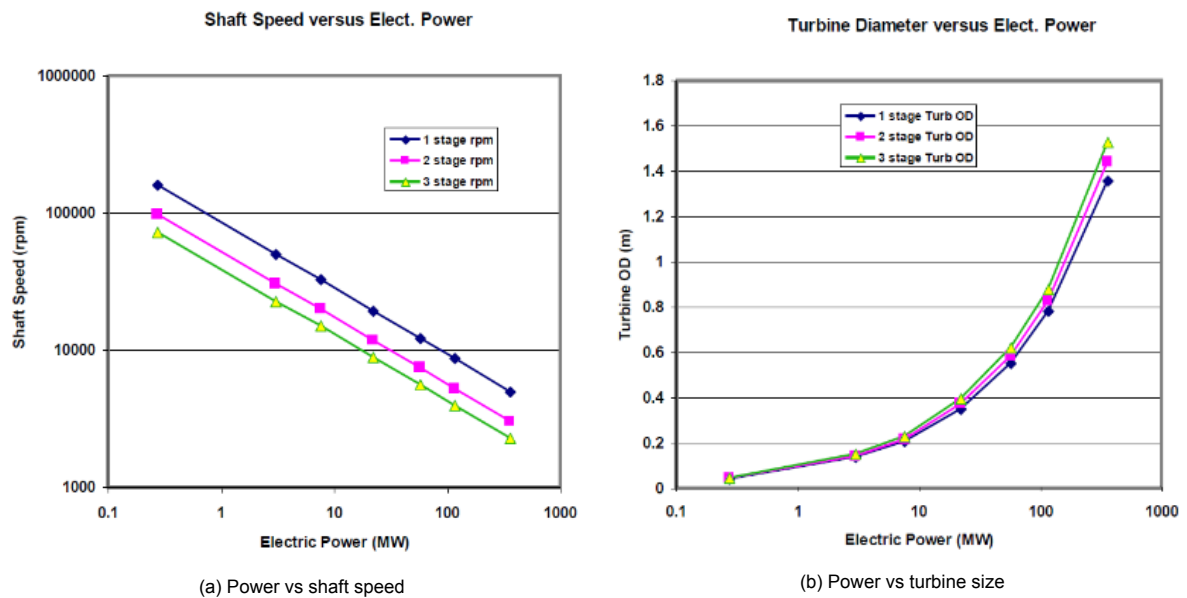


Figure 7.6: CO₂ recompression SBC turbine shaft speed, size, and electric power relations [33].

7.2.4. Other components

As mentioned before, energy conversion systems such as the power cycles investigated in this study consist of many more components than turbomachinery and heat exchangers. In this section, some general remarks and considerations are described in relation to a few other types of components.

The first is piping, which can differ in size substantially depending on the design and operating conditions of the cycle and configuration. It stands to reason to expect larger and more complex configurations to present with larger piping systems, simply because the main sizing factor of piping is the length of piping required. Configurations with the most processes will require the most piping to transport the working fluid to and from each process. To give an example, the combined reheating, intercooling, and recuperation air BC consists of five heat exchangers, two turbines, and two compressors, which amounts of ten connections being made with piping. In contrast, the basic SRC has two heat exchangers, one turbine, and one pump; which means it requires only four connections of piping.

⁽²⁾The figures refer to a cycle operating with a pressure ratio of 2.6 and a TIT of 650 °C.

Therefore, it can reasonably be expected the former would not only be larger due to the additional heat exchangers and turbomachinery, but also due to the increased piping requirements. However, the length of piping is not the only factor that determines the size of these components, and while it has a smaller influence, the diameter and thickness of the piping should also be considered. High density, high pressure fluids need to be transported through thick walled piping and casings, and would constitute an increase in the size of the piping system. This means that high pressure systems such as the TCSRC will require much thicker piping than the air BC configurations for example. As such, when it comes to piping, more complex configurations in terms of the number of main components, as well as systems operating at high pressures, will present with the largest space requirements.

The second type of component that will be discussed are the gearboxes, which are a crucial part connecting the turbines to the generators. The generators convert mechanical input power into the electrical power output, but they are typically operated on a designated rotational speed. As the turbines in the investigated systems may present with varying rotational speeds, it stands to reason that different cycles may require different gearboxes. In the previous section, some numbers were already mentioned regarding the rotational speeds of sCO₂ turbines, which can be as high as 100000 rpm. In that example, the high rotational speed of the turbine output shaft is a result of the small turbine diameter of around 10 cm. Therefore, if a waste heat recovery system can be equipped with a relatively small diameter turbine, it is likely the output shaft will have a relatively high rotational speed, which will subsequently require a gearbox able to handle a relatively large reduction ratio. It should be noted that the aforementioned considerations are only applicable when assuming each waste heat recovery system is equipped with the same type of generator and associated designed rotational speed. In that scenario, it can be expected that the small turbomachinery diameters associated with the CO₂-based cycles are likely to present with the largest gearbox requirements, followed by those of the air BC configurations, and finally the SRC and TCSRC systems.

Lastly, the waste heat recovery systems investigated require intricate control systems, and while it can be expected that the more complex systems and those with more severe operating conditions, such as high pressures, will require more extensive control systems, there has been found little to no literature supporting this substantially. Therefore, while control systems might have considerable spatial requirements and each investigated configuration is equipped with at least one such system, there can be said little of the differences between the various configurations, and it is presumed that these differences are small.

The components discussed in this section do not entirely make up a waste heat recovery system, with many more components being present; however, the considerations have been described nonetheless to provide some insight on how to approach the topic of spatial considerations and system sizing.

7.3. Conclusions

It has become evident that determining the volumetric size of power cycles is a difficult task, and is surprisingly enough a relatively unexplored topic in research. While no quantifiable conclusions will be drawn regarding the size of the turbomachines or the components discussed in the previous section, some general conclusions are presented.

Starting with the turbomachinery, it is expected that CO₂-based power cycles are likely to be equipped with significantly smaller turbomachinery than those based on air or steam. Additionally, while the pumps of the SRC and TCSRC configurations are most likely smaller than the compressors of the air BCs, the former are still expected to present with increased total turbomachinery volumes due to the large turbines as a result of the significantly higher pressure ratios. Finally, the very low density of steam at the outlet of the steam turbines will also result in increased turbine sizes. Based on the previously described parameters and literature, the turbomachinery of the TCSRC configurations is expected to be the largest, followed by that of the SRC configurations, and subsequently the air BC configurations; finally, the turbomachinery of the SBC and TCRC configurations is expected to be significantly smaller and present with similar dimensions. When considering the results from table B.1 containing the mass flow rate of each configuration and the electric power outputs as displayed in figure 7.1, it should be noted that those configurations presenting with relatively low mass flow rates and power outputs are likely to go accompanied by quite small turbomachines.

Regarding the size of the heat exchangers, their influence on the total system size becomes relatively insignificant when applying PCHes rather than STHes; this can be best seen when looking at the volumes of the heat exchangers as in appendix B table B.2. Only the total system size of the (TC)SRC configurations might be dominated by the size of the turbomachinery and other components when equipped with STHes, as these are still relatively small. The differences between the various cycles and configurations becomes clear in figures 7.3 and 7.4, where the (TC)SRC configurations present with the smallest sizes, followed by the CO₂-based cycles with recuperation and recompression, respectively. Finally the largest heat exchangers are required for the air BC configurations.

When considering the total system size, including heat exchangers, turbomachinery, and other components, further conclusions can be drawn. Firstly, the air BC configurations applying STHes are highly disadvantageous when it comes to size. Moreover, it is likely that the size of the heat exchangers will dominate the total system size, regardless of the size of the turbomachinery and the other components.

Secondly, the total system size of the CO₂-based cycles and the (TC)SRC configurations could be quite close together when applying STHes. This is a result of the latter having significantly smaller heat exchangers, but the former having significantly smaller turbomachinery. When it comes to the size of the other components discussed, it is likely the piping of the CO₂-based cycles takes up more space than that of the SRC configurations as the CO₂-based cycles encompass more processes and operate at higher pressures than the SRC configurations. Due to the maximum pressure of the TCSRC configurations being above those of the CO₂-based cycles, the same conclusions cannot be drawn when comparing these. Regarding the gearboxes it is expected that those of the CO₂-based cycles will be larger than those of the (TC)SRC configurations due to the high shaft speeds of the former. The combination of these results does not provide a clear answer to the comparison of the CO₂ and steam-based cycles, but it is expected they will have similar dimensions when applied with STHes.

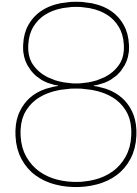
Thirdly, following from the previous point, it is likely the CO₂-based cycles will be relatively small compared to the other systems when applying PCHes. The combination of the small turbomachinery with the small volumes of the heat exchangers is expected to prove highly advantageous.

In short, when applying the configurations with PCHes, the size of the turbomachinery and the other components is expected to dominate the total system size, due to which the CO₂ TCRC and SBC configurations are most likely to be the smallest. These will be followed by the air BC configurations which are expected to have significantly smaller turbomachinery than the steam-based cycles. Finally, the SRC configurations will be slightly smaller than the TCSRC configurations due to the size of the turbomachinery of the former being smaller as a result of the lower pressure ratios.

When applying the configurations with STHes, the influence of the heat exchangers on the total system size becomes much more relevant. In this case, the air BC configurations present with significantly larger system sizes compared to the other systems, purely as a result of the heat exchangers. While no quantifiable conclusions could be drawn between the CO₂ and steam-based cycles, they are expected to present with comparable total system sizes due to the balance between the size of the heat exchangers, the turbomachinery, and the other components.

While the conclusions drawn here are rough and should be considered as such, they provide a qualitative estimation and general view on the comparative size of the different configurations; however, a potentially more interesting and relevant conclusion appears to be that insufficient research has been conducted regarding the detailed sizing of components for different power cycles.

It should be noted that the exact influence of the individual turbomachines and additional components present in each configuration has been omitted from these conclusions as no quantitative dimensions have been obtained. The most noteworthy example of this would be the difference between the combined reheating, intercooling, and recuperation air BC and the basic SRC. The conclusions drawn may point towards the former having a smaller total system size than the latter when applying PCHes, due to the smaller turbomachinery involved in air BCs, and the potentially negligible influence of the size of the heat exchangers. However, when considering that this specific air BC would have one more compressor and turbine, as well as three additional heat exchangers, all requiring extra piping, the difference in size between these two systems might become significantly smaller, if not up to the point where the basic SRC would present with a smaller total system size. This again proves the need for more detailed investigations on the size of turbomachinery and other components in different power cycles to be able to quantify the dimensions involved with these components and their influence on the total system size.



Component cost analysis

In addition to efficiency and size, another important parameter in determining suitable waste heat recovery systems is the associated cost of a configuration. While there are several approaches to determine the economics of a power conversion system, all with varying levels of detail, in this chapter, a simple approach to compare the costs of the different configurations is described and the results are presented.

8.1. Purchased equipment cost

As mentioned, there is more than one way to determine the costs or economic benefit associated with a power conversion system, some of which result in highly detailed cost estimates. However, in this study, the focus is on the comparison of different configurations, which allows for a more straightforward approach by calculating the cost of components. In this section, the determination of the component costs will be discussed for the heat exchangers and turbomachinery. While power conversion systems consist of many more components than heat exchangers and turbomachines, such as piping, bearings, and generators, to name a few, this section will focus on the former, as these are expected to drive the main differences in cost.

A commonly applied approach to determine the cost of a component is with the use of a so-called purchased equipment cost (PEC) correlation. This kind of correlation is derived from vendor data or typical cost expectations and contains a sizing factor in which a component can be expressed, such as the area for heat exchangers or power output for turbines. As PEC correlations are often determined empirically, several can be found for each type of component and they are not without uncertainty. To slightly decrease the uncertainty of the obtained results and to limit the influence of a single correlation, for each component, two correlations have been acquired from which the average PEC will be determined. Table 8.1 shows the applied cost correlations as obtained from the corresponding sources.

Table 8.1: Component cost correlations and the cycles to which they are applied.

Component	Cycle	Cost correlation (PEC [\$])	Units	Ref.	CEPCI
Pump ^a	(TC)SRC	$= 378 \left[1 + \left(\frac{1-0.808}{1-\eta_C} \right)^3 \right] W_C^{0.71}$	kW	[74]	359.2
	(TC)SRC	$= 442 (\dot{m} w_C)^{0.71} 1.41 \left[1 + \left(\frac{1-0.8}{1-\eta_C} \right) \right]$	kW^b	[102]	607.5
Compressor	BC	$= \left(\frac{39.5\dot{m}}{0.9-\eta_C} \right) \left(\frac{P_{out}}{P_{in}} \right) \ln \left(\frac{P_{out}}{P_{in}} \right)$	$\frac{kg}{s}$	[127]	368.1
	BC	$= 44.71\dot{m} \frac{1}{0.95-\eta_C} \left(\frac{P_{out}}{P_{in}} \right) \ln \left(\frac{P_{out}}{P_{in}} \right)$	$\frac{kg}{s}$	[100]	401.7
	TCRC/SBC	$= 1230000 W_C^{0.3992}$	MW	[133] ^c	567.5
	TCRC/SBC	$= 6898 W_C^{0.7865}$	kW	[18]	567.5
Turbine	(TC)SRC	$= -14000 + 1900 W_T^{0.75}$	kW	[122]	532.9
	(TC)SRC	$= -0.0018 W_T^2 + 137.39 W_T + 31647$	kW	[73] ^d	389.5
	BC	$= \left(\frac{266.3\dot{m}}{0.92-\eta_T} \right) \ln \left(\frac{P_{in}}{P_{out}} \right)$ $* [1 + \exp(0.036 T_{in} - 54.4)]$	$\frac{kg}{s}, K$	[127] ^e	368.1
	BC	$= 301.45\dot{m} \frac{1}{0.94-\eta_T} \ln \left(\frac{P_{in}}{P_{out}} \right)$ $* [1 + \exp(0.025 (T_{in} - 1570))]$	$\frac{kg}{s}, K$	[100] ^f	401.7
	TCRC/SBC	$= 4001.4 W_T^{0.6897}$	kW	[18] ^g	567.5
	TCRC/SBC	$= 406200 W_T^{0.8} * f$ with $f = 1$ if $T_{in} < 550$ °C, and $f = 1 + 1.137E-5 (T_{in} - 550)^2$ if ≥ 550	$MW, ^\circ C$	[133] ^h	607.5
STHE	All cycles	$= 28000 + 54 A_{HEX}^{1.2}$	m^2	[122] ⁱ	532.9
	All cycles	$= 125.87 A_{HEX} + 9583.8$	m^2	[73] ^j	389.5
PCHE	All cycles	$= 49.45 (\bar{U} A_{HEX})^{0.7544} * f$ with $f = 1$ if $T_{max} < 550$ °C, and $f = 1 + 0.02141 (T_{max} - 550)$ if ≥ 550	$\frac{W}{K}, ^\circ C$	[133] ^k	567.5
	All cycles	$= 5.2 (\bar{U} A_{HEX})^{0.8933} * C^*$	$\frac{W}{K}$	[47] ^l	556.8

^aFor the cost analysis, only the (TC)SRC configurations are assumed to be equipped with a pump, this is due to the pumping/compression process of the TCRC configurations being predominantly above the critical point of CO₂.

^bThe units of \dot{m} and w_C are kg/s and kJ/kg , respectively, which equals kW when multiplied.

^cIntegrally geared centrifugal-type compressor with a CEPCI from 2017, which is the cost year applied by the reference source.

^dThe correlation has been extrapolated by matching a polynomial fit to the data set provided by the reference source; additionally, a CEPCI from 1998 is applied, which is the year corresponding to the data set.

^eWhile the cost correlation is designed for gas turbines, it has been applied to air bottoming cycles as well [103]; additionally, T_{in} corresponds to the value of T_{max} assumed in section 6.1.

^f T_{in} corresponds to the value of T_{max} assumed in section 6.1.

^gThe correlation applied is for a radial expander.

^hThe correlation applied is for a single stage radial turbine; additionally, T_{in} corresponds to the value of T_{max} assumed in section 6.1.

ⁱA U-tube type heat exchanger is assumed, and the area is bounded between 10-1000 m^2 ; if it is larger, the area will be split into the nearest sufficient number of units.

^jThe correlation has been extrapolated by matching a linear fit to the data set provided by the reference source; as the data set only goes up to 70000 square feet, larger heat transfer areas will be split into the nearest sufficient number of units. Additionally, a CEPCI from 1998 is applied, which is the year corresponding to the data set.

^kThe correlation has been specifically designed for sCO₂ recuperators; additionally, a CEPCI from 2017 is taken, which is the cost year as applied by the reference source.

^lThe correlation has been specifically designed for sCO₂ recuperators; additionally, the values of C^* are taken from [18], ranging from approximately 24 for low $\bar{U} A_{HEX}$ values, to 1.0 for high $\bar{U} A_{HEX}$ values. In the PCHE cost calculation, the C^* values are read from figure 8.1.

In table 8.1, η_C is the isentropic efficiency of the pump/compressor, W_C is the pump/compressor power consumption, \dot{m} is the mass flow rate of the fluid through the component, w_C is the pump/compressor specific power consumption, P_{out} is the pressure of the fluid at the outlet of the component, P_{in} is the

pressure of the fluid at the inlet of the component, W_T is the turbine power output, η_T is the isentropic efficiency of the turbine, T_{in} is the temperature of the fluid at the inlet of the component, A_{HEX} is the heat transfer area, \bar{U} is the overall heat transfer coefficient of the heat exchanger, T_{max} is the maximum temperature of the fluid present in the heat exchanger, and C^* is a scaling factor as obtained from Carlson et al. [18] and visualized in figure 8.1.

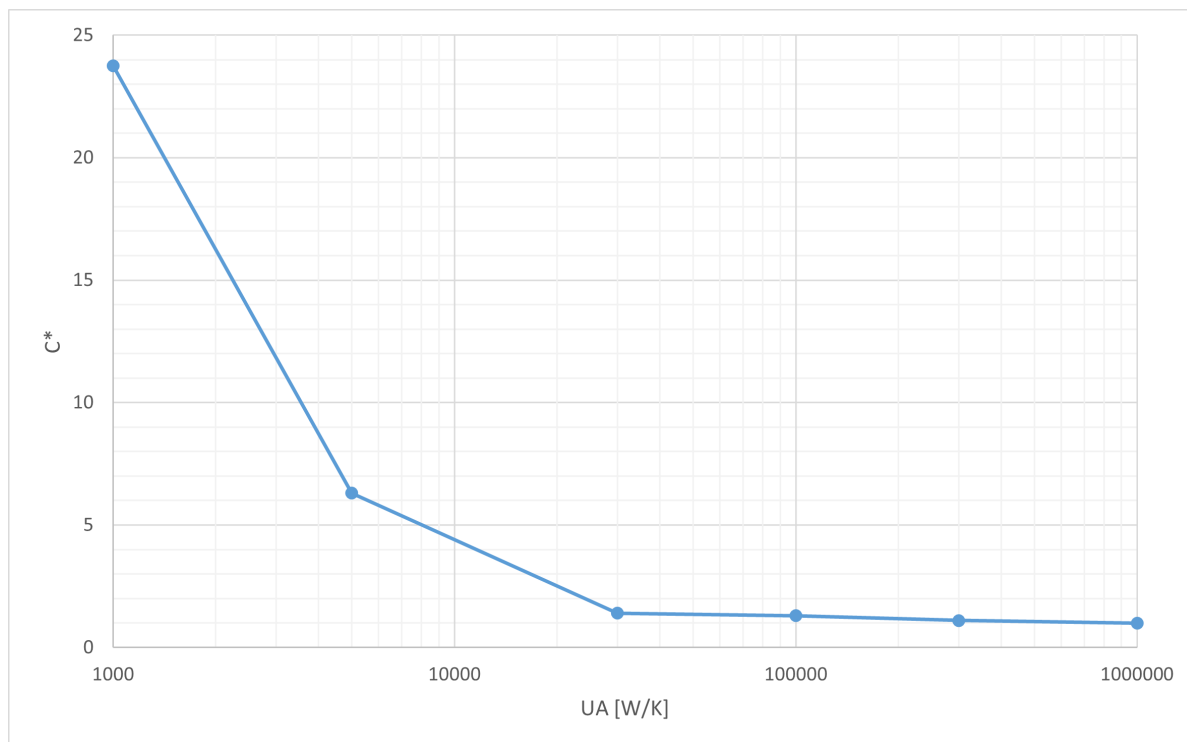


Figure 8.1: Visualisation of the scaling factors for PCHes, adapted from [18].

As previously mentioned, each cost correlation has at least one sizing factor, which can be determined for each component in every configuration, and subsequently applied to the respective PEC correlation. The values of the sizing factors, which are power and mass flow rate for turbomachinery, $\bar{U}A_{HEX}$ and temperature for PCHes, and heat transfer area for STHes, have been obtained from the models created in chapter 6 and 7. In appendix C, section C.1, the exact input values applied to the PEC correlations can be found.

It should be noted that while regeneration is commonly applied with the use of a single turbine divided into two stages with intermediate steam extraction, for the cost analysis, the stages are taken as separate turbines. This is done as the extraction of steam results in increased complexity of the turbine and cycle, which should be reflected in higher costs. Additionally, building on the assumption regarding the size of open FWHs in section 7.1.2, the cost of open FWHs will not be included in any calculations henceforth, unless specified otherwise. While this omission can be considered unrealistic, the small size of the open FWHs compared to the other heat exchangers, in combination with the already relatively small system size that can be associated with power conversion systems of approximately 600 kW, it is assumed that the influence of the cost of the open FWHs is insignificant.

8.1.1. Applied cost factors

As previously mentioned, the cost correlations from table 8.1 have been created empirically, often for a specific type of application and associated process conditions, which do not necessarily coincide with those applied in this study. Two main process conditions of a component that can experience variations between those assumed for the respective cost correlation, and those present in this study, are the operating pressure and temperature. These factors are especially important as increased pressures and temperatures can result in thicker or more expensive materials being required for the component.

Therefore, to account for such variations, considerations have to be made and correction factors should be added to the purchased equipment cost correlations when necessary. In this section, these considerations are discussed and the additional cost factors are presented.

Several components and their associated correlation require no additional correction factor as the operating temperature and/or pressure is not uncommonly high, or because the cost correlation can be assumed to account for such conditions.

First, the pumps do not operate at high temperatures and as the applied cost correlations from ref. [74] and [102] incorporate power consumption, the influence of pressure is assumed to be reasonably accounted for. Second, the compressors in the air BC configurations do not operate at high temperatures or pressures, and as such, the correlations from ref. [127] and [100] do not require a correction factor. Third, as the cost correlations of the CO₂ compressors in the TCRC and SBC configurations are specifically designed for high temperatures and pressures, these correlations are assumed to account for such operating conditions; the same applies to the correlations for the CO₂ turbines. Fourth, the turbines of the air BC configurations do not operate at high pressures, and as the cost correlations from ref. [127] and [100] contain the TIT, the influence of temperature is accounted for.

The cost correlations that require a correction factor are those of the steam turbines, STHes, and PCHEs. First, the turbines of the SRC and TCSRC configurations have a TIT of 800 °C, which is relatively high compared to typical steam turbine operating conditions, and the correlations from ref. [122] and [73] are designed for steam turbines constructed from carbon steel. To be better equipped to high temperatures, the steam turbine cost correlations are multiplied with a factor of 3 for nickel alloy construction, which can withstand high pressures and temperatures [18]. Second, similar to those of the steam turbines, the cost correlations of the STHes have also been designed for carbon steel construction; therefore, a nickel alloy construction factor of 3 will be applied to a number of STHes with high operating temperatures and/or pressures. The factor should be applied to STHes operating at temperatures above 480 °C, as this is the temperature limit for use of carbon steel [122]; additionally, the factor will also be applied to the LTRs in the CO₂-based cycles, which operate at lower temperatures but significant pressures.

Finally, the cost correlations for the PCHEs have both been designed specifically for sCO₂ applications, and while only the first correlation from ref. [133] applies an extended temperature factor, both are assumed to account for temperature influences. However, both correlations are also assumed to already account for high operating pressures, which could lead to the cost of PCHEs operating at low pressures to be overestimated; therefore, the PCHEs operating at relatively low pressures compared to sCO₂ applications should be corrected. Unfortunately, in the absence of detailed literature or data on the influence of low pressures on the cost of PCHEs, no accurate correction factor could be determined. When applying the cost correlations without correction factor to (for example) the heaters of the basic SRC and TCSRC, where the operating pressures are respectively 60 bar and 300 bar, the differences are very small which is highly unlikely. Therefore, the choice is made to reduce the cost of PCHEs operating at pressures below 100 bar by an intuitive factor of 20%.

8.1.2. Resulting purchased equipment costs

After applying the cost correlations and additional cost factors where required, the PEC of all the components applied in the different configurations is calculated. In this section, the resulting PEC of the configurations is provided for the cases applying PCHEs and STHes. In appendix C, the breakdown of the costs of the turbomachinery, PCHEs, and STHes is displayed separately, and the final total PEC is presented.

Figure 8.2 shows the total purchased equipment cost per kWe of the configurations in the cases applying either PCHEs or STHes. The cost is determined by applying the values from appendix C tables C.1, C.2, and C.4 to the two correlations of each component in table 8.1. After including the additional cost factors as described in section 8.1.1 and averaging the results, the total PEC can be determined, which after division by the power output results in the total PEC per unit power. The exact values from the component cost analysis that make up figure 8.2 are provided in appendix C.2.

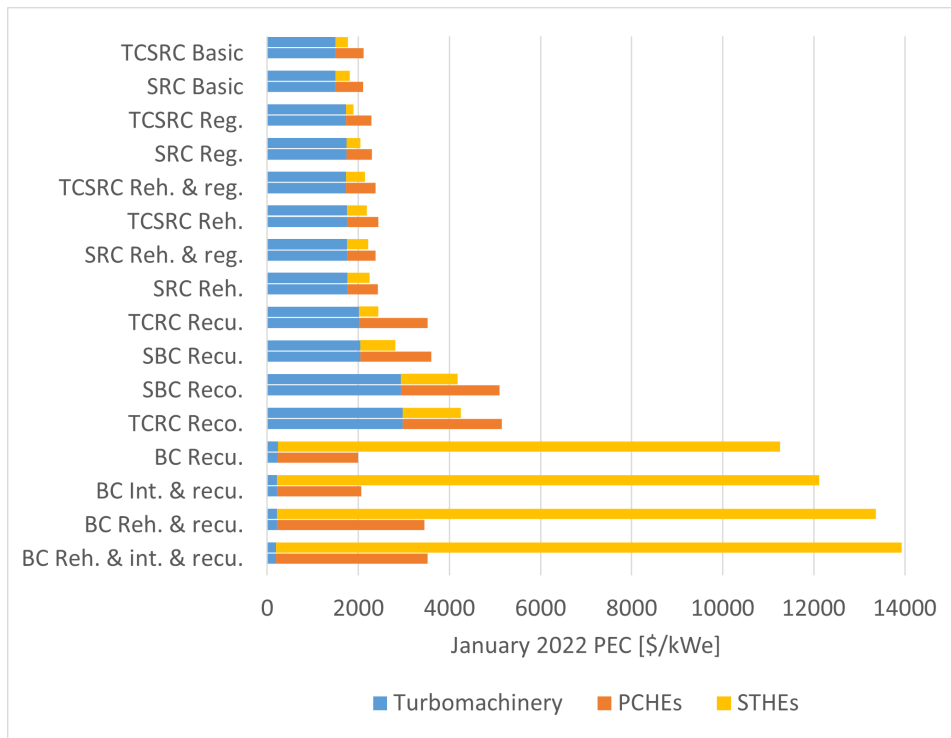


Figure 8.2: PEC per unit power of the configurations when applied with PCHEs or STHes.

8.2. Additional costs

In practice, the total cost of a waste heat recovery system consists of far more than the PEC of the turbomachinery and heat exchangers. While for the comparative purpose of this study, the cost quantification of only the latter is assumed sufficient, this section will briefly discuss some qualitative considerations that may prove useful when a wider scope of the cost analysis is desired.

8.2.1. Cost of other components

In section 7.2.4, some considerations were presented regarding the size of components other than turbomachinery and heat exchangers. In this section, such considerations will also be made regarding the cost of additional components.

Firstly, the piping, of which the size was discussed in the aforementioned section based on system complexity and operating conditions. The same aspects from the sizing considerations have a similar impact on the cost, as it is to be expected for larger sizes to be associated with higher cost and vice versa. It was concluded that systems with increased complexity such as cycles modified with additional processes, will see an increase in the amount of piping required, and therefore also an increase in cost. Similarly, systems operating at high pressures require thick walled piping and casings, which directly translates to higher cost as well. For example, from these considerations it can be concluded that a low pressure, low complexity system such as a recuperation air BC, will have significantly lower cost of piping compared to the high pressure, more complex, recompression CO₂ SBC.

Regarding the gearboxes as discussed in section 7.2.4, the considerations that should be made are the same when looking at the cost. Systems equipped with turbines rotating at high speeds are likely to require more complex gearboxes, which would result in higher associated component costs. These costs are again expected to be higher for the small diameter, high speed turbomachinery present in the CO₂-based cycles. In the discussion of component sizes, a short remark was made regarding the application of the same type of generator in each waste heat recovery system, concerning its designed rotational speed. However, the differences in the power produced by each system can still result in different "sizes" of generator being required, where higher mechanical power outputs may translate into higher associated costs.

Finally, there could be said little about the size of control systems for the investigated power cycles, and as such, no conclusions will be drawn about their cost. However, control systems can be highly advanced and complex, and their influence on the cost should be considered when applying cost considerations in a more practical setting. Again, not all components are discussed in this section and the considerations are predominantly presented to provide insight into the relevant aspects to consider when estimating the total cost of an energy conversion system.

8.2.2. Other cost factors

As mentioned before, estimating the cost of the investigated waste heat recovery systems does not end with the PEC of the main components, and it is common to apply cost factors to account for other aspects influencing the total cost. Such cost factors include those for additional components, installation cost, contingency cost, and operation & maintenance cost, to name a few well-known ones. In this section, these factors are briefly described as to why they are relevant, and what considerations should be made when comparing the investigated waste heat recovery systems.

As discussed in the previous section, the total equipment cost consists of more components than those described and quantitatively analysed in this study. However, this regards numerous components, and there is limited information available on their cost. It is not uncommon in economic analyses to apply a cost factor to include these components, which is often a percentage of the total main component cost.

Another commonly applied cost factor is that of installation costs. Including such a cost factor is considered relevant because following the cost of the individual components, the system has to be built and installed on the vessel. It is reasonable to expect that larger systems with more components require more installation costs, and more complex systems might require more specialized and therefore more expensive installation. To compare the waste heat recovery systems investigated in this study, it would not be unexpected for a system such as the combined reheating, intercooling, and recuperation air BC to have increased installation costs compared to the basic SRC.

A less common but nonetheless potentially influential cost factor is that of contingency costs. Acquiring and installing a waste heat recovery system presents with a level of uncertainty regarding the ultimate costs and economic benefit. This level of uncertainty can be best described as one of unknown field performance and unforeseen costs. While it can be modelled and calculated, a waste heat recovery system does not always operate in ideal design conditions, and it is uncertain whether it will produce the desired results. Additionally, unforeseen costs are often built into the cost estimation, as it is not uncommon for a project to experience them. These unforeseen costs are not identical to each investigated waste heat recovery system. For example, consider a new and innovative system that has experienced relatively limited field testing, such as a recompression CO₂ SBC, compared to a commonly applied and extensively proven system, such as a basic SRC. It can be reasonably expected that the former is significantly more likely to result in unforeseen costs than the latter, which can be accounted for by applying different contingency cost factors.

Finally, each of the investigated waste heat recovery systems must be operated and subjected to maintenance, both scheduled and unscheduled. These systems are complex pieces of engineering, with many moving parts, and they should be operated by trained personnel as well as being regularly checked to make sure they do not malfunction. Components and parts may present with fatigue and wear, and might therefore require replacing, systems with more components and more severe operating conditions are likely to require increased maintenance and thus higher costs. To again draw a connection with the systems included in this study, various components of the recompression CO₂ SBC operate at significant pressures, and the turbomachinery can present with high rotational speeds. On the other hand, a basic SRC has fewer components, operating at lower pressures, and the turbomachinery is likely to operate at lower rotational speeds. It can therefore be expected that the operation & maintenance costs of the former will be higher than those of the latter. These costs can also be included in an analysis through the application of a cost factor, which can for example be approximated as a percentage of total plant cost.

While the cost factors described are not the only possible ones, they are quite common, and this section serves predominantly to provide insight into the many facets that determine the cost of a waste heat recovery system.

8.3. Conclusions

This chapter describes an approach to estimate costs based on correlations and factors. In practice, such a cost analysis is typically applied for general comparison, after which more detailed cost analyses are conducted.

When looking solely at the calculated PEC of the different configurations, a few conclusions can be drawn. Firstly, it is evident that the PEC of the turbomachinery is significantly smaller for the air BC configurations than that of the other cycles, in which the CO₂-based cycles containing recompression present with the highest PEC of the turbomachinery. The cost of the turbomachinery for the remaining configurations can be considered comparable. Secondly, the PEC of the various configurations when applied with STHes is always lower, except for the air BC configurations in which the cost of the STHes is significantly higher than that of the PCHes. This directly follows from the very large size of the heat exchangers required in the air BC configurations. Thirdly, the PEC of the steam-based cycles is comparable regardless of the type of heat exchanger applied, and is only slightly lower than the PEC of the CO₂-based cycles with recuperation when applied with STHes. Finally, in the case applying PCHes, the PEC of the air BC configurations without reheating is comparable to that of the steam-based cycles, while the PEC of the air BC configurations with reheating is closer to that of the CO₂-based cycles.

Considering the cost of the additional components discussed in section 8.2.1, no quantifiable conclusions are drawn, but some general remarks are put forward. The cost of piping is expected to be highest for more complex systems or those that operate at higher pressures. The former includes systems with additional processes, the most clear example of which is the combined reheating, intercooling, and recuperation air BC. This configuration requires significantly more connections being made via piping compared to the basic SRC, which is the least complex system investigated. As such, it can be expected that a larger number of processes, requiring several additional components, results in more piping and therefore higher costs. Regarding the pressure, which has a significant influence on the thickness and therefore the cost of the piping, the systems that present with relatively high pressures are expected to present with increased costs of piping. It should be noted that pressures vary throughout each system, with for example the TCSRC configurations having the highest maximum pressure, but also the lowest minimum pressure. As such, systems with overall relatively high pressures, such as the CO₂-based cycles, will most likely require a relatively higher cost for piping.

Due to the high shaft speeds, the cost of the gearboxes is expected to be highest for the CO₂-based cycles; however, the exact influence on the total cost is uncertain, as well as how the different systems compare. Similarly, while some remarks have been made regarding the cost of generators and control systems, there is significant uncertainty and they will therefore not be taken into consideration.

In the previous section, a number of cost factors were discussed, including those for additional components, installation cost, contingency cost, and operation & maintenance cost. Omitting the cost factor for additional components, as this has just been discussed, the next factor is that of installation cost. Larger and more complex systems are expected to require increased installation costs. Examples of these would be the combined reheating, intercooling, and recuperation air BC, the reheating and regenerative TCSRC, and the CO₂-based cycles with recompression. All of which are either relatively large, consist of many components, or may require more specialized care to be installed. Regarding the factor for contingency costs, it stands to reason that the newest technologies present with increased uncertainty and therefore increased cost, in contrast to the more developed technologies. The former of which would be the CO₂-based cycles, while the latter would be the SRC and air BC. Finally, the cost for operation & maintenance was discussed, and it is likely these costs will be the highest for the CO₂-based cycles as their components operate at relatively high pressures and high rotational speeds in the case of the turbomachinery.

Combining the aforementioned conclusions regarding the PEC, the cost of additional components, and the cost factors, some more general conclusions regarding total system cost can be drawn. Firstly, in the case applying STHes, the air BC configurations are considerably more expensive and highly unsuitable from an economic point of view. Secondly, the CO₂-based cycles already present with the highest PEC, and combined with the potentially higher cost of piping and gearboxes, as well as increased installation costs, contingency costs, and operation & maintenance costs, the CO₂-based

cycles will be relatively even more expensive. Finally, when applied with PCHEs, the air BC configurations without reheating perform comparably to the (TC)SRC configurations. This is likely to remain after including considerations based on the cost of additional components and cost factors as these systems present with both advantages and disadvantages regarding these subjects. To further clarify, these air BC configurations may be equipped with more heat exchangers and turbomachines, requiring additional piping, but they also operate at lower pressures, reducing the cost of piping. Similarly, the (TC)SRC configurations may have a less complex system design, which would reduce installation costs, but they are also expected to be larger, which could potentially increase installation cost compared to the aforementioned air BC configurations.

While no quantitatively supported conclusions are drawn regarding the total system cost of each configuration including additional components and cost factors, the qualitative conclusions regarding these in combination with the calculated PEC provide relevant insights into the cost associated with the investigated waste heat recovery technologies. However, the resulting PEC in section 8.1.2 has been determined using cost correlations obtained from literature, as well as estimated additional cost factors. As a result, the presented conclusions can only be considered to hold under the condition that the applied correlations and estimated cost factors are valid.

Conclusions and recommendations

This chapter contains the most relevant conclusions that can be drawn from the investigations conducted in this study, as well as recommendations made for future research. The conclusions in the following section are focused solely on the waste heat recovery technologies subjected to the evaluations of efficiency, size, and cost. Waste heat recovery technologies that were omitted at any point during this study are not included in the final conclusions.

9.1. Conclusions

The goal of this study was to develop and execute a process-oriented approach to evaluate the efficiency, size, and cost of various waste heat recovery technologies when applied to a marine vessel powered by a 2MW SOFC. The process-oriented approach was described and undertaken for several possible waste heat recovery technologies regarding each separate aspect. Ideally, this would result in a dominant choice for one single waste heat recovery system, which would perform superior to the others with respect to efficiency, size, and cost. However, this was not the case as the various systems presented with both advantages as well as disadvantages in these areas. While no one optimal waste heat recovery system resulted from this study, relevant conclusions regarding each aspect were obtained.

Concerning the efficiency and electric power output produced, it is clear that the CO₂ TCRC and CO₂ SBC with recompression perform best. These two cycles show efficiencies between approximately 51 and 52%, with electric power outputs of around 670 kWe. This would constitute an improvement of approximately 33.5% relative to main engine power when considering the applied case study of the 2 MW SOFC system. The efficiencies of the remaining configurations lie in the range of approximately 41-48%, with electric power outputs between 530 and 641 kWe. When applying this to the 2 MW SOFC case study, relative improvements would be between 26.5 and 32.05%. In comparison, a marine ICE with an ORC system for waste heat recovery can present with improvements of 5-15% relative to main engine power as described by Zhu et al. [143]. This shows that besides the high efficiencies associated with SOFCs, their waste heat recovery potential is significant as well, allowing for even higher overall efficiencies.

Regarding the heat exchangers, the (TC)SRC configurations present with the smallest equipment sizes, followed by the CO₂-based cycles with recuperation and recompression, respectively. Finally the largest heat exchangers are required for the air BC configurations. However, from the results it also became clear that the influence of the heat exchangers on the total system size might be negligible compared to other components such as turbomachinery in the case of PCHEs. As a result, it is likely that the CO₂-based cycles will be smallest due to the reduced size of the turbomachines when applying PCHEs, while the steam-based cycles may become of comparable size when considering only STHes.

With respect to the cost of the various systems, it can be concluded that the steam-based cycles with either PCHEs or STHes, as well as the air BC configurations without reheating applied with PCHEs, present with the lowest PEC and perform comparably. On the other side are the air BC configurations applied with STHes, which are concluded to be unsuitable from an economic point of view. Omitting the air BC configurations applied with STHes, it can be furthermore concluded that the CO₂-based

cycles will be much more expensive than the remaining systems when including other aspects besides the PEC.

In conclusion, the best choice of waste heat recovery technology depends on the weight assigned to each area. When efficiency and power output, as well as size, are the most important factors, the best choice would most likely be one of the CO₂-based systems with recompression, applied with PCHes. These present with the largest power outputs at high efficiency, while being relatively small due to the PCHes in combination with small turbomachinery. However, the cost of such a system would be significant compared to other alternatives. In contrast, if cost dominates the choice a more suitable system would be the basic SRC or the air BC with recuperation. These systems present with a lower power output and a relatively large system size, but are considerably less expensive.

Despite the lack of a definitive superior waste heat recovery system, the approach developed in this study provides a solid basis for the evaluation of waste heat recovery technologies. Moreover, whether a waste heat recovery technology is a superior choice will mainly depend on the requirements and their importance as put forth by a ship designer or operator. As this study shows, no single system investigated proves to be the most desirable when looking at the combination of efficiency, size, and cost, and a balance must be found between them. It is suggested that for well substantiated choices to be made, more accurate results of the size and cost of the various waste heat recovery systems should be obtained, and further research into the exact sizing and cost of each entire waste heat recovery system would greatly improve the accuracy of the conclusions drawn. For that purpose, this study can be extended with more detailed analyses. Additionally, to apply the results from this study to real world scenarios, a connection to the benefits of the investigated waste heat recovery systems, such as fuel savings or reduced emissions, could further support the choice of system. Beyond that, future questions might arise relating the loss of space due to the installed waste heat recovery system to the associated economic losses of reduced cargo space or increased vessel size requirements. However, the results of this study already provide insight into the application of waste heat recovery, and the power outputs of the investigated systems show that significant amounts of energy can be recovered. It is therefore considered proven that fuel consumption, and depending on the marine fuel used emissions as well, can be reduced a great deal, which has the potential to translate into significant economic benefits. Finally, while this study has been conducted at the hand of a case study of a vessel powered by an SOFC, the same approach can be readily applied to a multitude of other sectors, power plants, and waste heat recovery applications.

9.2. Recommendations

This study was conducted for a specific case, and while some resulting findings can be applied to other cases as well, there are areas that have not been included or addressed in detail. These areas are the result of issues encountered which were left out of the scope of this study, but also assumptions that were made which led to the exclusion of the influence of certain parameters. Therefore, a number of recommendations are made for future research, specifically regarding the areas that have not been investigated in this study or that may require more attention. The following recommendations and remarks are supplemental to those suggested in the final paragraph of the previous section.

Recommendations regarding encountered issues and further remarks:

- The heat transfer area calculations resulted in very high cold source service fluid mass flow rates in the condenser of the RC-based configurations. While the impact of this was discarded due to its sensitivity to small variations of input parameters, in future works, this influence should be investigated further and cycles should be optimized while taking more suitable operating conditions into account.
- The investigated cycles, such as the SRC and TCSRC, have not been found to be practically applied with operating temperatures of 800 °C due to material considerations. While it has been assumed for the purpose of this study that such applications may be possible, it should be noted that as of yet such temperatures are potentially beyond the operating range of the investigated waste heat recovery systems.

- As obtained from the heat transfer area calculations, the type of heat exchanger has an enormous impact on the size of a configuration; a similar study should be conducted for more different types of heat exchangers to allow for the most practical choice of heat exchanger. An example of this is the application of simple plate heat exchangers in the air BCs, which could significantly reduce the size and cost associated with the heat exchangers.
- The size of the investigated configurations is most likely not linearly dependent on the cycle power output; as such, other cycles and configurations might prove more suitable for applications with different power output magnitudes.
- The results indicate that power outputs around 600 kW would be achieved; however, the investigated waste heat recovery systems, and especially the SBC, may experience issues with the turbomachinery due to these low power outputs. The issues would be a consequence of the turbomachines having relatively small diameters and very high rotational speeds [33]. In future studies, the practical feasibility of such turbomachinery should be investigated.
- Only the efficiency, size, and cost of the waste heat recovery systems have been investigated in this study. However, other factors such as safety and required personnel should also be considered in future works.

Recommendations regarding assumptions made:

- The assumption applied regarding equal pressure ratios for the intercooling, reheating, and regeneration pressures might not result in optimized cycles. As such, an optimization study could be conducted to investigate various pressure ratios in these configurations.
- The influence of the size and cost of open FWHS in regenerative cycles was omitted from this study due to the high heat transfer associated with direct contact condensation. A detailed study of the exact influence on the total system size and cost of these components could be performed to verify this assumption.
- The cathodic exhaust gas mass flow rate from the SOFC was estimated for the performance evaluation of the various waste heat recovery systems; as this mass flow rate might not linearly influence results such as heat transfer areas, a comparison of different cycles and their dependence on the exhaust gas mass flow rate should be conducted.
- The volume of the heat exchangers was based on estimated area-to-volume ratios, and did not include possible space requirements for maintenance; a more detailed investigation of these aspects should be considered in future works.
- The heat transfer areas were determined based on typical overall heat transfer coefficients, as well as being assumed constant throughout the flows; however, in future works, the overall heat transfer coefficients may be determined more accurately and the influence of inconstant heat transfer coefficients should be considered.
- The economic analysis in this study has been focused on comparing the PEC of the main components. In future works, attention may be given to the exact cost of other components such as gearboxes and generators, as well as additional cost factors, and the economic benefit that could be achieved by the various waste heat recovery systems.
- This study applied several assumptions and input parameters in the comparison of different cycles and their configurations; however, not all of the influences of these aspects were investigated. In future works, a more multidimensional approach should be considered to allow investigation of optimized configurations, as well as the influence and sensitivity of input parameters.

Bibliography

- [1] T. Adibi and O. Adibi. Evaluation of the optimum pressure of the intercooler and the regenerator in the bryton cycle based on exergy and energy analysis. *Thermophysics and Aeromechanics*, 28:879–889, 11 2021. ISSN 0869-8643. doi: 10.1134/S0869864321060123. URL <https://link.springer.com/10.1134/S0869864321060123>.
- [2] Habib Aghaali and Hans Erik Ångström. A review of turbocompounding as a waste heat recovery system for internal combustion engines. *Renewable and Sustainable Energy Reviews*, 49:813–824, 5 2015. ISSN 18790690. doi: 10.1016/j.rser.2015.04.144.
- [3] Y. Ahn, S.J. Bae, M. Kim, S.K. Cho, S. Baik, J.I. Lee, and J.E. Cha. Review of supercritical co2 power cycle technology and current status of research and development. *Nuclear Engineering and Technology*, 47:647–661, 10 2015. ISSN 2234358X. doi: 10.1016/j.net.2015.06.009.
- [4] K. H.M. Al-Hamed and I. Dincer. A new direct ammonia solid oxide fuel cell and gas turbine based integrated system for electric rail transportation. *eTransportation*, 2:100027, 11 2019. ISSN 2590-1168. doi: 10.1016/J.ETTRAN.2019.100027.
- [5] Regina Asariotis, Mark Assaf, Hassiba Benamara, Jan Hoffmann, Anila Premti, Luisa Rodríguez, Mathis Weller, and Frida Youssef. Review of maritime transport. Technical report, UNCTAD, 2018.
- [6] B. Ashok, S. Denis Ashok, and C. Ramesh Kumar. Lpg diesel dual fuel engine – a critical review. *Alexandria Engineering Journal*, 54:105–126, 6 2015. ISSN 1110-0168. doi: 10.1016/J.AEJ.2015.03.002.
- [7] G. Attolini, M. Bosi, C. Ferrari, and F. Melino. Design guidelines for thermo-photo-voltaic generator: The critical role of the emitter size. *Applied Energy*, 103:618–626, 2013. ISSN 03062619. doi: 10.1016/j.apenergy.2012.10.032.
- [8] Mojtaba Babaelahi and Hoseyn Sayyaadi. Modified psvl: A second order model for thermal simulation of stirling engines based on convective-polytropic heat transfer of working spaces. *Applied Thermal Engineering*, 85:340–355, 6 2015. ISSN 13594311. doi: 10.1016/j.applthermaleng.2015.03.018.
- [9] Francesco Baldi and Cecilia Gabriellii. A feasibility analysis of waste heat recovery systems for marine applications. *Energy*, 80:654–665, 2 2015. ISSN 03605442. doi: 10.1016/j.energy.2014.12.020.
- [10] Mohamed H.S. Bargal, Mohamed A.A. Abdelkareem, Qi Tao, Jing Li, Jianpeng Shi, and Yiping Wang. Liquid cooling techniques in proton exchange membrane fuel cell stacks: A detailed survey. *Alexandria Engineering Journal*, 59:635–655, 3 2020. ISSN 11100168. doi: 10.1016/j.aej.2020.02.005.
- [11] L. Basso, A. Crotwell, H. Dolman, L. Gatti, C. Gerbig, D. Griffith, B. Hall, A. Jordan, P. Krummel, M. Leuenberger, Z. Loh, S. Mikaloff-Fletcher, Y. Sawa, M. Schibig, O. Tarasove, J. Turnbull, and A. Vermeulen. Wmo greenhouse gas bulletin - no. 17: The state of greenhouse gases in the atmosphere based on global observations through 2020. Technical report, World Meteorological Organization, 10 2021.
- [12] Thomas Bauer. *Thermophotovoltaics: Basic principles and critical aspects of system design*, volume 7. Springer Verlag, 2011. ISBN 9783642199646. doi: 10.1007/978-3-642-19965-3.

- [13] M. Bianchi and A. De Pascale. Bottoming cycles for electric energy generation: Parametric investigation of available and innovative solutions for the exploitation of low and medium temperature heat sources. *Applied Energy*, 88:1500–1509, 2011. ISSN 03062619. doi: 10.1016/j.apenergy.2010.11.013.
- [14] M. Biondi. Business case for sco 2 waste heat recovery system. Technical report, European Turbine Network, 2020.
- [15] S. Bouckaert, A. Fernandez Pales, C. McGlade, U. Remme, and B. Wanner. Net zero by 2050 - a roadmap for the global energy sector. Technical report, International Energy Agency, 2021.
- [16] Hendrik W. Brinks and Christos Chryssakis. Lpg as a marine fuel. Technical report, Group Technology & Research, DNV GL, 2017.
- [17] Klaus Brun, Peter Friedman, and Richard Dennis. *Fundamentals and Applications of Supercritical Carbon Dioxide (sCO₂) Based Power Cycles*. Woodhead Publishing, 2017. ISBN 978-0-08-100804-1.
- [18] M.D. Carlson, B.M. Middleton, and C.K. Ho. Techno-economic comparison of solar-driven sco₂ brayton cycles using component cost models baselined with vendor data and estimates. 2017.
- [19] Francesco Catapano, Carmela Perozziello, and Bianca Maria Vaglieco. Heat transfer of a stirling engine for waste heat recovery application from internal combustion engines. *Applied Thermal Engineering*, 198, 11 2021. ISSN 13594311. doi: 10.1016/j.applthermaleng.2021.117492.
- [20] Amrit Chandan, Mariska Hattenberger, Ahmad El-Kharouf, Shangfeng Du, Aman Dhir, Valerie Self, Bruno G. Pollet, Andrew Ingram, and Waldemar Bujalski. High temperature (ht) polymer electrolyte membrane fuel cells (pemfc)-a review. *Journal of Power Sources*, 231:264–278, 2013. ISSN 03787753. doi: 10.1016/j.jpowsour.2012.11.126.
- [21] International Maritime Organization. Marine Environment Protection Committee. *MARPOL, Annex VI and NTC 2008 with guidelines for implementation*. International Maritime Organization, 2017. ISBN 9789280116588.
- [22] MAN Diesel. Man b&w k98me-c6 project guide. Technical report, MAN Diesel, 2 2009. URL www.mandiesel.com.
- [23] Vaclav Dostal. A supercritical carbon dioxide cycle for next generation nuclear reactors, 2004.
- [24] Peter Durcansky, Radovan Nosek, and Jozef Jandacka. Use of stirling engine for waste heat recovery. *Energies*, 13, 8 2020. ISSN 19961073. doi: 10.3390/en13164133.
- [25] VDI e. V., editor. *VDI Heat Atlas*. Springer, 2nd edition, 2010. ISBN 978-3-540-77876-9. doi: 10.1007/978-3-540-77877-6.
- [26] Ulrich Eberle, Michael Felderhoff, and Ferdi Schüth. Chemical and physical solutions for hydrogen storage. *Angewandte Chemie International Edition*, 48:6608–6630, 8 2009. ISSN 1521-3773. doi: 10.1002/ANIE.200806293. URL <https://onlinelibrary.wiley.com/doi/full/10.1002/anie.200806293>.
- [27] Khosrow Ebrahimi, Gerard F. Jones, and Amy S. Fleischer. A review of data center cooling technology, operating conditions and the corresponding low-grade waste heat recovery opportunities. *Renewable and Sustainable Energy Reviews*, 31:622–638, 3 2014. ISSN 1364-0321. doi: 10.1016/J.RSER.2013.12.007.
- [28] Echogen. Eps100 heat recovery solution, 2022. URL <https://www.echogen.com/our-solution/product-series/eps100/>.
- [29] M. Morsy El-Gohary. Overview of past, present and future marine power plants. *Journal of Marine Science and Application*, 12:219–227, 2013. doi: 10.1007/s11804-013-1188-8.

- [30] Mohamed M Elgohary, Ibrahim S Seddiek, and Ahmed M Salem. Overview of alternative fuels with emphasis on the potential of liquefied natural gas as future marine fuel. *Proc IMechE Part M: J Engineering for the Maritime Environment*, 229:365–375, 2015. doi: 10.1177/1475090214522778.
- [31] Jasper Faber, Shinichi Hanayama, Shuang Zhang, Paula Pereda, Bryan Comer, Elena Hauerhof, Wendela Schim van der Loeff, Tristan Smith, Yan Zhang, Hiroyuko Kosaka, Masaki Adachi, Jean-Marc Bonello, Connor Galbraith, Ziheng Gong, Koichi Hirata, David Hummels, Anne Kleijn, David S. Lee, Yiming Liu, Andrea Lucchesi, Xiaoli Mao, Eiichi Muraoka, Liudmila Osipova, Haoqi Qian, Dan Rutherford, Santiago Suárez de la Fuente, Haichao Yuan, Camilo Velandia Perico, Libo Wu, Deping Sun, Dong-Hoon Yoo, and Hui Xing. Fourth imo greenhouse gas study 2020. Technical report, IMO, 2021.
- [32] Claudio Ferrari and Francesco Melino. Thermo - photo - voltaic generator development. *Energy Procedia*, 45:150–159, 2014. ISSN 18766102. doi: 10.1016/j.egypro.2014.01.017.
- [33] D. Fleming, T. Holschuh, T. Conboy, J. Pasch, S. Wright, and G. Rochau. Scaling considerations for a multi-megawatt class supercritical co2 brayton cycle and path forward for commercialization. *Proceedings of the ASME Turbo Expo*, 2012.
- [34] Maria Gallucci. The ammonia solution: Ammonia engines and fuel cells in cargo ships could slash their carbon emissions. *IEEE Spectrum*, 58:44–50, 3 2021. doi: 10.1109/MSPEC.2021.9370109.
- [35] A A Genbach, V O Baibekova, K S Olzhabayeva, A Mergalimova, A S Rasmukhametova, A A Begimbetova, A Zhauyt, and K S Olzha-bayeva. Research and modelling of the cooling system in steam turbine bearings. *Metalurgija*, 60:145–148, 2021. ISSN 0543-5846.
- [36] Federico Ghirardo, Marco Santin, Alberto Traverso, and Aristide Massardo. Heat recovery options for onboard fuel cell systems. *International Journal of Hydrogen Energy*, 36:8134–8142, 7 2011. ISSN 0360-3199. doi: 10.1016/J.IJHYDENE.2011.01.111.
- [37] Nathan Gray, Shane McDonagh, Richard O’Shea, Beatrice Smyth, and Jerry D. Murphy. Decarbonising ships, planes and trucks: An analysis of suitable low-carbon fuels for the maritime, aviation and haulage sectors. *Advances in Applied Energy*, 1, 2 2021. ISSN 26667924. doi: 10.1016/j.adapen.2021.100008.
- [38] Mirko Grljušić, Vladimir Medica, and Gojmir Radica. Calculation of efficiencies of a ship power plant operating with waste heat recovery through combined heat and power production. *Energies*, 8:4273–4299, 2015. ISSN 19961073. doi: 10.3390/en8054273.
- [39] KH Grote and H Hefazi, editors. *Handbook of Mechanical Engineering*. Springer, 2 edition, 2021.
- [40] Pavan K. Gupta, Vineet Kumar, and Sudip Maity. Renewable fuels from different carbonaceous feedstocks: a sustainable route through fischer-tropsch synthesis. *Journal of Chemical Technology & Biotechnology*, 96:853–868, 4 2021. ISSN 0268-2575. doi: 10.1002/jctb.6644.
- [41] Seyfettin Can Gülen. Steam turbine—quo vadis? *Frontiers in Energy Research*, 8:384, 2 2021. ISSN 2296598X. doi: 10.3389/FENRG.2020.612731/BIBTEX.
- [42] Ali Haseltalab, Lindert van Biert, Harsh Sapra, Benny Mestemaker, and Rudy R. Negenborn. Component sizing and energy management for sofc-based ship power systems. *Energy Conversion and Management*, 245, 10 2021. ISSN 01968904. doi: 10.1016/j.enconman.2021.114625.
- [43] Heatric. Characteristics of diffusion-bonded heat exchangers, 2022. URL http://www.heatric.com/typical_characteristics_of_PCHes.html.
- [44] Jerzy Herdzik. Decarbonization of marine fuels—the future of shipping. *Energies*, 14, 7 2021. ISSN 19961073. doi: 10.3390/en14144311.

- [45] Koichi Hirata and Masakuni Kawada. Discussion of marine stirling engine systems. pages 1–5, 2005. URL www.dieselduck.net.
- [46] S. E. Hirdaris, Y. F. Cheng, P. Shallcross, J. Bonafoux, D. Carlson, B. Prince, and G. A. Saris. Considerations on the potential use of nuclear small modular reactor (smr) technology for merchant marine propulsion. *Ocean Engineering*, 79:101–130, 3 2014. ISSN 0029-8018. doi: 10.1016/J.OCEANENG.2013.10.015.
- [47] C.K. Ho, M. Carlson, P. Garg, and P. Kumar. Cost and performance tradeoffs of alternative solar-driven s-co2 brayton cycle configurations. 2015.
- [48] G. Hoogers. *Fuel Cell Technology Handbook*. CRC Press, 2003. ISBN 9780429120473. doi: 10.1201/9781420041552. URL <https://www-taylorfrancis-com.tudelft.idm.oclc.org/books/mono/10.1201/9781420041552/fuel-cell-technology-handbook-gregor-hoogers>.
- [49] Cara A. Horowitz. *Paris Agreement*, volume 55, pages 740–755. Cambridge University Press, 8 2016. doi: 10.1017/S0020782900004253. URL <https://www-cambridge-org.tudelft.idm.oclc.org/core/journals/international-legal-materials/article/paris-agreement/1EC0C66C41C86DE533D3BD777B997B16>.
- [50] Md Jubayer Hossain, Jahedul Islam Chowdhury, Nazmiye Balta-Ozkan, Faisal Asfand, Syamimi Saadon, and Muhammad Imran. Design optimization of supercritical carbon dioxide (s-co2) cycles for waste heat recovery from marine engines. *Journal of Energy Resources Technology, Transactions of the ASME*, 143, 12 2021. ISSN 15288994. doi: 10.1115/1.4050006.
- [51] Chuankun Huang, Yuzhuo Pan, Yuan Wang, Guozhen Su, and Jincan Chen. An efficient hybrid system using a thermionic generator to harvest waste heat from a reforming molten carbonate fuel cell. *Energy Conversion and Management*, 121:186–193, 8 2016. ISSN 01968904. doi: 10.1016/j.enconman.2016.05.028.
- [52] S. Imran, D. R. Emberson, A. Diez, D. S. Wen, R. J. Crookes, and T. Korakianitis. Natural gas fueled compression ignition engine performance and emissions maps with diesel and rme pilot fuels. *Applied Energy*, 124:354–365, 7 2014. ISSN 0306-2619. doi: 10.1016/J.APENERGY.2014.02.067.
- [53] F P Incropera, D P DeWitt, T L Bergman, and A S Lavine. *Fundamentals of Heat and Mass Transfer*. John Wiley & Sons, 7th edition, 2011. ISBN 9780470501979.
- [54] S. Ishiyama, Y. Muto, Y. Kato, S. Nishio, T. Hayashi, and Y. Nomoto. Study of steam, helium and supercritical co2 turbine power generations in prototype fusion power reactor. *Progress in Nuclear Energy*, 50:325–332, 3 2008. ISSN 01491970. doi: 10.1016/j.pnucene.2007.11.078.
- [55] J.S. Jadhao and D.G. Thombare. Review on exhaust gas heat recovery for ic engine. *International Journal of Engineering and Innovative Technology*, 2, 2013. ISSN 2277-3754. URL <https://www.researchgate.net/publication/284685429>.
- [56] Brian David James, Daniel Allan DeSantis, and Genevieve Saur. Hydrogen production pathways cost analysis (2013 – 2016). Technical report, Golden Field Office, 9 2016. URL <http://www.osti.gov/servlets/purl/1346418/>.
- [57] Hussam Jouhara, Navid Khordehgah, Sulaiman Almahmoud, Bertrand Delpech, Amisha Chauhan, and Savvas A. Tassou. Waste heat recovery technologies and applications. *Thermal Science and Engineering Progress*, 6:268–289, 6 2018. ISSN 2451-9049. doi: 10.1016/J.TSEP.2018.04.017.
- [58] Satish G. Kandlikar and Zijie Lu. Thermal management issues in a pemfc stack - a brief review of current status. *Applied Thermal Engineering*, 29:1276–1280, 5 2009. ISSN 13594311. doi: 10.1016/j.applthermaleng.2008.05.009.

- [59] A Sinan Karakurt and Yasin Ust. Marine steam turbines. pages 713–723, 2011. URL <https://www.researchgate.net/publication/270239382>.
- [60] Kamarul Aizat Abdul Khalid, Thye Jien Leong, and Khairudin Mohamed. Review on thermionic energy converters. *IEEE Transactions on Electron Devices*, 63:2231–2241, 6 2016. ISSN 00189383. doi: 10.1109/TED.2016.2556751.
- [61] Riza Kizilel, Rami Sabbah, J. Robert Selman, and Said Al-Hallaj. An alternative cooling system to enhance the safety of li-ion battery packs. *Journal of Power Sources*, 194:1105–1112, 12 2009. ISSN 03787753. doi: 10.1016/j.jpowsour.2009.06.074.
- [62] Sirichai Koonaphapdeelert, Pruk Aggarangsi, and James Moran. *Biomethane : production and applications*. Springer, 2020. ISBN 9789811383076. doi: 10.1007/978-981-13-8307-6. URL <http://link.springer.com/10.1007/978-981-13-8307-6>.
- [63] Jan Kopyscinski, Tilman J. Schildhauer, and Serge M.A. Biollaz. Production of synthetic natural gas (sng) from coal and dry biomass – a technology review from 1950 to 2009. *Fuel*, 89:1763–1783, 8 2010. ISSN 0016-2361. doi: 10.1016/J.FUEL.2010.01.027.
- [64] K Kolwzan and M Narewski. Alternative fuels for marine applications. *Latvian Journal of Chemistry*, pages 398–406, 2012. doi: 10.2478/v10161-012-0024-9. URL <https://www.researchgate.net/publication/264972038>.
- [65] Ngoc Anh Lai, Martin Wendland, and Johann Fischer. Working fluids for high-temperature organic rankine cycles. *Energy*, 36:199–211, 2011. ISSN 03605442. doi: 10.1016/j.energy.2010.10.051.
- [66] James Larminie and Andrew Dicks. *Fuel cell systems explained*. John Wiley & Sons Ltd, 2 edition, 2003. ISBN 9781118878330. doi: 10.1002/9781118878330.
- [67] Roland Arthur Lee and Jean-Michel Lavoie. From first- to third-generation biofuels: Challenges of producing a commodity from a biomass of increasing complexity. *Animal Frontiers*, 3:6–11, 4 2013. ISSN 2160-6056. doi: 10.2527/AF.2013-0010. URL <https://academic.oup.com/af/article/3/2/6/4638639>.
- [68] T. J. Leo, M. A. Raso, E. Navarro, E. Sánchez De La Blanca, M. Villanueva, and B. Moreno. Response of a direct methanol fuel cell to fuel change. *International Journal of Hydrogen Energy*, 35:11642–11648, 10 2010. ISSN 0360-3199. doi: 10.1016/J.IJHYDENE.2010.02.115.
- [69] Trevor M. Letcher. *Introduction with a focus on atmospheric carbon dioxide and climate change*, pages 3–17. Elsevier, 1 2020. ISBN 9780081028865. doi: 10.1016/B978-0-08-102886-5.00001-3.
- [70] Mingjia Li, Ge Wang, Jinliang Xu, Jingwei Ni, and Enhui Sun. Life cycle assessment analysis and comparison of 1000 mw s-co₂ coal fired power plant and 1000 mw usc water-steam coal-fired power plant. *Journal of Thermal Science*, 31:463–484, 4 2022. ISSN 1993033X. doi: 10.1007/s11630-020-1327-x.
- [71] Shi Jun Liang, Bo Liu, Wei Hu, Kun Zhou, and L. K. Ang. Thermionic energy conversion based on graphene van der waals heterostructures. *Scientific Reports*, 7, 4 2017. ISSN 20452322. doi: 10.1038/srep46211.
- [72] Xingyu Liang, Xiangxiang Wang, Gequn Shu, Haiqiao Wei, Hua Tian, and Xu Wang. A review and selection of engine waste heat recovery technologies using analytic hierarchy process and grey relational analysis. *International Journal of Energy Research*, 39:453–471, 3 2015. ISSN 1099114X. doi: 10.1002/er.3242.
- [73] H.P. Loh, J. Lyons, and C.W. White. Process equipment cost estimation final report. Technical report, U.S. Department of Energy National Energy Technology Laboratory, 1 2002.

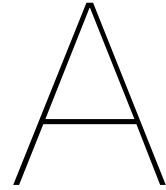
- [74] M.A. Lozano, A. Valero, and L.M. Serra. Theory of exergetic cost and thermoeconomic optimization. pages 339–350, 1993. URL <https://www.researchgate.net/publication/255821269>.
- [75] Fangrui Ma and Milford A. Hanna. Biodiesel production: a review. *Bioresource Technology*, 70: 1–15, 10 1999. ISSN 0960-8524. doi: 10.1016/S0960-8524(99)00025-5.
- [76] Patrycja Makos, Edyta Słupek, Joanna Sobczak, Dawid Zabrocki, Jan Hupka, and Andrzej Rogala. Dimethyl ether (dme) as potential environmental friendly fuel. volume 116, page 00048. EDP Sciences, 9 2019. doi: 10.1051/E3SCONF/201911600048. URL https://www.e3s-conferences.org/articles/e3sconf/abs/2019/42/e3sconf_asee18_00048/e3sconf_asee18_00048.html.
- [77] Matteo Marchionni, Giuseppe Bianchi, and Savvas A. Tassou. Review of supercritical carbon dioxide (sco2) technologies for high-grade waste heat to power conversion. *SN Applied Sciences*, 2, 4 2020. ISSN 25233971. doi: 10.1007/s42452-020-2116-6.
- [78] Charles J. McKinlay, Stephen R. Turnock, and Dominic A. Hudson. Route to zero emission shipping: Hydrogen, ammonia or methanol? *International Journal of Hydrogen Energy*, 46: 28282–28297, 8 2021. ISSN 03603199. doi: 10.1016/j.ijhydene.2021.06.066.
- [79] Charlie Mckinlay, Stephen R Turnock, and Dominic Antony Hudson. A comparison of hydrogen and ammonia for future long distance shipping fuels. 2020. URL <https://www.researchgate.net/publication/339106527>.
- [80] Anthony F Mills. *Heat Transfer*. Prentice Hall, 2nd edition, 1999.
- [81] Mohamed T. Mito, Mohamed A. Teamah, Wael M. El-Maghlany, and Ali I. Shehata. Utilizing the scavenge air cooling in improving the performance of marine diesel engine waste heat recovery systems. *Energy*, 142:264–276, 1 2018. ISSN 03605442. doi: 10.1016/j.energy.2017.10.039.
- [82] Szymon Mocarski and Aleksandra Borsukiewicz-Gozdur. Selected aspects of operation of supercritical (transcritical) organic rankine cycle. *Archives of Thermodynamics*, 36:85–103, 11 2015. ISSN 20836023. doi: 10.1515/aoter-2015-0017.
- [83] L. Mofor, P. Nuttall, and A. Newell. Renewable energy options for shipping (techreport). Technical report, IRENA, 2015. URL https://www.irena.org/-/media/Files/IRENA/Agency/Publication/2015/IRENA_Tech_Brief_RE_for-Shipping_2015.pdf.
- [84] Kamaljit Moirangthem and David Baxter. Alternative fuels for marine and inland waterways. Technical report, European Commission, 2016. URL <https://ec.europa.eu/jrc>.
- [85] Soo Young No. Application of straight vegetable oil from triglyceride based biomass to ic engines – a review. *Renewable and Sustainable Energy Reviews*, 69:80–97, 3 2017. ISSN 1364-0321. doi: 10.1016/J.RSER.2016.11.007.
- [86] M. Noaman, G. Saade, T. Morosuk, and G. Tsatsaronis. Exergoeconomic analysis applied to supercritical co2 power systems. *Energy*, 183:756–765, 9 2019. ISSN 03605442. doi: 10.1016/j.energy.2019.06.161.
- [87] Tiancheng Ouyang, Zhongkai Zhao, Jie Lu, Zixiang Su, Jiawei Li, and Haozhong Huang. Waste heat cascade utilisation of solid oxide fuel cell for marine applications. *Journal of Cleaner Production*, 275:124133, 12 2020. ISSN 0959-6526. doi: 10.1016/J.JCLEPRO.2020.124133.
- [88] Tiancheng Ouyang, Zhongkai Zhao, Zixiang Su, Jie Lu, Zhiping Wang, and Haozhong Huang. An integrated solution to harvest the waste heat from a large marine solid oxide fuel cell. *Energy Conversion and Management*, 223:113318, 11 2020. ISSN 0196-8904. doi: 10.1016/J.ENCONMAN.2020.113318.
- [89] T. Paanu, S. Niemi, and P. Rantanen. Waste heat recovery - bottoming cycle alternatives. University of Vaasa, 2012. ISBN 978-952-476-389-9. URL www.uwasa.fi.

- [90] V. Pattabathula and J. Richardson. Introduction to ammonia production. *CEP Magazine*, 2: 69–75, 2016.
- [91] Michael Persichilli, Alex Kacludis, Edward Zdankiewicz, and Timothy Held. Supercritical co2 power cycle developments and commercialization: Why sco 2 can displace steam. *Power-Gen India & Central Asia*, 2012. URL www.echogen.com.
- [92] Ahmad Pesaran, Andreas Vlahinos, and Thomas Stuart. Cooling and preheating of batteries in hybrid electric vehicles. 3 2003. URL <http://www.ctts.nrel.gov/BTM>.
- [93] Andreas Poullikkas. An overview of current and future sustainable gas turbine technologies. *Renewable and Sustainable Energy Reviews*, 9:409–443, 10 2005. ISSN 13640321. doi: 10.1016/j.rser.2004.05.009.
- [94] Radoslav Radonja, Dragan Bebić, and Darko Glujić. Methanol and ethanol as alternative fuels for shipping. *Promet - Traffic & Transportation*, 31:321–327, 6 2019. ISSN 0353-5320. doi: 10.7307/PTT.V31I3.3006.
- [95] Mohammad Mizanur Rahman, Ji Dongxu, Nusrat Jahan, Massimo Salvatores, and Jiyun Zhao. Design concepts of supercritical water-cooled reactor (scwr) and nuclear marine vessel: A review. *Progress in Nuclear Energy*, 124:103320, 6 2020. ISSN 0149-1970. doi: 10.1016/J.PNUCENE.2020.103320.
- [96] A. S. Rangwala. *Theory and Practice in Gas Turbines*. New Academic Science, 2 edition, 2013. ISBN 9781781830017. URL https://books.google.com/books/about/Theory_and_Practice_in_Gas_Turbines.html?hl=nl&id=J24DwgEACAAJ.
- [97] Hannah Ritchie and Max Roser. Co2 and greenhouse gas emissions. *Our World in Data*, 5 2020. URL <https://ourworldindata.org/emissions-by-sector>.
- [98] D Roemmich. Voyager: How long until ocean temperature goes up a few more degrees?, 3 2014. URL <https://scripps.ucsd.edu/news/voyager-how-long-until-ocean-temperature-goes-few-more-degrees>.
- [99] Masoud Rokni. Thermodynamic analysis of sofc (solid oxide fuel cell)-stirling hybrid plants using alternative fuels. *Energy*, 61:87–97, 11 2013. ISSN 03605442. doi: 10.1016/j.energy.2013.06.001.
- [100] P. Roosen, S. Uhlenbruck, and K. Lucas. Pareto optimization of a combined cycle power system as a decision support tool for trading off investment vs. operating costs. *International Journal of Thermal Sciences*, 42:553–560, 2003. ISSN 12900729. doi: 10.1016/S1290-0729(03)00021-8.
- [101] Shad Roundy, Paul Kenneth Wright, and Jan M. Rabaey. *Energy Scavenging for Wireless Sensor Networks*. Springer US, 2004. doi: 10.1007/978-1-4615-0485-6.
- [102] M. Saghafifar and M. Gadalla. A critical assessment of thermo-economic analyses of different air bottoming cycles for waste heat recovery. *International Journal of Energy Research*, 43: 1315–1341, 2019. ISSN 1099114X. doi: 10.1002/er.4243.
- [103] M. Saghafifar, A. Omar, K. Mohammadi, A. Alashkar, and M. Gadalla. A review of unconventional bottoming cycles for waste heat recovery: Part i – analysis, design, and optimization. *Energy Conversion and Management*, 198, 2019. ISSN 01968904. doi: 10.1016/j.enconman.2018.10.047.
- [104] Harsh Sapra, Jelle Stam, Jeroen Reurings, Lindert van Biert, Wim van Sluijs, Peter de Vos, Klaas Visser, Aravind Purushothaman Vellayani, and Hans Hopman. Integration of solid oxide fuel cell and internal combustion engine for maritime applications. *Applied Energy*, 281, 1 2021. ISSN 03062619. doi: 10.1016/j.apenergy.2020.115854.
- [105] S. Schöffner. A solid oxide fuel cell- sco2 brayton cycle hybrid system: system concepts and analysis, 2017.

- [106] S. I. Schöffler, S. A. Klein, P. V. Aravind, and R. Pecnik. A solid oxide fuel cell- supercritical carbon dioxide brayton cycle hybrid system. *Applied Energy*, 283, 2 2021. ISSN 03062619. doi: 10.1016/j.apenergy.2020.115748.
- [107] R K Shah and D R Sekulic. *Heat Exchangers*. McGraw-Hill, 3rd edition, 1998. ISBN 0070535558.
- [108] Amir Sharafian, Omar E Herrera, and Walter M Erida. Performance analysis of liquefied natural gas storage tanks in refueling stations. *Journal of Natural Gas Science and Engineering*, 36:496–509, 11 2016. doi: 10.1016/j.jngse.2016.10.062. URL <http://dx.doi.org/10.1016/j.jngse.2016.10.062>.
- [109] Gequn Shu, Youcai Liang, Haiqiao Wei, Hua Tian, Jian Zhao, and Lina Liu. A review of waste heat recovery on two-stroke ic engine aboard ships. *Renewable and Sustainable Energy Reviews*, 19:385–401, 2013. ISSN 13640321. doi: 10.1016/j.rser.2012.11.034.
- [110] R K Singal and Mehrzad Tabatabaian. *Direct Energy Conversion Technologies*. Mercury Learning & Information, 2019. ISBN 9781683924548. URL <http://ebookcentral.proquest.com/lib/delft/detail.action?docID=5977204>.
- [111] Dig Vijay Singh and Eilif Pedersen. A review of waste heat recovery technologies for maritime applications. *Energy Conversion and Management*, 111:315–328, 3 2016. ISSN 0196-8904. doi: 10.1016/J.ENCONMAN.2015.12.073.
- [112] Saima Siouane, Slaviša Jovanović, and Philippe Poure. Equivalent electrical circuits of thermo-electric generators under different operating conditions. *Energies*, 10, 2017. ISSN 19961073. doi: 10.3390/en10030386.
- [113] Binyang Song, Weilin Zhuge, Rongchao Zhao, Xinqian Zheng, Yangjun Zhang, Yong Yin, and Yanting Zhao. An investigation on the performance of a brayton cycle waste heat recovery system for turbocharged diesel engines. *Journal of Mechanical Science and Technology*, 27:1721–1729, 6 2013. ISSN 1738494X. doi: 10.1007/s12206-013-0422-2.
- [114] Ankit Sonthalia and Naveen Kumar. Hydroprocessed vegetable oil as a fuel for transportation sector: A review. *Journal of the Energy Institute*, 92:1–17, 2 2019. ISSN 1743-9671. doi: 10.1016/J.JOEI.2017.10.008.
- [115] Charles Sprouse and Christopher Depcik. Review of organic rankine cycles for internal combustion engine exhaust waste heat recovery. *Applied Thermal Engineering*, 51:711–722, 2013. ISSN 13594311. doi: 10.1016/j.applthermaleng.2012.10.017.
- [116] S. P. Stolyarov and A. S. Stolyarov. Stirling generators: Challenges and opportunities. *Russian Electrical Engineering* 2017 88:12, 88:778–782, 2 2018. ISSN 1934-8010. doi: 10.3103/S1068371217120161. URL <https://link.springer.com/article/10.3103/S1068371217120161>.
- [117] D. Sánchez, R. Chacartegui, M. Torres, and T. Sánchez. Stirling based fuel cell hybrid systems: An alternative for molten carbonate fuel cells. *Journal of Power Sources*, 192:84–93, 7 2009. ISSN 03787753. doi: 10.1016/j.jpowsour.2008.12.061.
- [118] D. Sánchez, J. M. Muñoz De Escalona, R. Chacartegui, A. Muñoz, and T. Sánchez. A comparison between molten carbonate fuel cells based hybrid systems using air and supercritical carbon dioxide brayton cycles with state of the art technology. *Journal of Power Sources*, 196:4347–4354, 5 2011. ISSN 03787753. doi: 10.1016/j.jpowsour.2010.09.091.
- [119] Bertrand F. Tchanche, Gr Lambrinos, A. Frangoudakis, and G. Papadakis. Low-grade heat conversion into power using organic rankine cycles - a review of various applications. *Renewable and Sustainable Energy Reviews*, 15:3963–3979, 2011. ISSN 13640321. doi: 10.1016/j.rser.2011.07.024.
- [120] Heather Thomson, James J. Corbett, and James J. Winebrake. Natural gas as a marine fuel. *Energy Policy*, 87:153–167, 12 2015. ISSN 0301-4215. doi: 10.1016/J.ENPOL.2015.08.027.

- [121] Youssef Timoumi, Iskander Tlili, and Sassi Ben Nasrallah. Performance optimization of stirling engines. *Renewable Energy*, 33:2134–2144, 9 2008. ISSN 0960-1481. doi: 10.1016/J.RENENE.2007.12.012.
- [122] G Towler and R Sinnott. *Chemical Engineering Design: Principles, Practice, and Economics of Plant and Process Design*. Butterworth-Heinemann, 2nd edition, 2013. ISBN 9780080966595.
- [123] Allen D. Uhler, Scott A. Stout, Gregory S. Douglas, Edward M. Healey, and Stephen D. Emsbo-Mattingly. Chemical character of marine heavy fuel oils and lubricants. *Standard Handbook Oil Spill Environmental Forensics*, pages 641–683, 2016. doi: 10.1016/B978-0-12-803832-1.00013-1. URL <http://dx.doi.org/10.1016/B978-0-12-809659-8.00013-9>.
- [124] Stefan Unnasch and Love Goyal. Life cycle analysis of lpg transportation fuels under the californian lcfs. Technical report, Life Cycle Associates, prepared for WPGA, 2017. URL www.LifeCycleAssociates.com.
- [125] Zafer Utlu and Büsra Selenay Önal. Thermodynamic analysis of thermophotovoltaic systems used in waste heat recovery systems: An application. *International Journal of Low-Carbon Technologies*, 13:52–60, 3 2018. ISSN 17481325. doi: 10.1093/ijlct/ctx019.
- [126] Guillermo E. Valencia, Luis G. Obregon, and Jorge Duarte. First-law-based thermodynamic study of reheat and regeneration rankine cycles using an educational software. *Contemporary Engineering Sciences*, 11:1253–1260, 2018. ISSN 13136569. doi: 10.12988/ces.2018.83104.
- [127] A. Valero, M.A. Lozano, L. Serra, G. Tsatsaronis, J. Pisa, C. Frangopoulos, and M.R. von Spakovsky. Cgam problem: Definition and conventional solution. *Energy*, 19:279–286, 1994. ISSN 0360-5442. doi: 10.1016/0360-5442(94)90112-0.
- [128] L. van Biert, M. Godjevac, K. Visser, and P. V. Aravind. A review of fuel cell systems for maritime applications. *Journal of Power Sources*, 327:345–364, 9 2016. ISSN 03787753. doi: 10.1016/j.jpowsour.2016.07.007.
- [129] P. F. van den Oosterkamp. Critical issues in heat transfer for fuel cell systems. *Energy Conversion and Management*, 47:3552–3561, 12 2006. ISSN 01968904. doi: 10.1016/j.enconman.2006.03.013.
- [130] Sundaramurthy Vedachalam, Nathalie Baquerizo, and Ajay K. Dalai. Review on impacts of low sulfur regulations on marine fuels and compliance options. *Fuel*, 310, 2 2022. ISSN 00162361. doi: 10.1016/j.fuel.2021.122243.
- [131] Philip P. Walsh and Paul Fletcher. *Gas turbine performance*. Blackwell Science, 2 edition, 2004. ISBN 9781405151030. doi: 10.1002/9780470774533.
- [132] Yuan Wang, Ling Cai, Tie Liu, Junyi Wang, and Jincan Chen. An efficient strategy exploiting the waste heat in a solid oxide fuel cell system. *Energy*, 93:900–907, 12 2015. ISSN 03605442. doi: 10.1016/j.energy.2015.09.088.
- [133] N.T. Weiland, B.W. Lance, and S. Pidaparti. sco2 power cycle component cost correlations from doe data spanning multiple scales and applications. volume 9, 6 2019. ISBN 9780791858721. doi: 10.1115/GT2019-90493.
- [134] Peng Wu and Richard Bucknall. Marine propulsion using battery power. 2016.
- [135] Christina Wulf, Petra Zapp, and Andrea Schreiber. Review of power-to-x demonstration projects in europe. *Frontiers in Energy Research*, 8, 9 2020. ISSN 2296598X. doi: 10.3389/fenrg.2020.00191.
- [136] Jiayi Xia, Jiangfeng Wang, Juwei Lou, Pan Zhao, and Yiping Dai. Thermo-economic analysis and optimization of a combined cooling and power (ccp) system for engine waste heat recovery. *Energy Conversion and Management*, 128:303–316, 11 2016. ISSN 01968904. doi: 10.1016/j.enconman.2016.09.086.

- [137] Gang Xiao, Guanghua Zheng, Min Qiu, Qiang Li, Dongsheng Li, and Mingjiang Ni. Thermionic energy conversion for concentrating solar power. *Applied Energy*, 208:1318–1342, 12 2017. ISSN 03062619. doi: 10.1016/j.apenergy.2017.09.021.
- [138] Hui Xing, Charles Stuart, Stephen Spence, and Hua Chen. Alternative fuel options for low carbon maritime transportation: Pathways to 2050. *Journal of Cleaner Production*, 297:126651, 5 2021. ISSN 0959-6526. doi: 10.1016/J.JCLEPRO.2021.126651.
- [139] Jyoti Yadav, Dinesh Yadav, D P Goyal, and Ph D Scholar. A review on advance piezoelectric energy harvesting and their circuitry system. *International Journal of R&D in Engineering*, 4: 8–17, 2016. URL <http://rndpublications.com/Nov2016/>.
- [140] C. Zamfirescu and I. Dincer. Using ammonia as a sustainable fuel. *Journal of Power Sources*, 185:459–465, 10 2008. ISSN 0378-7753. doi: 10.1016/J.JPOWSOUR.2008.02.097.
- [141] Lianjie Zhang, Tianrui Deng, Ting Ma, Min Zeng, and Qiuwang Wang. Selection of working medium and model for brayton cycle at different heat source temperatures. *Chemical Engineering Transactions*, 81:739–744, 2020. ISSN 22839216. doi: 10.3303/CET2081124.
- [142] Xinxin Zhang, Maogang He, and Ying Zhang. A review of research on the kalina cycle. *Renewable and Sustainable Energy Reviews*, 16:5309–5318, 9 2012. ISSN 13640321. doi: 10.1016/j.rser.2012.05.040.
- [143] Sipeng Zhu, Kun Zhang, and Kangyao Deng. A review of waste heat recovery from the marine engine with highly efficient bottoming power cycles. *Renewable and Sustainable Energy Reviews*, 120:109611, 3 2020. ISSN 1364-0321. doi: 10.1016/J.RSER.2019.109611.
- [144] Andreas Züttel. Materials for hydrogen storage. *Materials Today*, 6:24–33, 9 2003. ISSN 1369-7021. doi: 10.1016/S1369-7021(03)00922-2.
- [145] O. İpek, M. M. Mohammedsalih, B. Gürel, and B. Kılıç. Experimental investigation of low-temperature organic rankine cycle using waste heat from gas turbine bearings for different conditions. *International Journal of Environmental Science and Technology*, 2021. ISSN 17352630. doi: 10.1007/s13762-021-03172-x.



Verification of intermediate pressures

A.1. Verification of reheating, intercooling, and regeneration pressures

In section 6.1, the assumption was made to apply equal pressure ratios in configurations having reheating, intercooling, and/or regeneration. To make sure this assumption has merit, a verification for each of these three configurations has been conducted by varying the intermediate pressure and plotting this against both the theoretical efficiency and the specific net work. The verification has been conducted for a reheating SRC, an intercooling air BC, and a regeneration SRC; the resulting graphs are displayed in figures A.1a, A.1b, and A.1c respectively. Apart from the pressure ratio assumption, the other assumptions from section 6.1 are still applied. Additionally, for the reheating and regeneration SRCs, a P_{max} of 60 bar was used; for the intercooling air BC, a P_{min} and P_{max} of respectively 1 and 3 bar were used.

For the reheating SRC, a maximum theoretical efficiency of 44.46% is achieved when reheating at 5.69 bar; at this pressure, a specific net work of 2152 kJ/kg is produced. However, the maximum specific net work that can be produced is 2226.298 kJ/kg when reheating takes place at 1.63 bar; at this pressure, a theoretical efficiency of 43.36% is attained. When applying equal pressure ratios, an intermediate pressure of 1.60 bar is used, and a theoretical efficiency and specific net work of 43.32% and 2226.255 kJ/kg are obtained respectively. It can be concluded that by applying equal pressure ratios, the theoretical efficiency and specific net work are lower than when the intermediate pressure is optimized for maximum specific net work. However, while a balance between theoretical efficiency and specific net work would have been desirable, the reductions in efficiency and net work are significantly small, leading to the conclusion that applying equal pressure ratios for reheating does not produce invalid results.

For the intercooling air BC, a maximum theoretical efficiency of 16.97% is achieved when intercooling takes place at 1.26 bar; at this pressure, a specific net work of 121.8 kJ/kg is produced. However, the maximum specific net work that can be produced is 125.689 kJ/kg when intercooling is applied at an intermediate pressure of 1.75 bar; at this pressure, a theoretical efficiency of 16.51% is attained. When applying equal pressure ratios, an intermediate pressure of 1.73 bar is used, and a theoretical efficiency and specific net work of 16.54% and 125.685 kJ/kg are obtained respectively. It can be concluded that by applying equal pressure ratios, some efficiency is gained compared to the maximum net work, and some net work is gained compared to the maximized efficiency; therefore, it is concluded that the application of equal pressure ratios for intercooling is valid.

For the regeneration SRC, a maximum theoretical efficiency of 44.06% is achieved when the steam extraction for regeneration takes place at 3.64 bar; at this pressure, a specific net work of 1558 kJ/kg is produced. However, the maximum specific net work that can be produced is 1631 kJ/kg when regeneration is applied at an intermediate pressure of 0.28 bar; at this pressure, a theoretical efficiency of 42.45% is attained. When applying equal pressure ratios, an intermediate pressure of 1.60 bar is used, and a theoretical efficiency and specific net work of 43.87% and 1602 kJ/kg are obtained respectively.

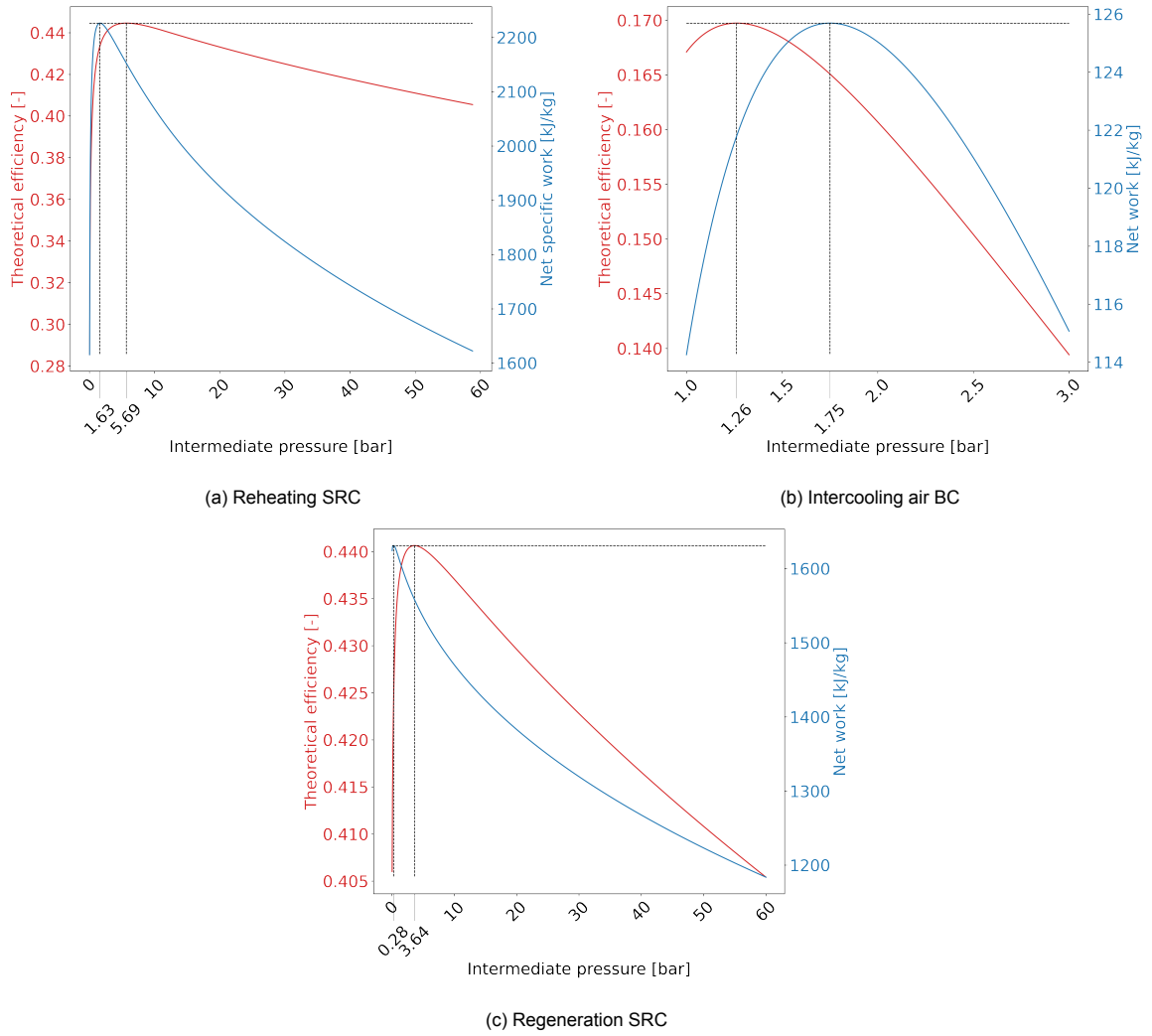


Figure A.1: Verification of intermediate pressures for reheating, intercooling, and regeneration.

It can be concluded that by applying equal pressure ratios, some efficiency is gained compared to the maximum net work, while some net work is gained compared to the maximized efficiency; therefore, the assumption to apply equal pressure ratios across the pumps before and after the open FWH is verified to produce valid results.

B

Size of configurations

This appendix contains tables of the resulting data obtained from the models created in chapter 7, as well as data which was visually represented by the figures present in the aforementioned chapter.

B.1. Electric power produced

Table B.1 shows the resulting mass flow rates and power outputs of the different configurations as obtained from the models created in section 7.1. The mass flow rates displayed are those present in the main parts of each configuration. In cycles containing regeneration or recompression, the flow experiences a split and the mass flow rates of the split flows vary from those provided in table B.1. The electric power outputs displayed are those visualized in figure 7.1.

Table B.1: Resulting mass flow rate and net electric power output of each configuration when applied with the same heat input.

Cycle	Configuration	Mass flow rate [<i>kg/s</i>]	Electric power output [<i>kWe</i>]
SRC	Basic	0.344	530.43
SRC	Reheating	0.268	565.91
SRC	Regeneration	0.377	573.08
SRC	Reheating & regeneration	0.296	587.06
TCSRC	Basic	0.356	582.30
TCSRC	Reheating	0.265	610.99
TCSRC	Regeneration	0.405	634.92
TCSRC	Reheating & regeneration	0.306	641.11
TCRC	Recuperation	4.02	572.22
TCRC	Recompression	5.77	673.02
BC	Recuperation	5.18	534.46
BC	Reheating & recuperation	4.96	564.84
BC	Intercooling & recuperation	5.18	575.84
BC	Reheating, intercooling & recuperation	4.96	604.51
SBC	Recuperation	4.04	572.82
SBC	Recompression	5.63	667.08

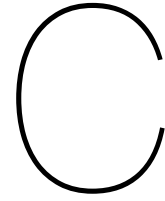
B.2. Heat transfer area and heat exchanger volume

Table B.2 shows the results of the heat transfer area and heat exchanger volume calculations for both the case applying PCHEs and the one applying STHes as described in section 7.1. The heat transfer areas displayed are those visualized in figures 7.3 and 7.4. The heat exchanger volumes displayed are

those obtained by the multiplication of the heat transfer areas and the area-to-volume ratios discussed in section 7.1.3.

Table B.2: Resulting heat transfer area and associated equipment volume for the PCHE and STHE.

Cycle	Configuration	Area [m^2]		Volume [m^3]	
		PCHE	STHE	PCHE	STHE
SRC	Basic	12.81	85.27	0.0092	0.866
SRC	Reheating	13.59	108.47	0.0097	1.10
SRC	Regeneration	12.64	86.74	0.0090	0.881
SRC	Reheating & regeneration	13.55	109.36	0.0097	1.11
TCSRC	Basic	11.63	76.76	0.0097	0.830
TCSRC	Reheating	12.37	94.03	0.0103	1.02
TCSRC	Regeneration	11.46	79.17	0.0096	0.856
TCSRC	Reheating & regeneration	12.30	95.40	0.0103	1.03
TCRC	Recuperation	34.66	354.30	0.0315	3.97
TCRC	Recompression	75.54	769.96	0.0687	8.63
BC	Recuperation	345.05	6513.16	0.2380	65.20
BC	Reheating & recuperation	422.12	8070.30	0.2911	80.78
BC	Intercooling & recuperation	404.73	7581.85	0.2791	75.89
BC	Reheating, intercooling & recuperation	478.56	9078.49	0.3300	90.88
SBC	Recuperation	35.13	356.30	0.0335	4.05
SBC	Recompression	72.45	735.26	0.0690	8.36



Cost of configurations

This appendix contains data obtained from the models created in chapter 7, as well as detailed results from the cost analysis conducted in chapter 8 and the data visually represented by the figures in this chapter.

C.1. Applied inputs to the PEC correlations

This section contains the detailed inputs applied to the cost correlations displayed in table 8.1.

Table C.1 shows the applied turbomachinery equipment in each configuration and the relevant measurement units; the inputs were obtained from the models created in chapter 6, combined with the values from table B.1.

Table C.1: Overview of the turbomachinery equipment applied in each cycle and their relevant units of measurement.

Turbomachines		Compressor & Pump $W_c [kW]$ or $\dot{m} [kg/s]$ & $W_c [kW]$		Turbine $W_T [kW]$ or $\dot{m} [kg/s]$	
Cycle	Configuration	1	2	1	2
SRC	Basic	2.58		560.93	
SRC	Reh.	2.01		297.58	300.12
SRC	Reg.	0.065	2.90	418.87	187.33
SRC	Reh. & reg.	0.051	2.27	328.72	291.55
TCSRC	Basic	13.33		626.27	
TCSRC	Reh.	9.91		316.59	336.47
TCSRC	Reg.	0.149	16.08	483.95	200.62
TCSRC	Reh. & reg.	0.112	12.13	365.20	321.90
TCRC	Recu.	106.64		708.98	
TCRC	Reco.	92.00	180.37	980.81	
BC	Recu.	5.18		5.18	
BC	Reh. & recu.	4.96		4.96	4.96
BC	Int. & recu.	5.18	5.18	5.18	
BC	Reh., int. & recu.	4.96	4.96	4.96	4.96
SBC	Recu.	111.89		714.87	
SBC	Reco.	97.51	159.69	959.39	

The heat exchangers applied in the case of PCHEs and STHs (and their relevant measurement units) are shown in tables C.2 and C.4, respectively; the values resulted from the extension of the models described in section 6.2 by those described in section 7.1.

Table C.2: Applied PCHEs with their respective values of $\bar{U}A_{HEX}$ and T_{max} .

Cycle	PCHE Configuration	$\bar{U}A_{HEX} [W/K] / T_{max} [^{\circ}C]^a$					
		Heater	Reheat.	Cooler / cond.	Intercool.	(LT)R	HTR
SRC	Basic	3771		54499			
SRC	Reh.	2936	1635	44849			
SRC	Reg.	3964		51503			
SRC	Reh. & reg.	3111	1589	43568			
TCSRC	Basic	4363		50855			
TCSRC	Reh.	3244	1688	44221			
TCSRC	Reg.	4725		47159			
TCSRC	Reh. & reg.	3566	1615	42305			
TCRC	Recu.	11562		37221		35720/656	
TCRC	Reco.	15021		32110		44595/202	85474/661
BC	Recu.	12822		38786		140311/580	
BC	Reh. & recu.	10479	10271	37203		171707/689	
BC	Int. & recu.	12822		28889	22390	163905/580	
BC	Reh., int. & recu.	10479	10271	27801	21465	193896/689	
SBC	Recu.	11630		39993		38844/656	
SBC	Reco.	14778		34854		49452/199	79746/661

^aHeaters and reheaters all have a T_{max} of 850 °C, as per the assumption in section 7.1.2; additionally, all (inter)coolers and condensers have values of T_{max} below 550 °C.

Table C.3 shows the scaling factors applied in the calculation of the cost of PCHEs. The values have been approximated from figure 8.1 and may be subject to inaccuracies.

Table C.3: Applied scaling factors (C^*) for the cost correlation of PCHEs, approximated from figure 8.1.

Cycle	Configuration	Scaling factor (C^*) [-]					
		Heater	Reheat.	Cooler / cond.	Intercool.	(LT)R	HTR
SRC	Basic	9		1.4			
SRC	Reh.	12	18	1.4			
SRC	Reg.	9		1.4			
SRC	Reh. & reg.	11.5	18	1.4			
TCSRC	Basic	8		1.4			
TCSRC	Reh.	11.5	18	1.4			
TCSRC	Reg.	6.5		1.4			
TCSRC	Reh. & reg.	9.5	18	1.4			
TCRC	Recu.	4		1.4		1.4	
TCRC	Reco.	3		1.4		1.4	1.3
BC	Recu.	3.5		1.4		1.25	
BC	Reh. & recu.	4.5	4.5	1.4		1.2	
BC	Int. & recu.	3.5		1.5	2	1.2	
BC	Reh., int. & recu.	4.5	4.5	1.5	2.1	1.2	
SBC	Recu.	4		1.4		1.4	
SBC	Reco.	3		1.4		1.4	1.3

Table C.4: Applied STHEs and their respective heat transfer areas.

Cycle	STHE Configuration	Area [m^2]					(LT)R	HTR
		Heater	Reheater	Cooler / condenser	Intercooler			
SRC	Basic	58.02		27.25				
SRC	Reh.	45.17	40.88	22.42				
SRC	Reg.	60.99		25.75				
SRC	Reh. & reg.	47.86	39.71	21.78				
TCSRC	Basic	51.33		25.43				
TCSRC	Reh.	38.16	33.76	22.11				
TCSRC	Reg.	55.59		23.58				
TCSRC	Reh. & reg.	41.95	32.30	21.15				
TCRC	Recu.	154.16		57.26		142.88		
TCRC	Reco.	200.28		49.40		178.38	341.90	
BC	Recu.	512.87		387.86		5612.42		
BC	Reh. & recu.	419.18	410.82	372.03		6868.27		
BC	Int. & recu.	512.87		288.89	223.90	6556.18		
BC	Reh., int. & recu.	419.18	410.82	278.01	214.65	7755.82		
SBC	Recu.	145.37		61.53		149.40		
SBC	Reco.	184.72		53.62		190.20	306.72	

C.2. Detailed results of PEC

This section contains the detailed cost breakdown of all components which makes up the visualization in figure 8.2. The cost of each component is determined by applying the values from tables C.1, C.2, and C.4 to the two correlations displayed in table 8.1 for each component. After applying the additional cost factors as discussed in section 8.1.1 and averaging the results, the PEC of each component is obtained and the total PEC is determined.

Table C.5 shows the resulting component cost of the turbomachinery for each configuration.

Table C.5: Overview of the purchased equipment costs of each turbomachine in USD, with a CEPCI of 797.6 as per January 2022.

Turbomachines		Compressor/Pump PEC [\$]		Turbine PEC [\$]	
Cycle	Configuration	1	2	1	2
SRC	Basic	3154		792417	
SRC	Reh.	2642		496494	499512
SRC	Reg.	231.1	3427	636525	360630
SRC	Reh. & reg.	194.5	2880	533211	489312
TCSRC	Basic	10121		861918	
TCSRC	Reh.	8200		518979	542259
TCSRC	Reg.	416.5	11563	708849	377604
TCSRC	Reh. & reg.	340.1	9466	575514	525222
TCRC	Recu.	544457		606492	
TCRC	Reco.	503293	724663	774439	
BC	Recu.	12358		115500	
BC	Reh. & recu.	11833		55297	53102
BC	Int. & recu.	3567	3774	115500	
BC	Reh., int. & recu.	3416	3614	55297	53102
SBC	Recu.	558656		610281	
SBC	Reco.	519076	677622	761659	

Table C.6 shows the resulting component cost of the heat exchangers when PCHEs are applied in each configuration.

Table C.6: Overview of the purchased equipment costs of the applied PCHEs in USD, with a CEPCI of 797.6 as per January 2022.

PCHE		Component PEC [\$]					
Cycle	Configuration	Heater	Reheat.	Cooler / cond.	Intercool.	(LT)R	HTR
SRC	Basic	144967		175040			
SRC	Reh.	130030	94631	149471			
SRC	Reg.	150834		167198			
SRC	Reh. & reg.	134249	92462	146005			
TCSRC	Basic	196836		165491			
TCSRC	Reh.	173535	97118	147774			
TCSRC	Reg.	198961		155677			
TCSRC	Reh. & reg.	176112	93690	142568			
TCRC	Recu.	363179		128536		369991	
TCRC	Reco.	425269		114065		185982	739794
BC	Recu.	307955		132891		496266	
BC	Reh. & recu.	274941	270670	128486		1152794	
BC	Int. & recu.	307955		107603	99000	554842	
BC	Reh., int. & recu.	274941	270670	104309	97846	1266649	
SBC	Recu.	364841		136228		394909	
SBC	Reco.	419935		121883		202227	700955

Table C.7 shows the resulting component cost of the heat exchangers when STHEs are applied in each configuration.

Table C.7: Overview of the purchased equipment costs of the applied STHEs in USD, with a CEPCI of 797.6 as per January 2022.

STHE		Component PEC [\$]					
Cycle	Configuration	Heater	Reheat.	Cooler / cond.	Intercool.	(LT)R	HTR
SRC	Basic	130578		36411			
SRC	Reh.	121497	118515	35344			
SRC	Reg.	132705		36078			
SRC	Reh. & reg.	123381	117705	35204			
TCSRC	Basic	125826		36007			
TCSRC	Reh.	116637	113625	35276			
TCSRC	Reg.	128844		35598			
TCSRC	Reh. & reg.	119256	112635	35066			
TCRC	Recu.	203094		43345		194271	
TCRC	Reco.	239814		41488		222255	357627
BC	Recu.	507177		132384		5249367	
BC	Reh. & recu.	424389	417096	127825		6456702	
BC	Int. & recu.	507177		104254	86325	6156801	
BC	Reh., int. & recu.	424389	417096	101219	83815	7280520	
SBC	Recu.	196212		44364		199362	
SBC	Reco.	227316		42482		231705	327759

Table C.8 shows the total purchased equipment cost of the configurations in the cases applying either PCHEs or STHes.

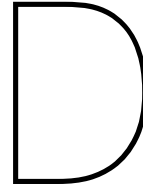
Table C.8: Overview of the total purchased equipment costs of the waste heat recovery configurations in USD, with a CEPCI of 797.6 as per January 2022.

Cycle	Configuration	Total PEC [\$]				
		Turbo-machinery	PCHEs	Turbomach. + PCHEs	STHes	Turbomach. + STHes
SRC	Basic	795571	320007	1115578	166989	962560
SRC	Reh.	998648	374132	1372780	275356	1274004
SRC	Reg.	1000813	318032	1318845	168783	1169596
SRC	Reh. & reg.	1025598	372716	1398314	276290	1301888
TCSRC	Basic	872039	362327	1234366	161833	1033872
TCSRC	Reh.	1069438	418427	1487865	265538	1334976
TCSRC	Reg.	1098433	354638	1453071	164442	1262875
TCSRC	Reh. & reg.	1110542	412370	1522912	266957	1377499
TCRC	Recu.	1150949	861706	2012655	246439	1397388
TCRC	Reco.	2002395	1465110	3467505	861184	2863579
BC	Recu.	127858	937112	1064970	5888928	6016786
BC	Reh. & recu.	120232	1826891	1947123	7426012	7546244
BC	Int. & recu.	122841	1069400	1192241	6854557	6977398
BC	Reh., int. & recu.	115429	2014415	2129844	8307039	8422468
SBC	Recu.	1168937	895978	2064915	439938	1608875
SBC	Reco.	1958357	1445000	3403357	829262	2787619

Table C.9 shows the total purchased equipment cost per kWe of the configurations in the cases applying either PCHEs or STHes.

Table C.9: Overview of the total purchased equipment costs of the waste heat recovery configurations in USD/kWe, with a CEPCI of 797.6 as per January 2022.

Cycle	Configuration	Total PEC per kW [\$/kWe]				
		Turbo-machinery	PCHEs	Turbomach. + PCHEs	STHes	Turbomach. + STHes
SRC	Basic	1500	603	2103	315	1815
SRC	Reh.	1765	661	2426	487	2252
SRC	Reg.	1746	555	2301	295	2041
SRC	Reh. & reg.	1747	635	2382	471	2218
TCSRC	Basic	1498	622	2120	278	1776
TCSRC	Reh.	1750	685	2435	435	2185
TCSRC	Reg.	1730	559	2289	159	1989
TCSRC	Reh. & reg.	1732	643	2375	416	2148
TCRC	Recu.	2011	1506	3517	431	2442
TCRC	Reco.	2975	2177	5152	1280	4255
BC	Recu.	239	1753	1992	11018	11257
BC	Reh. & recu.	213	3234	3447	13147	13360
BC	Int. & recu.	213	1857	2070	11904	12117
BC	Reh., int. & recu.	191	3332	3523	13742	13933
SBC	Recu.	2041	1564	3605	768	2809
SBC	Reco.	2936	2166	5102	1243	4179



Alternative approaches

The original approach was to apply the same heat input to each configuration, which resulted in the mass flow rate and power output; this in turn determined the size and cost of the components. In this section, results of two other paths are provided.

D.1. Same power output

A different way to compare the various waste heat recovery systems is to apply the same power output, instead of the same heat input. Here, the electric power output is fixed at 900 kWe, after which the heat transfer areas and heat exchanger volumes of the PCHEs and STHes are determined and displayed in table D.1. Additionally, the parameters relevant to the cost correlations from table 8.1 are presented in tables D.2, D.3, and D.4 for the turbomachinery, PCHEs, and STHes, respectively.

Table D.1: Resulting heat transfer area and associated equipment volume for the PCHE and STH.

Cycle	Configuration	Area [m^2]		Volume [m^3]	
		PCHE	STHE	PCHE	STHE
SRC	Basic	22.13	149.18	0.016	1.51
SRC	Reheating	22.09	177.80	0.016	1.81
SRC	Regeneration	20.18	139.99	0.014	1.42
SRC	Reheating & regeneration	21.25	173.05	0.015	1.76
TCSRC	Basic	18.25	121.85	0.015	1.32
TCSRC	Reheating	18.58	142.61	0.015	1.54
TCSRC	Regeneration	16.48	114.92	0.014	1.24
TCSRC	Reheating & regeneration	17.65	138.36	0.015	1.50
TCRC	Recuperation	57.81	594.69	0.053	6.66
TCRC	Recompression	104.08	1064.36	0.095	11.93
BC	Recuperation	591.04	11167.68	0.408	111.79
BC	Reheating & recuperation	710.48	13616.75	0.490	136.30
BC	Intercooling & recuperation	639.83	11995.06	0.441	120.07
BC	Reheating, intercooling & recuperation	737.84	14023.26	0.509	140.37
SBC	Recuperation	58.36	595.31	0.056	6.76
SBC	Recompression	100.65	1024.71	0.096	11.64

Table D.2: Overview of the turbomachinery equipment applied in each cycle and their relevant units of measurement.

Turbomachines		Compressor & Pump W_C [kW] or \dot{m} [kg/s] & [kW]		Turbine W_T [kW] or \dot{m} [kg/s]	
Cycle	Configuration	1	2	1	2
SRC	Basic	4.38		951.75	
SRC	Reh.	3.20		473.26	477.30
SRC	Reg.	0.101	4.55	657.82	294.19
SRC	Reh. & reg.	0.078	3.48	503.96	446.97
TCSRC	Basic	20.60		967.97	
TCSRC	Reh.	14.60		466.34	495.63
TCSRC	Reg.	0.211	22.79	686.00	284.38
TCSRC	Reh. & reg.	0.158	17.04	512.68	451.89
TCRC	Recu.	167.73		1115.10	
TCRC	Reco.	123.03	241.20	1311.59	
BC	Recu.	8.72		8.72	
BC	Reh. & recu.	7.91		7.91	7.91
BC	Int. & recu.	8.09	8.09	8.09	
BC	Reh., int. & recu.	7.39	7.39	7.39	7.39
SBC	Recu.	175.80		1123.17	
SBC	Reco.	131.56	215.45	1294.38	

Table D.3: Applied PCHEs with their respective values of $\bar{U}_{A_{HEX}}$ and T_{max} .

PCHE		$\bar{U}_{A_{HEX}}$ [W/K] / T_{max} [°C] ^a					
Cycle	Configuration	Heater	Reheat.	Cooler / cond.	Intercool.	(LT)R	HTR
SRC	Basic	6691		92471			
SRC	Reh.	5158	2511	71325			
SRC	Reg.	6471		80884			
SRC	Reh. & reg.	5275	2340	66793			
TCSRC	Basic	7017		78602			
TCSRC	Reh.	5231	2425	65138			
TCSRC	Reg.	6927		66849			
TCSRC	Reh. & reg.	5503	2196	59389			
TCRC	Recu.	20992		58543		56182/656	
TCRC	Reco.	22692		42940		59636/202	114301/661
BC	Recu.	26590		65314		236273/580	
BC	Reh. & recu.	27361	24645	59279		273593/689	
BC	Int. & recu.	23668		45152	34994	256172/580	
BC	Reh., int. & recu.	22794	20774	41391	31958	288675/689	
SBC	Recu.	21113		62836		61030/656	
SBC	Reco.	22555		47024		66719/199	107591/661

^aHeaters and reheaters all have a T_{max} of 850 °C, as per the assumption in section 7.1.2; additionally, all (inter)coolers and condensers have values of T_{max} below 550 °C.

Table D.4: Applied STHes and their respective heat transfer areas.

Cycle	STHE Configuration	Area [m^2]					
		Heater	Reheat.	Cooler / cond.	Intercool.	(LT)R	HTR
SRC	Basic	102.94		46.24			
SRC	Reh.	79.35	62.79	35.66			
SRC	Reg.	99.55		40.44			
SRC	Reh. & reg.	81.16	58.49	33.40			
TCSRC	Basic	82.55		39.30			
TCSRC	Reh.	61.54	48.50	32.57			
TCSRC	Reg.	81.49		33.42			
TCSRC	Reh. & reg.	64.74	43.93	29.69			
TCRC	Recu.	279.90		90.07		224.73	
TCRC	Reco.	302.56		66.06		238.54	457.20
BC	Recu.	1063.60		653.14		9450.94	
BC	Reh. & recu.	1094.45	985.79	592.79		10943.72	
BC	Int. & recu.	946.71		451.52	349.94	10246.89	
BC	Reh., int. & recu.	911.78	830.98	413.91	319.58	11547.01	
SBC	Recu.	263.91		96.67		234.73	
SBC	Reco.	281.94		72.34		256.61	413.81

It becomes clear from table D.1 that the conclusions are the same as when the same heat input is applied to each configuration. The heat exchangers of the air BC configurations are largest, followed by those of the CO₂-based cycles, and are the smallest for the (TC)SRC configurations. The application of the same (larger) power output has resulted in an increase of heat transfer area for each configuration, albeit slightly larger increases for some configurations more than others. This result is to be expected since the differences between the power outputs when the same heat input is applied are not that enormous.

This statement is also applicable to the data displayed in tables D.2, D.3, and D.4. The fixed larger power output has increased turbomachinery power and mass flow rates, as well as $\bar{U}A_{HEX}$ -values and STHE areas, across the board.

While this alternative approach has not been extended to the component cost analysis, it is reasonable to expect that the same conclusions would result in line with the aforementioned statements. Herein, all configurations would show an increased total PEC with again some more than others. However, as cost correlations rarely scale linearly with power output, the PEC per unit power is likely to improve for all configurations, but the most for those experiencing the largest increase in power output, such as the basic SRC.

D.2. No additional cost correction

In section 8.1.1, a few correction factors were discussed regarding the operating temperature and/or pressure of the steam turbines, PCHes, and STHes; however, as these factors were obtained from other studies and estimations, they are not without uncertainty. Therefore, the resulting PEC when applying the same heat input has also been determined without the application of correction factors. The approach to obtain the total PEC is similar to before, with the PEC of each component following from the application of the relevant input parameters to the two respective correlations in table 8.1, and averaging the results.

Table D.5 shows the resulting component cost of the turbomachinery for each configuration.

Table D.5: Overview of the purchased equipment costs of each turbomachine in USD, with a CEPCI of 797.6 as per January 2022.

Turbomachines		Compressor/Pump PEC [\$]		Turbine PEC [\$]	
Cycle	Configuration	1	2	1	2
SRC	Basic	3154		264139	
SRC	Reh.	2642		165498	166504
SRC	Reg.	231.1	3427	212175	120210
SRC	Reh. & reg.	194.5	2880	177737	163104
TCSRC	Basic	10121		287306	
TCSRC	Reh.	8200		172993	180753
TCSRC	Reg.	416.5	11563	236283	125868
TCSRC	Reh. & reg.	340.1	9466	191838	175074
TCRC	Recu.	544457		606492	
TCRC	Reco.	503293	724663	774439	
BC	Recu.	12358		115500	
BC	Reh. & recu.	11833		55297	53102
BC	Int. & recu.	3567	3774	115500	
BC	Reh., int. & recu.	3416	3614	55297	53102
SBC	Recu.	558656		610281	
SBC	Reco.	519076	677622	761659	

Table D.6 shows the resulting component cost of the heat exchangers when PCHEs are applied in each configuration.

Table D.6: Overview of the purchased equipment costs of the applied PCHEs in USD, with a CEPCI of 797.6 as per January 2022.

PCHE		Component PEC [\$]					
Cycle	Configuration	Heater	Reheat.	Cooler / cond.	Intercool.	(LT)R	HTR
SRC	Basic	181209		218800			
SRC	Reh.	162538	118289	186839			
SRC	Reg.	188542		208998			
SRC	Reh. & reg.	167811	115577	182506			
TCSRC	Basic	196836		206864			
TCSRC	Reh.	173535	121397	184718			
TCSRC	Reg.	198961		194596			
TCSRC	Reh. & reg.	176112	117112	178210			
TCRC	Recu.	363179		160670		369991	
TCRC	Reco.	425269		142581		185982	739794
BC	Recu.	384944		166114		620332	
BC	Reh. & recu.	343676	338337	160607		1440992	
BC	Int. & recu.	384944		134504	123750	693553	
BC	Reh., int. & recu.	343676	338337	130386	122307	1583311	
SBC	Recu.	364841		170285		394909	
SBC	Reco.	419935		152354		202227	700955

Table D.7 shows the resulting component cost of the heat exchangers when STHes are applied in each configuration.

Table D.7: Overview of the purchased equipment costs of the applied STHEs in USD, with a CEPCI of 797.6 as per January 2022.

STHE		Component PEC [\$]					
Cycle	Configuration	Heater	Reheat.	Cooler / cond.	Intercool.	(LT)R	HTR
SRC	Basic	43526		36411			
SRC	Reh.	40499	39505	35344			
SRC	Reg.	44235		36078			
SRC	Reh. & reg.	41127	39235	35204			
TCSRC	Basic	41942		36007			
TCSRC	Reh.	38879	37875	35276			
TCSRC	Reg.	42948		35598			
TCSRC	Reh. & reg.	39752	37545	35066			
TCRC	Recu.	67698		43345		64757	
TCRC	Reco.	79938		41488		74085	119209
BC	Recu.	169059		132384		1749789	
BC	Reh. & recu.	141463	139032	127825		2152234	
BC	Int. & recu.	169059		104254	86325	2052267	
BC	Reh., int. & recu.	141463	139032	101219	83815	2426840	
SBC	Recu.	65404		44364		66454	
SBC	Reco.	75772		42482		77235	109253

Table D.8 shows the total purchased equipment cost of the configurations in the cases applying either PCHes or STHEs (excluding the correction factors).

Table D.8: Overview of the total purchased equipment costs of the waste heat recovery configurations in USD, with a CEPCI of 797.6 as per January 2022.

		Total PEC [\$]				
Cycle	Configuration	Turbo- machinery	PCHes	Turbomach. + PCHes	STHEs	Turbomach. + STHEs
SRC	Basic	267293	400009	667302	79937	347230
SRC	Reh.	334644	467666	802310	115348	449992
SRC	Reg.	336043	397540	733583	80313	416356
SRC	Reh. & reg.	343916	465894	809810	115566	459482
TCSRC	Basic	297427	403700	701127	77949	375376
TCSRC	Reh.	361946	479650	841596	112030	473976
TCSRC	Reg.	374131	393557	767688	78546	452677
TCSRC	Reh. & reg.	376718	471434	848152	112363	489081
TCRC	Recu.	1150949	893840	2044789	175800	1326749
TCRC	Reco.	2002395	1493626	3496021	314720	2317115
BC	Recu.	127858	1171390	1299248	2051232	2179090
BC	Reh. & recu.	120232	2283612	2403844	2560554	2680786
BC	Int. & recu.	122841	1336751	1459592	2411905	2534746
BC	Reh., int. & recu.	115429	2518017	2633446	2892369	3007798
SBC	Recu.	1168937	930035	2098972	176222	1345159
SBC	Reco.	1958357	1475471	3433828	304742	2263099

When comparing the results from table D.8 to those in table C.8, the differences observed are significant. This indicates how large the influence of cost correction factors can be, and why any uncertainty in these factors can have a tremendous impact on the final results.

While the results provided in table D.8 do not support the inclusion or exclusion of correction factors, they do indicate that in the case of PCHEs, the (TC)SRC configurations still present with a relatively low total PEC, followed by the air BCs and CO₂-based cycles. This can be said similarly for the case applying STHs, however, the air BCs show a significantly lower total PEC, close to that of recompression CO₂ cycles, than when the correction factors are included.

In conclusion, the results indicate what was to be expected: the exclusion of correction factors significantly alters the total PEC. However, to a certain extent the results from the comparison of the cycles and their PEC remains relatively unchanged, with the steam cycles showing a lower total PEC compared to the other cycles, between which the differences highly depend on the exact configuration and the type of heat exchanger applied.